AQUIFER DELINEATION WITHIN THE OXNARD FOREBAY GROUNDWATER BASIN USING SURFACE GEOPHYSICS

Open-File Report 2013-06
June 2013

THIS REPORT IS PRELIMINARY AND IS SUBJECT TO MODIFICATION BASED UPON FUTURE ANALYSIS AND EVALUATION

PREPARED BY

GROUNDWATER
RESOURCES
DEPARTMENT

UNITED WATER
CONSERVATION DISTRICT

UWCD OFR 2013-06

AQUIFER DELINEATION WITHIN THE OXNARD FOREBAY GROUNDWATER BASIN USING SURFACE GEOPHYSICS

United Water Conservation District
Open-File Report 2013-06

PREPARED BY

GROUNDWATER RESOURCES DEPARTMENT

JUNE 2013

THIS REPORT IS PRELIMINARY AND IS SUBJECT TO MODIFICATION BASED UPON FUTURE ANALYSIS AND EVALUATION

Cover Photo: Geophysical data collection in Santa Clara River flood plain within the Oxnard Forebay groundwater basin fall 2011.

Preferred Citation: United Water Conservation District, 2013, Aquifer Delineation within the Oxnard Forebay Groundwater Basin using Surface Geophysics, United Water Conservation District Open-File Report 2013-06.

Principal Author: Tim Moore - Staff Hydrogeologist.

AQUIFER DELINEATION WITHIN THE OXNARD FOREBAY GROUNDWATER BASIN USING SURFACE GEOPHYSICS

TABLE OF CONTENTS

LIST OF FIGURES

AQUIFER DELINEATION WITHIN THE OXNARD FOREBAY GROUNDWATER BASIN USING SURFACE GEOPHYSICS

UWCD OPEN-FILE REPORT 2013-06

EXECUTIVE SUMMARY / ABSTRACT

United Water Conservation District (United Water) conducted a Time Domain Electromagnetics (TDEM or TEM) geophysical survey in the Oxnard Forebay (Forebay) groundwater basin in fall 2011 and summer 2012. The purpose of the study is to advance current understanding of the subsurface geologic conditions in the Forebay that affect natural and managed groundwater recharge. The project was supported by a Fox Canyon Groundwater Management Agency (FCGMA) Groundwater Supply Enhancement and Assistance Program (GSEAP) grant.

The field survey area was approximately 12 square miles. In all, 139 high quality soundings were obtained in and around recharge basins, agricultural fields, orchards, dry Santa Clara River floodplain, open private land, and preservation land within and near the Forebay. Data were collected outside the Forebay in neighboring locations to define the boundary conditions of the Forebay. Geophysical software was used to model the data associated with each sounding in the study area. Model results were used to correlate the individual soundings in 21 resistivity cross-sections.

The depths of the geoelectric layers may not exactly coincide with the actual aquifer depths. The methodology maps the modeled resistivity values which may or may not correspond with the vertical aquifer boundaries. There is, however reasonable agreement between the aquifer delineation observed from this study and the findings of previous investigators in the Forebay. The TDEM method provides an indication of grain size and porosity (sands and gravels are relatively less porous but more permeable than silts and clays) but there is not a direct relationship due to the many variables that influence the measured resistivity for a given sounding.

The modeled resistivity data collected for this project is notably conductive at depth. Very low resistivities may correspond to the Lower Hueneme and Fox Canyon aquifers, but they may also correspond to discontinuous clay lenses (aquitards) that are present at more shallow depths in some locations in the Forebay. Clay lenses are discontinuous and appear as anomalies (blobs of low resistivity) within the dataset. Whereas, the deeper Lower Hueneme and Fox Canyon aquifers appear as a somewhat continuous geoelectric layer. Clay lenses, at these deeper depths, if present, are not readily distinguished from the Lower Hueneme and Fox Canyon aquifers using the TDEM surface geophysical technique in the Forebay.

Aquifer delineation can be difficult using TDEM surface geophysical methods alone. The large transmitter loop laid on the ground surface required to obtain the desired depth of investigation for

this project produces significant lateral influence (averaging) of the modeled geoelectric layers. The method is good for showing the degree of lateral continuity of units, but not absolute depths of aquifer units. Other sources of data such as available borehole electrical resistivity logs (electrical logs) are useful for comparison when interpreting surface geophysical data.

The resistivity data from this project can be roughly divided into three geoelectric layers. This grouping does not hold true for all of the soundings, especially across the Forebay boundary, but it is useful for the purpose of general interpretation of the data. Geoelectric Layer 1 is highly resistive and continuous throughout the Forebay and ranges in thickness from approximately 200 to 280 feet (approximately 61 to 85m). Although it protrudes down into the Upper Mugu aquifer, it roughly corresponds to the Oxnard aquifer.

Geoelectric Layer 2 is interpreted to roughly correspond to the Lower Mugu and Upper Hueneme aquifers. This geoelectric layer is approximately 800 feet (244m) thick in the middle of the Forebay and nearly pinches out near South Mountain. Layer 2 contains several notable anomalies (blobs). The high-resistivity anomalies are interpreted as aquifer material (areas of comparatively low porosity and high permeability) and the low-resistivity anomalies are interpreted as silts and clays (areas of high porosity and low permeability).

Geoelectric Layer 3 is fairly continuous, and likely corresponds with the Lower Hueneme and Fox Canyon aquifers, and the Santa Barbara Formation. The Lower Hueneme and Fox Canyon aquifers both appear to be relatively conductive and cannot be distinguished from each other with the surface geophysical method employed here.

Several of the northwest-southeast cross-sections imply offset in the low resistivity intervals in geoelectric Layer 3, but the offset is not so apparent in geoelectric Layer 2, and absent in geoelectric Layer 1. Changes in the geoelectric layers are apparent in the cross-sections that transverse both the mapped Forebay/Mound and Forebay Oxnard Plain basin boundaries. These facies changes are interpreted to be changes in depositional/erosional environments and/or suspected faulting.

Findings for this study include anomalous zones of high and low resistivity (indicating sands/gravels and silts/clays respectively) identified within and near United Water's recharge facilities. This study will aid in United Water's future recharge planning.

1 INTRODUCTION

United Water Conservation District (United Water) is a public agency within Ventura County, California that is charged with conserving the water of the Santa Clara River and its tributaries. United Water works to manage the surface water and groundwater resources within eight groundwater basins, including the Oxnard Forebay basin (Forebay). Figure 1.1-1 is a location map showing all of the basins including the Forebay. United Water and Fox Canyon Groundwater Management Agency's (FCGMA) boundaries are also shown in the figure.

1.1 UNITED WATER CONSERVATION DISTRICT AND FOX CANYON GROUNDWATER MANAGEMENT AGENCY

United Water encompasses nearly 213,000 acres of central Ventura County, including the Ventura County portion of the Santa Clara River Valley and the Oxnard Plain. The District serves as a steward for managing the surface water and groundwater resources, and is governed by a seven-person board of directors elected by region. The developed areas within the District boundaries of United Water are a mix of agriculture and urban areas, with prime agricultural land supporting high-dollar crops such as avocados, strawberries, row crops, lemons, and flowers. More than 370,000 people live within the United Water's District boundaries, including those living in the cities of Oxnard, Port Hueneme, Santa Paula, Fillmore and eastern Ventura.

United Water and the Fox Canyon Groundwater Management Agency (FCGMA) have complementary roles in the management of groundwater resources in Ventura County. FCGMA has regulatory powers to limit pumping while United Water has authority to construct water supply projects.

United Water is authorized under the California Water Code to conduct water resource investigations, acquire water rights, build facilities to store and recharge water, construct wells and pipelines for water deliveries, commence actions involving water rights and water use, and prevent interference with or diminution of stream/river flows and their associated natural subterranean supply of water (California Water Code, section 74500 et al.).

The current project was supported by a FCGMA Groundwater Supply Enhancement and Assistance Program (GSEAP) grant. This grant program was established by FCGMA in 2010 to provide grant funding to local water agencies pursuing projects intended to alleviate overdraft conditions within its boundary. Groundwater recharge to the Oxnard Forebay groundwater basin is a key component in the overall groundwater management strategy to reduce the severity of the overdraft in the Oxnard Plain and Pleasant Valley basins. The Forebay is the main source of recharge to the aquifers beneath the Oxnard Plain (FCGMA, 2007; UWCD, 2012a), as well as other adjacent groundwater basins.

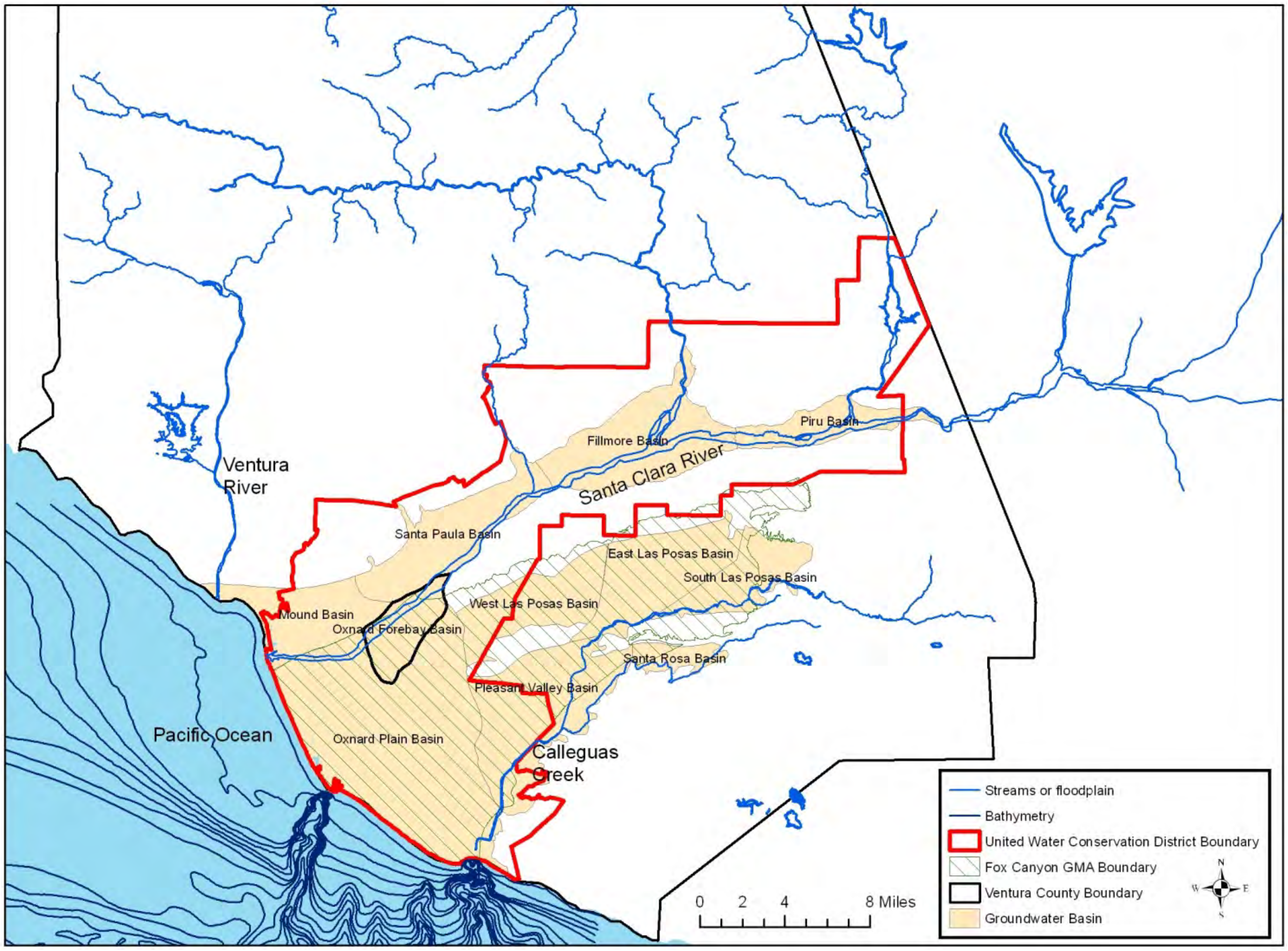

Figure 1.1-1: Location map of the Oxnard Forebay basin with respect to the other basins, United Water Conservation District and the Fox Canyon Groundwater Management Agency boundaries.

1.2 GEOLOGIC / HYDROLOGIC SETTING

United Water overlies all or part of eight groundwater basins in Ventura County. An overview of the geologic setting of the coastal basins, the regional aquifers, and some specifics of the Oxnard Forebay and other groundwater basins are discussed in this section.

The basins within United Water's District boundary are part of the Transverse Ranges geologic province, in which the mountain ranges and basins are oriented east-west rather than the typical northwest-southeast trend over much of California. The groundwater basins are within the more regional Ventura basin, which is an elongate east to west trending structurally complex syncline within the Transverse Range province (Yeats, et. al., 1981). The geology associated with the Transverse Range is primarily east to west trending folding and faulting that creates the elongate mountains and valleys that dominate Santa Barbara County and Ventura County.

Active thrust faults border the basins of the Santa Clara River valley, causing uplift of the adjacent mountains and down-dropping of the basins. The total stratigraphic thickness of upper Cretaceous, Tertiary, and Quaternary strata exceeds 55,000 feet (Sylvester and Brown, 1988). The sediments were deposited in both marine and terrestrial settings. Figure 1.2-1 is a geologic map of the region showing the general geology and location of the basins.

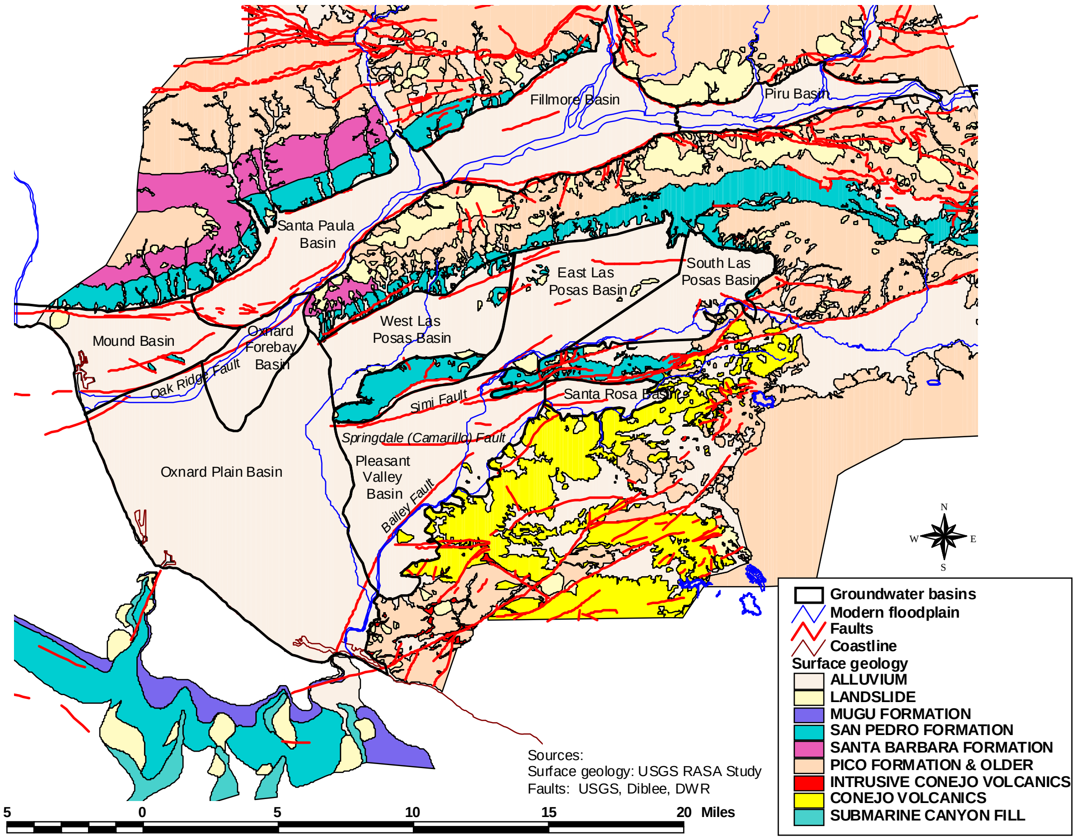

Figure 1.2-1: Geologic map for United Water Conservation District showing groundwater basins including Forebay Basin.

The aquifers within United Water's District boundary are generally grouped into the Upper Aquifer System (UAS) and Lower Aquifer System (LAS) (e.g., Turner, 1975; Mukae and Turner, 1975). The aquifers contain gravel and sand deposited by the ancestral Santa Clara River, within alluvial fans along the flanks of the mountains, and in a coastal plain/delta complex at the terminus of the recent and ancestral Santa Clara River (Oxnard Plain basin). The aquifers are recharged by infiltration of stream flow (primarily the Santa Clara River), artificial recharge of diverted stream flow (recharge basins), mountain-front recharge along the exterior boundary of the basins, direct infiltration of precipitation on the valley floors of the basins and on bedrock outcrops in adjacent mountain fronts, and irrigation return flow in agricultural areas.

Figure 1.2-2 is a schematic (depths in feet) of the UAS and LAS showing their subsurface sequence. However, more recent work with geophysical logs has suggested that some of the aquifers are actually deeper than originally thought as indicated from this schematic. Also note that the clay layers (aquitards) shown in the UAS are absent or discontinuous in the field area where this study was conducted.

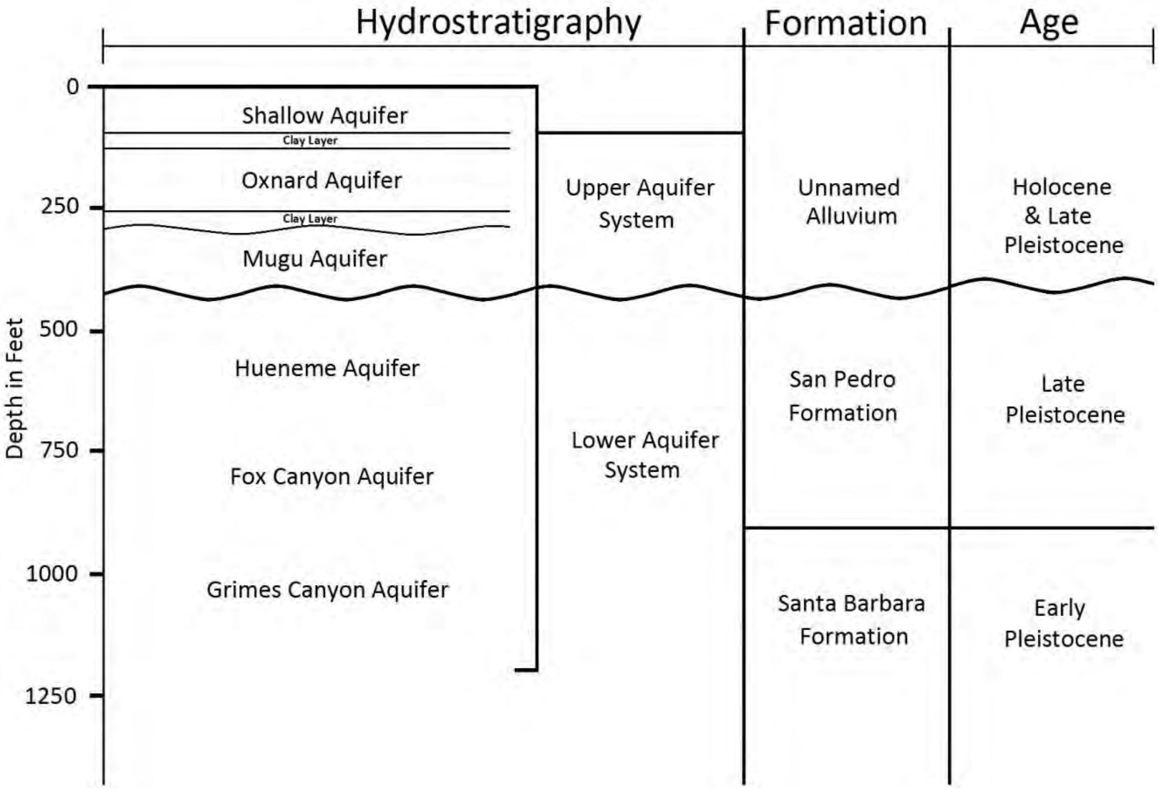

Figure 1.2-2: Schematic diagram of the Oxnard Plain aquifer system.

The LAS consists of the Hueneme, Fox Canyon, and Grimes Canyon aquifers. The LAS is part of the Santa Barbara, San Pedro, and Saugus formations of Pleistocene age (Hanson et al, 2003). The lowest water-bearing unit of the East Las Posas, Pleasant Valley, and Oxnard Plain basins is commonly referred to as the Grimes Canyon aquifer (CA DWR, 1954; Turner, 1975). The Fox Canyon aquifer overlies the Grimes Canyon aquifer. The Hueneme aquifer overlies the Fox Canyon aquifer. In some areas, the aquifers of the LAS may be isolated from each other vertically by low permeability units. The LAS is folded and tilted in many areas, and has been eroded along an unconformity that separates the upper and lower aquifer systems.

The UAS of the Oxnard Plain consists of the Mugu and Oxnard aquifers of Late Pleistocene and Holocene age. The UAS rests unconformably on the LAS, with basal conglomerates in many areas (Hanson et al, 2003). In the Oxnard Plain and Forebay, these coarse-grained basal deposits are referred to as the Mugu aquifer (Turner, 1975). The Oxnard aquifer rests unconformably on the Mugu aquifer and is a highly-permeable assemblage of sand and gravel generally found at depths that range between approximately 100 feet to 300 feet below land surface elevation. Recent river channel deposits comprise the uppermost water-bearing units along portions of the Santa Clara River basins.

In the Forebay, the UAS and LAS delineation is less defined. In the area between the El Rio and Saticoy spreading grounds (see Figure 1.2-3), the LAS has been uplifted and truncated along its contact with the UAS. Recharge from surface sources may enter both the UAS and the underlying LAS in this area. The U.S. Geological Survey estimates that about 20% of the water recharged to this area reaches the LAS, with the remainder recharging the UAS (United, 2012a). The Mugu and Hueneme aquifers pinch out near the northeast boundary of the Forebay at the base of South Mountain. The Fox Canyon aquifer outcrops in several locations on South Mountain.

On the Oxnard Plain, in some places the uppermost silt and clay deposits of the Oxnard aquifer are overlain by sand layers comprising the "semi-perched zone," which generally produces poor-quality water. This zone extends from the surface to no more than about 100 feet in depth. This semi-perched zone is absent or discontinuous in the Forebay permitting deeper percolation of natural and artificial groundwater recharge.

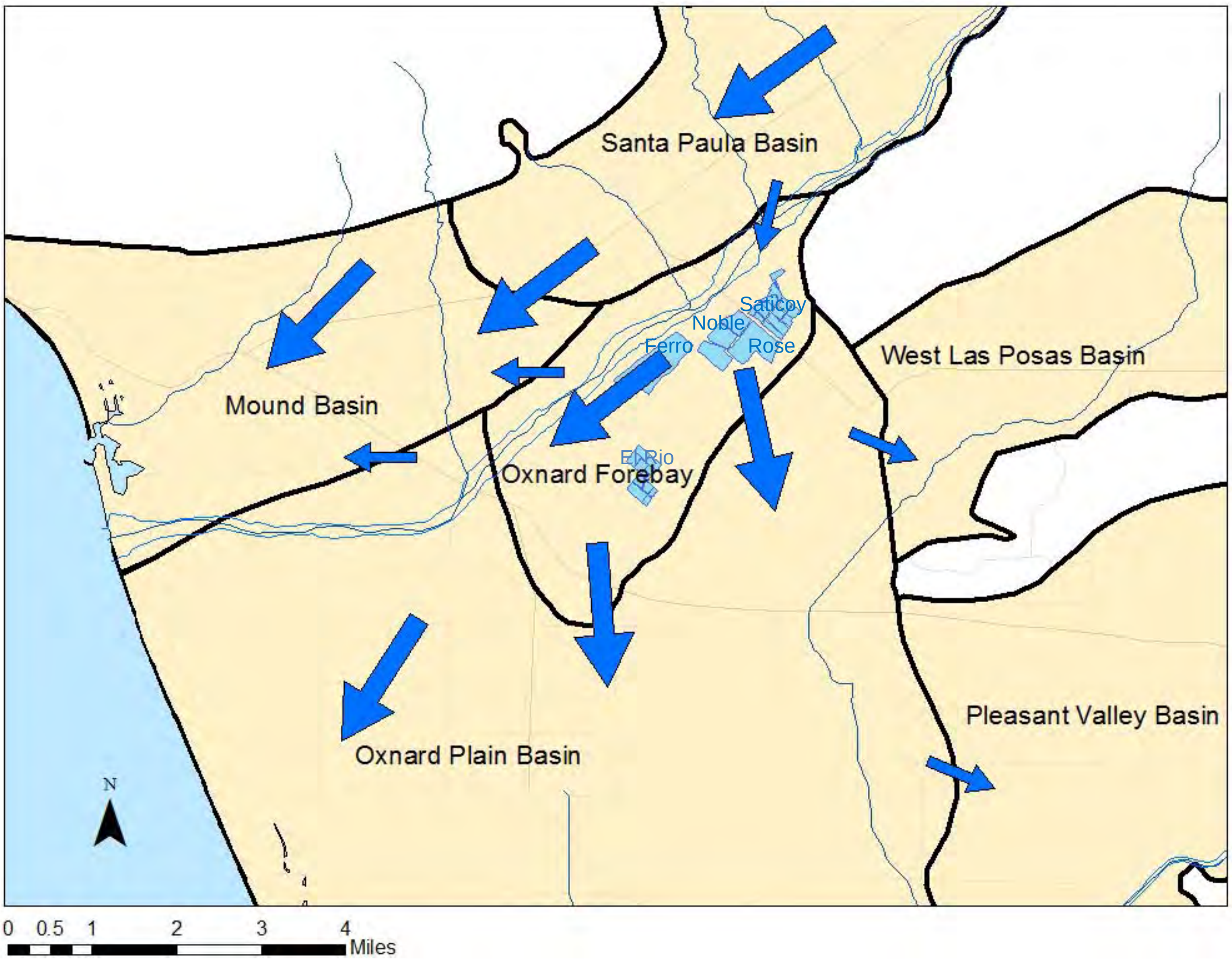

Figure 1.2-3: Generalized conceptual groundwater flow paths and United Water's Recharge Facilities.

The Forebay is a source of recharge to adjacent groundwater basins. Sources of recharge to the Forebay include: percolation of Santa Clara River flows (Figure 1.2-3), artificial recharge from United Water's spreading grounds, irrigation return flows, percolation of rainfall, and lesser amounts of underflow from adjacent basins. In 2011, United Water's spreading grounds in the Forebay recharged a total of 71,960 acre-feet. Figures C-1 through C-4 in Appendix C are spring high and fall low 2011 UAS and LAS groundwater elevation contour maps.

The land surface elevation of the Forebay ranges about 170 feet above mean see level (amsl) near the toe of South Mountain to about 70 feet amsl at the most southern edge of United Water's mapped Oxnard Forebay boundary. The Forebay has a typical coastal climate of warm dry summers and cool wet winters. The precipitation generally occurs from November through April with a mean annual precipitation (1950-1992) of 15.46 inches at El Rio Gage #239.

2 PROJECT PURPOSE

As mentioned earlier, the semi-perched zone is absent or discontinuous in the Forebay. Recent investigations (e.g., Daniel B. Stephens & Associates, 2008) depict the presence of clay units (aquitards) near the Santa Clara River in the southern Forebay but the lateral continuity and presence/absence of faulting were not addressed.

United Water was awarded a grant in 2011 through the FCGMA's Groundwater Supply Enhancement and Assistance Program (GSEAP). The purpose of the project is to conduct detailed surface geophysical surveys to refine the current understanding of the subsurface geologic conditions in the Oxnard Forebay that affect recharge operations.

2.1 FUTURE PLANNING AND DEVELOPMENT

The Oxnard Forebay groundwater basin readily accepts large volumes of recharge water when the water is available under wet hydrologic conditions. Figure C-5 in Appendix C is a historical time series of estimated changes in available groundwater storage within the Forebay. The graphic shows that storage in the basin can change rapidly, especially when the basin is filling.

The Forebay is a critical component of the region's water supply system as both an important area of groundwater recharge and also groundwater extractions (totaling nearly 18,500 acre-feet reported in 2011) (United, 2012a). The Forebay is envisioned as a potential location for increased groundwater pumping and a possible location for aquifer recharge with recycled water.

As the groundwater resource utilization in the Forebay intensifies, a more refined understanding of the hydrogeologic conditions is needed to facilitate optimization of this resource. A more detailed understanding of the lateral and vertical extent of both the discontinuous low-permeability units and the anomalous units of high electrical resistance (high permeability) within the Forebay's aquifers, as revealed in this geophysical study, will allow more informed decisions when locating new recharge projects and optimizing current management practices.

2.2 GROUNDWATER FLOW MODEL

United Water is currently developing detailed groundwater basin conceptual models utilizing the large number of oil and water well borehole (downhole) electrical resistivity logs within United Water's District boundary. This Oxnard Forebay geophysical survey will provide additional detail and refinement to the model. The conceptual model will serve as the foundation for United Water's efforts to construct an updated numerical groundwater flow model.

3 TECHNICAL APPROACH

In order to refine the current understanding of the subsurface geologic conditions in the Oxnard Forebay, a geophysical survey was designed and conducted in this area. The field survey area (Figure 3.3-1) encompassed approximately 12 square miles (the Forebay itself is approximately 10 square miles) and is utilized for agricultural, commercial and residential uses. Over 140 soundings were collected on United Water's properties, agricultural fields, orchards, dry Santa Clara River floodplain, open private land, and preservation land (The Nature Conservancy) within and near the Forebay. Data were collected outside the Forebay in neighboring locations to define the boundary conditions of the Forebay. A portion of the study area contains streets, houses, commercial buildings and other structures which completely cover the land surface, making data collection impossible due to electromagnetic interferences.

An overview of the methodology and interpretation are given here. Further explanation is in Appendix A and there is a discussion of apparent resistivity in TDEM soundings in Appendix B.

3.1 METHODOLOGY AND DATA INTERPRETATION

The geophysical methodology that was used was Time Domain Electromagnetics (TDEM or TEM). This surface geophysical method allows for rapid, cost-effective data collection compared to invasive borehole geophysical surveys such as electrical resistivity logging that require an open, uncased, fluid-filled borehole. The theory of operation for the TDEM method and data interpretation are summarized in this section with a more detailed explanation in Appendix A.

TDEM techniques are effective for determining electrical resistivity of soils at depths from about 30 feet to more than a thousand feet. Since electrical resistivity of earth materials correlates strongly with soil properties and the groundwater properties, TDEM is a powerful tool for mapping soils and changes in soil type and groundwater conditions in this depth range. TDEM can be used for numerous purposes some of which include: salt water intrusion, depth to bedrock, leachate in groundwater, mapping sand and gravel aquifers, mapping clay layers, mineral exploration, etc. TDEM went through a renaissance in the 1980s with the development of efficient and effective field equipment and computer interpretation techniques.

The TDEM technique induces electrical currents in the earth's subsurface using electromagnetic induction. A time-varying magnetic field is created using a loop of wire laid on the earth surface. Faraday's Law of induction indicates that a changing magnetic field will produce an electric field, which will in turn create an electric current. Thus the primary magnetic field from the transmitter loop will create a secondary electric current in the earth. Finally, instrumentation measures the secondary magnetic field produced by those secondary electric currents (eddy currents) in the earth.

The instrument measures the voltage against time of the decaying secondary magnetic field associated with the eddy currents produced by the primary current transmitter. An inversion must be performed on the data to get apparent resistivity, and then the apparent resistivity is modeled to generate true depth-dependent resistivity values for each sounding. IX1D 3.51 modeling software (Interpex, Inc.) was used to model the data utilizing a consistent automatically generated smooth modeling approach for processing all of the soundings in the study area. One model for each sounding location and 26-37 depth intervals, with a corresponding resistivity value (I-Data), was automatically generated for each model by this process. Cross-sections were constructed that correlate the individual soundings.

3.2 GENERAL FIELD PROCEDURE

Figure 3.2-1 shows a typical layout for a central loop TDEM sounding. United Water used the Monex GeoScope terraTEM Time-Domain Electromagnetic Surveying System and a terraTX-50 External terraTEM Transmitter. The system is battery powered and uses deep marine cycle 12-volt batteries connected in series (upper right in cover photo) as the transmitter power source. The external transmitter allows additional amperes (maximum of 50 amperes) to be generated and consequently a deeper depth of investigation to be obtained before the elevated signal-to-noise ratio decays to below a measurable level (disappears into the system noise).

Field procedures involve placing a square transmitter loop of wire on the ground surface. There is a tradeoff between resolution and depth of investigation associated with the loop size. A smaller loop is easier to handle in the field and produces higher resolution data, but the depth of investigation is proportionately shallower. A 350-foot (approximately 110m) on a side square loop of 10-gauge wire was determined to be the optimal loop for this investigation.

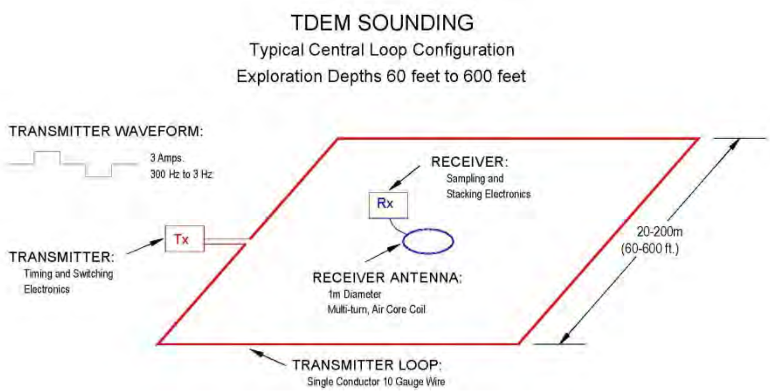

Figure 3.2-1: TDEM Field Setup.

Square wave current from the transmitter loop is abruptly turned off and on, which creates eddy currents and the subsequent decay of their measurable secondary magnetic fields in the ground. Measurements are made with a receiver coil (lower left in cover photo) in the center of the transmitter loop, as the induced eddy currents penetrate and diffuse through the earth. The receiver may also be placed outside of the transmitter loop in an “offset” configuration but this configuration was not employed in this study. For typical groundwater applications the measurement times range from 0.006 to 50 milliseconds (ms) after the primary transmitter current is turned off.

The receiver averages over tens or hundreds of repetitious measurements ("stacks") to increase the signal-to-noise ratio performance of the instrument. Data are recorded digitally and then reviewed by the field geophysicist or technician and stored in memory. Data are downloaded at the end of the day's survey for further processing and interpretation at the office.

3.3 SCOPE OF PROJECT DATA ACQUISTION

Figure 3.3-1 is a location map indicating the location of the 139 high-quality TDEM soundings obtained during the data acquisition phase of this project.

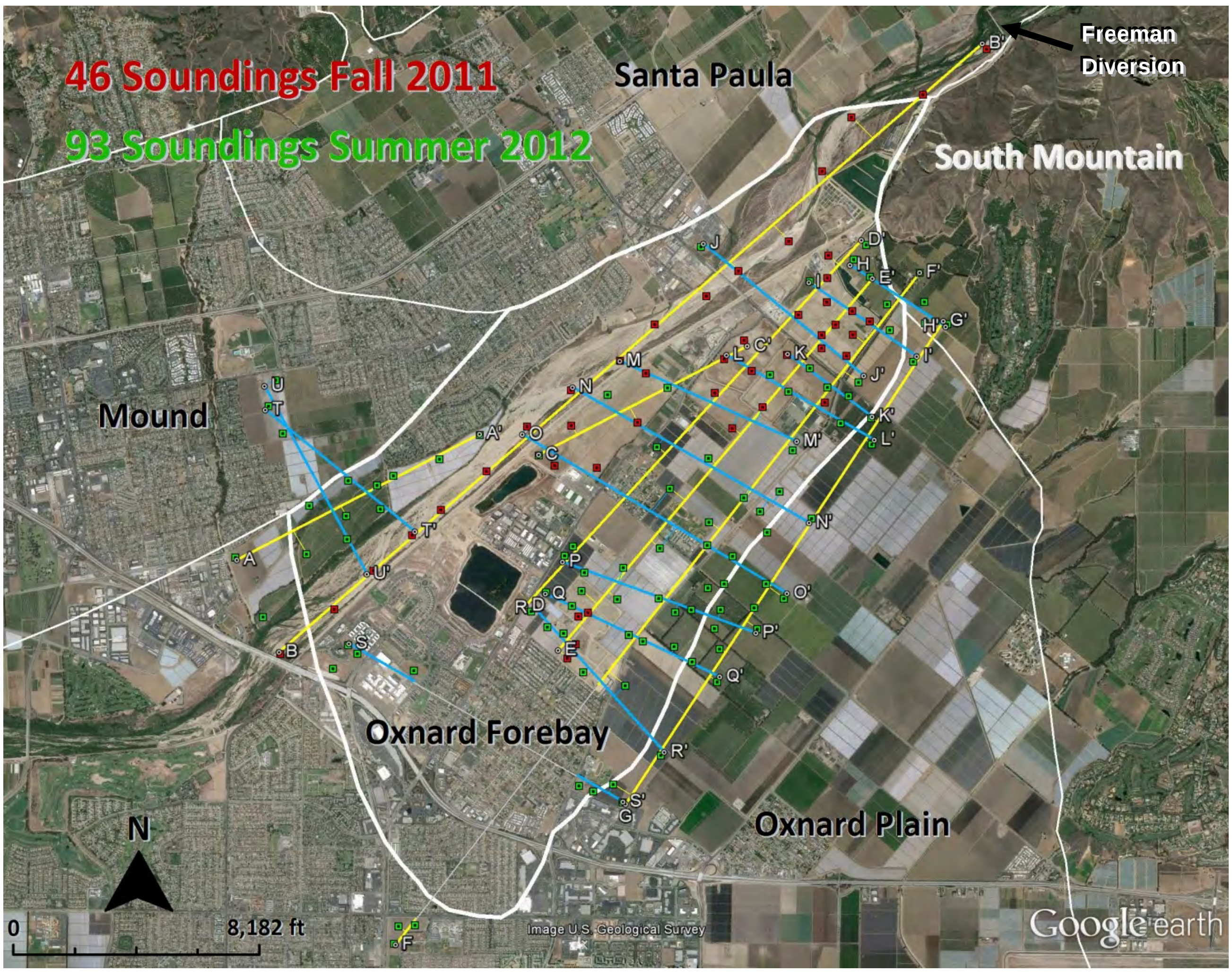

Figure 3.3-1: Location Map TDEM soundings collected during fall 2011 and summer 2012 and cross-section lines.

Each of the sounding locations represents a single transmitter loop laid on the ground surface where measurements were obtained at that location with the receiver coil in the center of the transmitter loop. The soundings are unevenly spaced due to access restrictions imposed by several obstacles including infrastructure and irrigation pipe containing metallic material and power lines.

Most of the data collected during the fall of 2011 (red squares in Figure 3.3-1) were collected on United Water's property and the dry Santa Clara River floodplain. United Water was diverting Santa Clara River flow at the Freeman Diversion and spreading surface water in percolation basins during the majority of the field data acquisition phase of this project.

Some of the soundings were collected in actively-farmed strawberry fields. There is a short window of time each summer when the crops have been harvested and aluminum irrigation piping are not in the fields. A concentrated field effort was performed during this window of time in the summer of 2012.

United Water worked closely with the land owners and ranch managers to access fields between planting of the various crops. Voluntary cooperation from many individuals made this project possible. There were a few fields and areas where United Water could not gain access to collect data. In general, a good distribution of data points was achieved by working in all areas that were accessible.

Each sounding was located with GPS. The GPS point on the map is the receiver coil location in the center of the transmitting loop. The receiver coil is the theoretical location for a given sounding; the data are assumed to be from directly below the receiver coil. The GPS accuracy (laterally on the land surface) ranged from approximately 10 to 20 feet depending on field conditions and satellite reception.

Data were stored on the instrument receiver console during a given field day. At the end of the day the data were downloaded for processing back in the office. One day worth of data typically consisted of 3 to 6 soundings. Prior to performing the modeling, the raw data was converted to USF format (Universal Sounding Format). This process takes the raw data and formats it for import into a modeling program.

Overall, a reasonable signal-to-noise ratio was achieved in a field area that contained significant ambient electrical noise. The terraTEM Time-Domain Electromagnetic Surveying System has a filter that is able to remove some of the effects of the background noise from power lines. The frequency of the waveform oscillations in transmitted alternating current (AC) through power lines in North America is 60 Hertz (Hz). Power lines and high voltage lines trended through parts of the field area, and data collected near power lines were often deemed to be unusable.

Limiting the effects of power lines was achieved by collecting data as far away from a given line as possible, while attempting to maintain an evenly-spaced distribution of sounding locations. Up to 2048 stacks were used during data acquisition to increase the signal-to-noise ratio. The use of an external transmitter also helped increase the signal-to-noise ratio by generating a stronger signal (up to 50 amperes).

Quality control of the data was conducted both in the field and in the office. Careful field inspection of the data in real time allowed possible identification of interferences so the sounding could be relocated. Typically problems were discovered and resolved in the field by making appropriate adjustments.

Data obtained on a given day was usually looked at the same day back in the office. If there were any apparent problem with the data (e.g., interference, wrong settings, instrument malfunction, etc.) that was not detected in the field, the sounding was relocated (when possible) and data was obtained properly.

4 STUDY RESULTS

The results of this study are presented in this section of the report. The 139 high-quality soundings allowed the construction of 21 cross-sections labeled A-A' through U-U' that correlate the individual modeled soundings. The cross-section figures are in Appendix D.

The methodology maps the modeled resistivity values which may or may not correspond with the vertical aquifer boundaries. The distinguishable zones or layers apparent from the data are termed "geoelectric layers". The depths of the geoelectric layers generally do not exactly coincide with the actual aquifer depths. There is, however, reasonable agreement between the aquifer delineation observed from this study and the findings of previous investigators in Oxnard Forebay.

4.1 RESISTIVITY VALUES

In this study, modeled resistivity values ranged from less than 1 Ohm-m to over 100 Ohm-m. Coarse-grained materials (sand, gravel, etc.) typically have relatively higher resistivity values than fine-grained materials (silt, clay, etc.). The TDEM method provides an indication of grain size and porosity (sands and gravels are relatively less porous but more permeable than silts and clays) but there is not a direct relationship due to the many variables that influence the measured resistivity for a given sounding.

Solid, dry rock has a very high resistivity and composition also plays a significant factor in resistivity. However, the presence of water significantly reduces the resistivity of all earth materials. Water quality can also affect the measured resistivity values. In general, water with a high salinity has a very low resistivity. Water with a low concentration of salts or salinity is characterized by relatively higher resistivity. Measured resistivity values represent a contribution from the water content, water type, and host materials (United, 2010). Water quality generally does not very significantly within the depth of investigation in the Forebay.

The selected transmitter loop size and the programmed instrument parameters also affect the measured resistivity values at a given location. All of the data for this project was collected using consistent instrument parameters, transmitter loop size, and general field technique.

4.2 DATA CHARACTERISTICS

The large transmitter loop required to obtain the desired depth of investigation for this project introduced notable lateral influence (averaging) of the modeled geoelectric layers. The TDEM equipment configuration used for this project was selected to balance the depth of investigation versus the level of detail. A smaller transmitter loop could have been utilized for this project that would have yielded greater vertical detail, but the depth of investigation would have been sacrificed. The data are good for showing the degree of continuity of geoelectric layers, but not absolute depths of individual aquifers.

The modeled resistivity data collected for this project are notably conductive at depth. This is not surprising since the Lower Hueneme and Fox Canyon aquifers (San Pedro Formation) includes more fined-grained marine sands, in contrast to the predominately coarse-grained terrestrial deposits (with intermixed marine deposits due to changes in sea level) of the Upper Hueneme, Mugu and Oxnard aquifers (Hanson et al, 2003).

Within the dataset collected for this project a particular resistivity value range cannot necessarily be associated with certainty to a particular grain size or aquifer due to the many variables that complicate the relationship. Very low resistivities may correspond to the Lower Hueneme and Fox Canyon aquifers, but they may also correspond to the discontinuous clay lenses (aquitards) that are present at some locations in the Forebay.

Therefore, silts and clays may be displayed as the same color when cross-sections are constructed based on the correlated depth dependent resistivity values from each sounding. The more shallow clay lenses are discontinuous and appear as anomalies (blobs of low resistivity) within the dataset. The deeper Lower Hueneme and Fox Canyon aquifers appear as a somewhat continuous geoelectric layer. The deeper clay lenses, if present, may not be distinguishable from the Lower Hueneme and Fox Canyon aquifers using the TDEM surface geophysical technique in the Forebay.

4.3 CROSS-SECTIONS

Cross-sections labeled A-A’ through U-U’ were constructed to analyze the vertical and horizontal relationship between the resistivity values modeled for each sounding. Each of the cross-sections were constructed from approximately +325 feet (+100m) to -1475 feet (-450m) of elevation above mean sea level (amsl), but the horizontal length of each cross-sections varies. The number of soundings used to construct each cross-section ranges from 5 to 19. The 21 cross-section locations are identified in Figure 3.3-1. The yellow lines in the figure represent the 7 southwest to northeast trending cross-sections and the blue lines represent the 14 northwest to southeast trending cross-sections. The individual cross-section figures are in Appendix D.

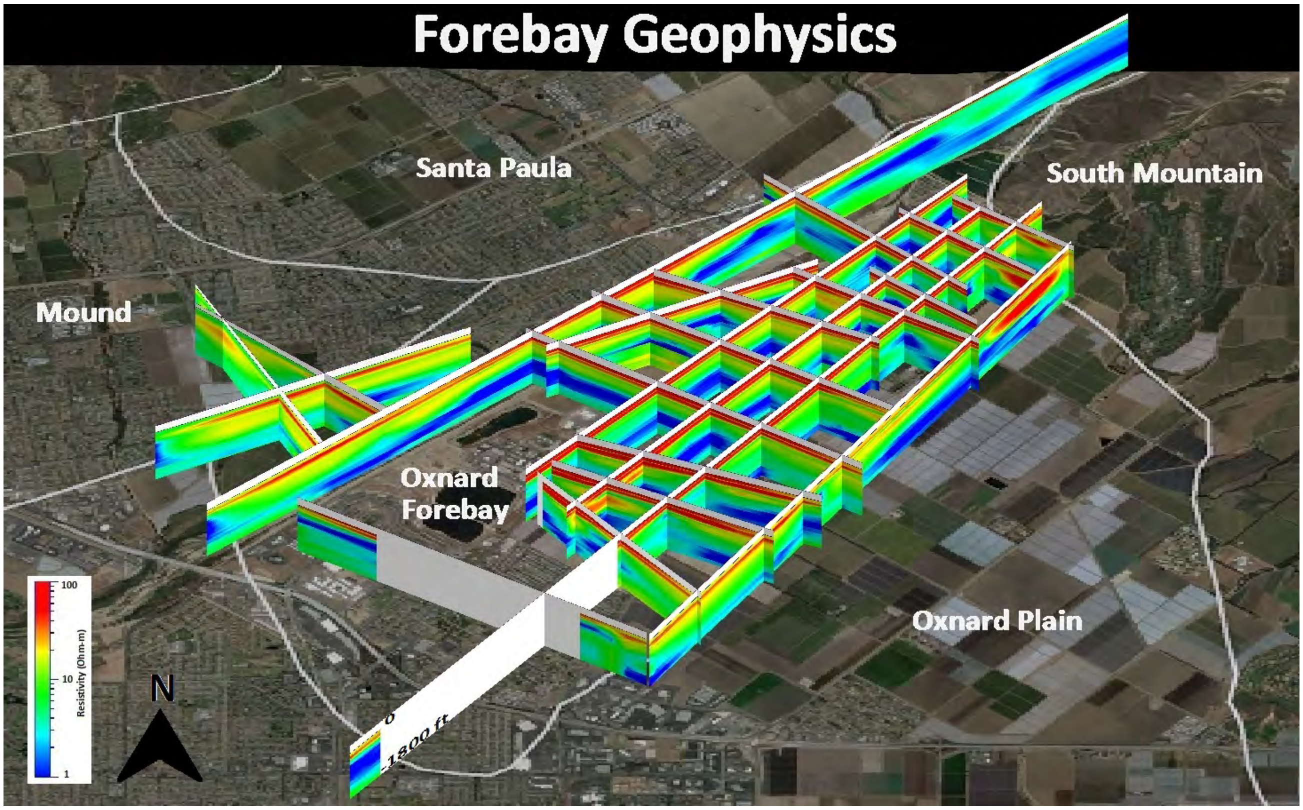

Figure 4.2-1: Fence Diagram with 1 to 50 Ohm-m color ramp looking obliquely north.

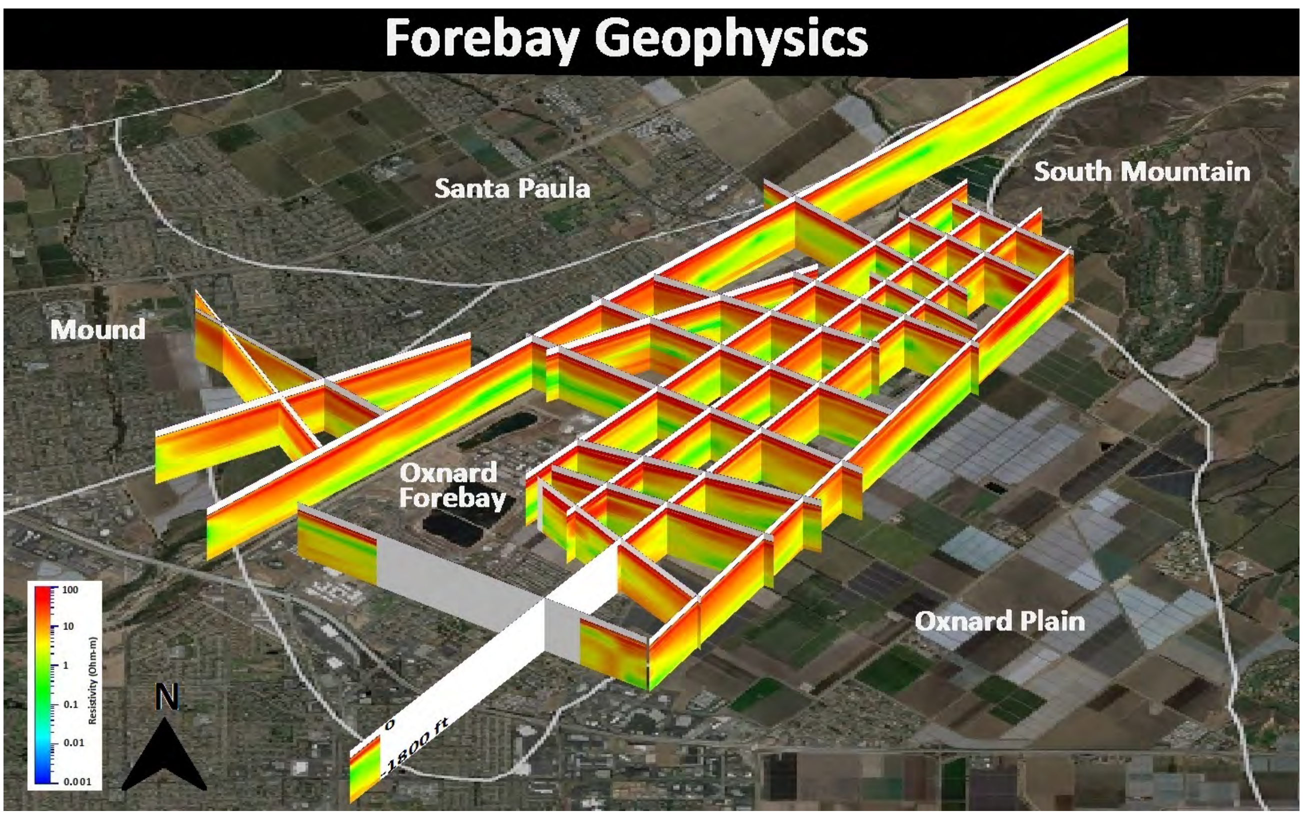

Figure 4.2-2: Fence Diagram with 0.001 to 50 Ohm-m color ramp looking obliquely north.

Figures 4.2-1 and 4.2-2 are fence diagrams showing the cross-sections in 3D vertically offset to display above the ground surface. The blanked-out areas in cross-sections F-F' and S-S' are due to large data gaps between soundings. Two different color ramps were used in correlating the individual soundings associated with each of the cross-sections.

In both color ramps, warm colors correspond with higher resistivity and cool colors correspond with lower resistivity. Log scales were used for both color ramps. 1 to 50 Ohm-m was selected for one of the color ramps and 0.001 to 50 Ohm-m was selected for the other color ramp. Because the depth-dependent resistivity values for a given sounding were sometimes higher than 50 Ohm-m, those values were filled with the color that represents the highest resistivity values for the selected color ramp (red). The 1 to 50 Ohm-m color ramp reveals the smaller (greater contrast) vertical and lateral difference in resistivity, and the 0.001 to 50 Ohm-m color ramp better illustrates the general geoelectric layers observed in the dataset.

Cross-section lines represent best-fit lines drawn through the selected soundings. The IX1D modeling software projects the selected soundings onto a cross-section line. All soundings shown on a cross-section were located within 1000 feet (perpendicular) of the line.

5 DISCUSSION

The discussion of the study results are presented in this section of the report. Included in this section are selected cross-section figures with annotation where appropriate.

5.1 RESISTIVITY ELECTRICAL LOG COMPARISON

Aquifer delineation using surface geophysical methods is best accomplished using complementary data. Other sources of data such as available borehole electrical resistivity logs (electrical logs) are useful for comparison when interpreting surface geophysical data.

There are approximately 290 active or destroyed water wells and approximately 30 active or destroyed oil and gas wells in the Forebay. Available oil and water well electrical logs have been projected onto cross-sections F-F', K-K' and Q-Q' (from this study) in Figures 5.1-1, 5.5.2-1 and 5.1-2 respectively.

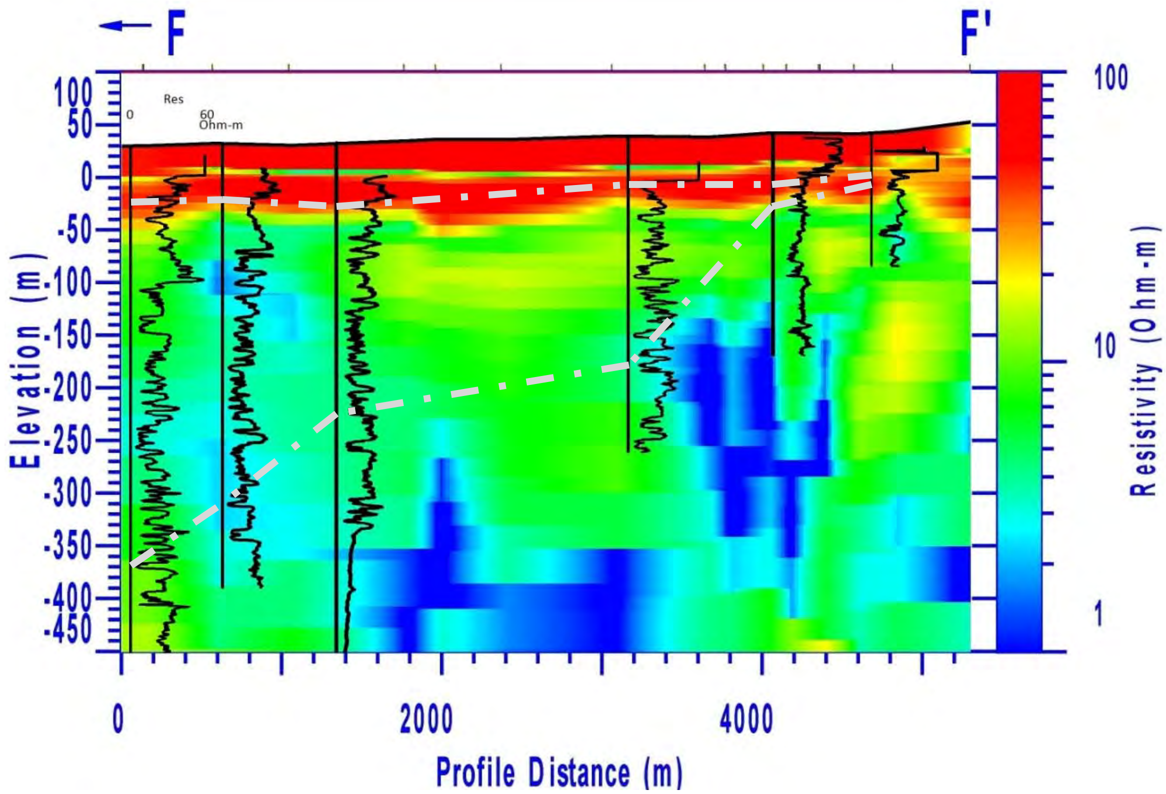

Figure 5.1-1: Cross-section F-F' (note only part of cross-section shown) with superimposed nearby borehole resistivity electrical logs.

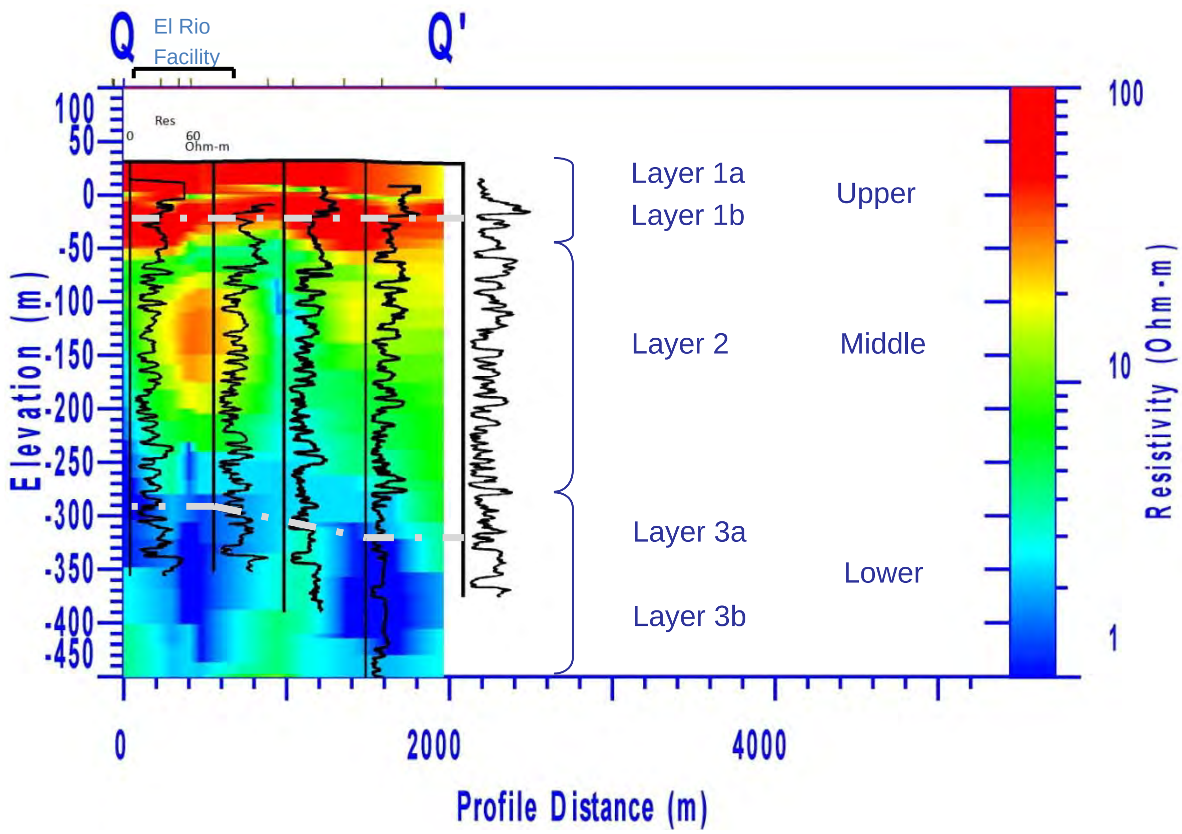

Figure 5.1-2: Cross-section Q-Q' with superimposed nearby borehole resistivity electrical logs.

The superimposed electrical logs in Figures 5.1-1 and 5.1-2 provide an example of the greater vertical detail obtained from the available electrical logs in the Forebay (compared to the TDEM cross-sections). Electrical logs provide a high level of vertical detail of the geologic formation material within a few feet laterally of the borehole wall, but may not always be representative of the geologic formation that is greater than a few feet away. The grey dashed lines in Figure 5.1-1 and 5.1-2 are explained in the following section.

5.2 GEOELECTRIC LAYERS DELINEATION

The pronounced resistivity patterns (geoelectric layers) labeled in Figure 5.1-2 can be roughly grouped into three layers (Layers 1-3 in Figure 5.1-2). This grouping does not hold true for all of the soundings, especially across the Forebay boundary, but it is useful for the purpose of general interpretation of the data. Figure 5.1-2 employs the 1-50 Ohm-m color ramp but these same general layers can also be seen with the 0.001-50 Ohm-m color ramp (with less color contrast).

The warm-colored upper geoelectric layer (Layer 1) in Figure 5.1-2 is continuous throughout the Forebay. It ranges in thickness from approximately 200 to 280 feet (approximately 61 to 85m). There is a thin conductive, continuous layer that roughly bisects this upper geoelectric layer, resulting in the interpreted delineation of resistive geoelectric Layers 1a and 1b. This thin conductive zone does not correlate with any recognized aquifer boundary (it is within the Oxnard Aquifer).

The upper grey dashed line in Figures 5.1-1 and 5.1-2 approximates the boundary between the bottom of the Oxnard aquifer and the top of the Mugu aquifer as identified from the electrical logs superimposed on cross-sections F-F' and Q-Q'. Geoelectric Layer 1, although protruding down into the Upper Mugu aquifer, roughly corresponds to this boundary.

The intermediate colored (yellow and green) geoelectric Layer 2 identified in Figure 5.1-2 is interpreted to roughly correspond to the Lower Mugu and Upper Hueneme aquifers. This geoelectric layer is approximately 800 feet (244m) thick in the middle of the Forebay and nearly disappears as the unit pinches out near South Mountain (Figure 4.2-1) in cross-section B-B'. Geoelectric Layer 2 contains several noticeable anomalies (blobs). The warm-colored anomalies are interpreted as aquifer material (coarse-grained) and the cool colored-anomalies are interpreted as silts and clays (fine-grained deposits).

Geoelectric Layer 3 in interpreted to correspond with the Lower Hueneme and Fox Canyon aquifers, and the Santa Barbara Formation, which is often considered to be the deepest local unit containing fresh water. Layer 3 can be divided into two sub-layers. Layer 3a is a highly-conductive geoelectric layer resting on top of the less-conductive (comparatively more resistive) Layer 3b (blue and green in color respectively in Figure 5.1-2).

The lower grey dashed line in Figure 5.1-1 and 5.1-2 approximates the boundary between the bottom of the Hueneme aquifer and the top of the Fox Canyon aquifer identified from the electrical logs superimposed on cross-sections F-F' and Q-Q'. As has been stated earlier, the Lower

Hueneme and Fox Canyon aquifers both appear to be relatively conductive and cannot be distinguished from each other with the surface geophysics method employed here. The boundary between Geoelectric Layer 2 and Layer 3 roughly corresponds to the boundary between the Upper Hueneme and Lower Hueneme aquifer.

5.3 INTERPRETATION OF LOW RESISTIVITY ZONES

As stated in section 4.2 of this report, the Lower Hueneme and Fox Canyon aquifers (Layer 3) have similar resistivity values to the clay lenses present within the study area. Clay lenses appear to be discontinuous and appear as anomalies (blobs) within the dataset. The Lower Hueneme and Fox Canyon aquifers appear as a somewhat continuous geoelectric layer (Layer 3).

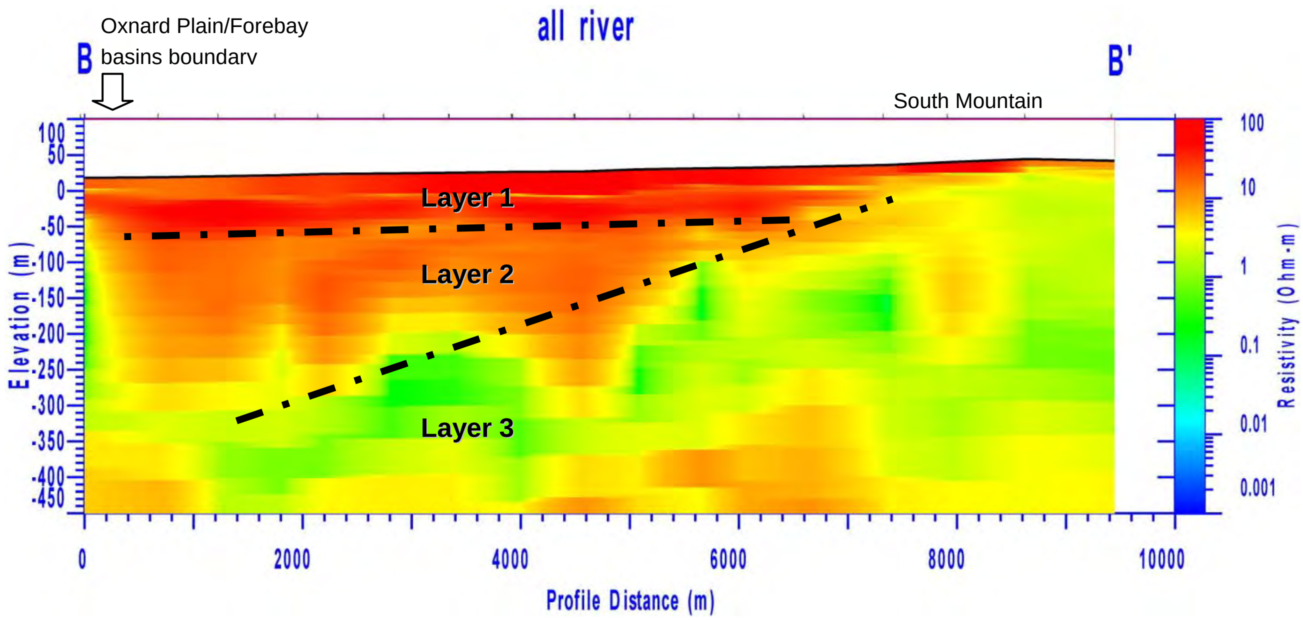

Figure 5.3-1: Cross-section B-B' (with annotation).

Cross-section B-B' (Figure 5.3-1 and Appendix D) correlates the 17 soundings collected in the Santa Clara River flood plain. The section runs southwest from across the Forebay/Oxnard Plan basin boundary northeast to a location just downstream of the Freeman Diversion (Figure 3.3-1). The Fox Canyon aquifer is interpreted to be uplifted to near the ground surface in the northeast part of the Forebay, and the Mugu and Hueneme aquifers are thought to have been eroded away and pinch out in this area (Turner, 1975). The lower black dashed line in Figure 5.3-1 generally illustrates the upward slope of geoelectric Layer 3 in the direction of South Mountain.

There is an anomalous low-resistivity zone located beneath United Water's western-most groundwater recharge pond (#10) at the El Rio Facility (see Figure 1.2-3), as shown in cross-section R-R' in Appendix D. There is a destroyed 1783 foot deep production well (02N22W23K04S El Rio #9) located on the bank of the eastern corner of the pond. The drillers report and electrical log from this well suggests the low-resistivity layer is not vertically continuous but rather is interfingered with zones of higher resistivity.

United Water's Ferro property (former gravel mining pit intended for future use as a recharge basin) northwest of the El Rio Facility (adjacent to the Santa Clara River flood plain) is thought to have a clay layer from 150 to 340 feet of depth beneath the southwest portion of the basin, based on the driller's log from an 800-foot deep well located on the artificial southeastern terrace of the property. This low-resistivity zone was not identified by this surface geophysical study. The electrical log from with this well suggests the low-resistivity layer is not vertically continuous but rather is interfingered with zones of higher resistivity that possibly can be interpreted to be the Mugu and Upper Hueneme aquifers.

5.4 INTERPRETATION OF ANOMALOUS HIGH RESISTIVITY ZONES

There are high-resistivity anomalies within geoelectric Layer 2 underlying several of United Water's properties (see Figure 1.3-3). Cross-sections E-E' and Q-Q' (Appendix D and Figure 5.1-2) show a high-resistivity anomaly at United Water's El Rio Facility. From the data, the lateral extent of this anomaly covers most of the El Rio Facility (except for the low-resistivity zone associated with percolation pond #10) and extends into the southwest portion of the private agricultural land adjacent to the northeast boundary of the El Rio Facility. The data affirms that this facility is well situated for managed aquifer recharge.

Soundings from United Water's Noble basin and the Rose basin (not currently plumbed to receive recharge water) show a high-resistivity anomaly (cross-section L-L'). This cross-section runs northwest from Noble southeast through Rose and terminates across the Forebay/Oxnard Plain basin boundary. The anomaly extends laterally to encompass most of the Noble and Rose properties, except for the northeastern part of the Rose basin near Highway 118 (observed in cross-section K-K').

There is a prominent high-resistivity zone underlying private agricultural land adjacent to the southeast boundary United Water's Saticoy Facility (northeast of Highway 118), observed in cross-sections G-G' and I-I'. The anomaly is located just across the Forebay basin boundary and located in the mapped extent of the confined Oxnard Plain basin. It may appear to extend further laterally in cross-section than it really does due to the sparseness of soundings in this area. Alternatively, the anomaly may be the result of unknown interferences (one sounding in this area could not be modeled due to interference).

5.5 OXNARD FOREBAY BOUNDARY

The Oxnard Forebay boundary (Figure 3.3-1) is typically mapped as the axis of the Montalvo Anticline/Oak Ridge fault zone, which distinguishes the Forebay from the Mound and Santa Paula groundwater basins (United, 2012b). The boundary between the Forebay and Oxnard Plain is mapped based on the presence of relatively continuous aquitards separating the UAS and LAS in the Oxnard Plain basin and the absence or discontinuity of these aquitards in Oxnard Forebay basin. The eastern boundary of the Forebay is formed by the uplifted South Mountain.

5.5.1 Forebay/Mound Basin Boundary

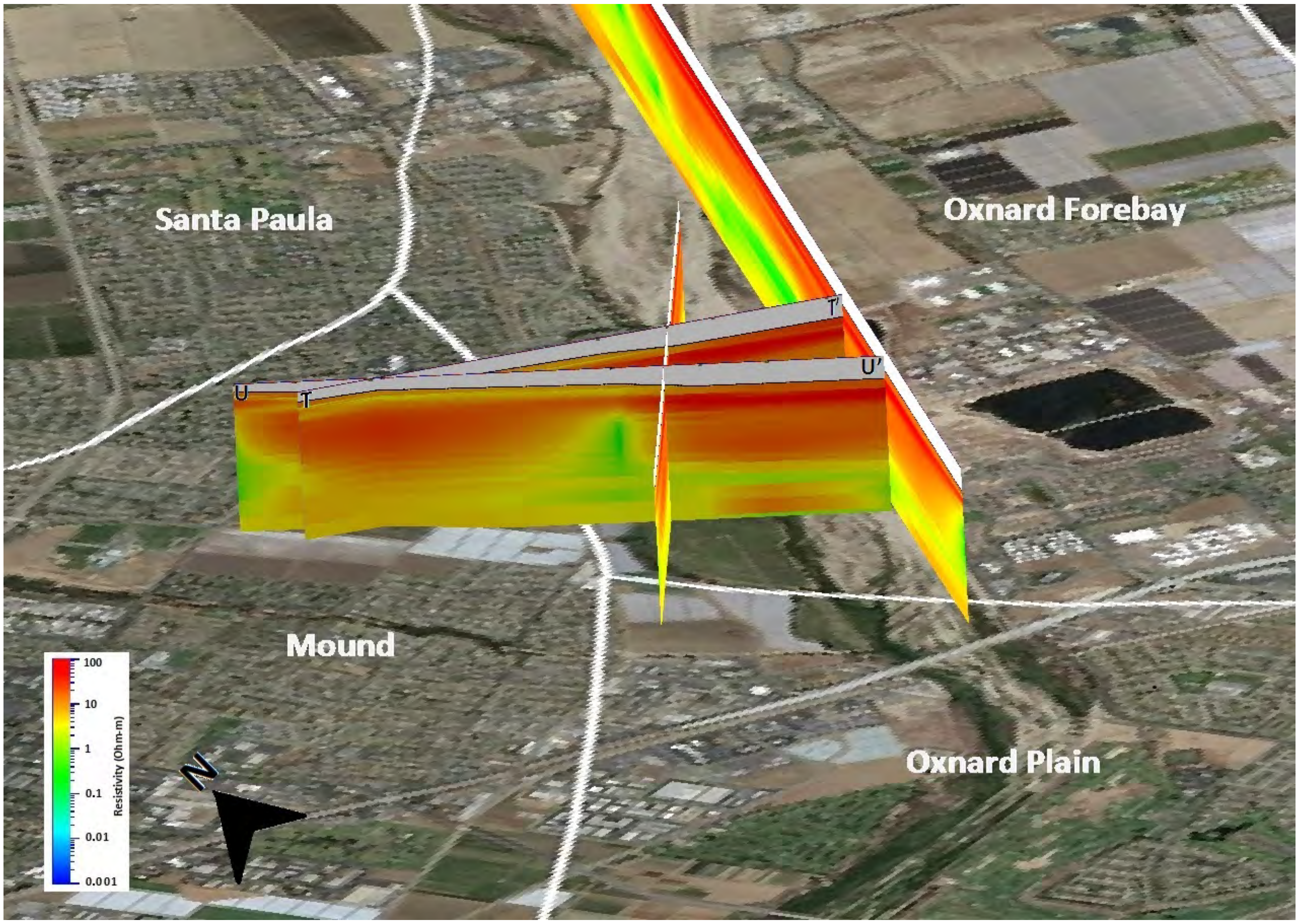

Figure 5.5.1-1: Fence diagram of cross-section T-T' and U-U' (0.001 -50 Ohm-m color ramp) across Mound Oxnard Forebay basins boundary looking obliquely northeast.

Figure 5.5.1-1 shows fence diagrams of cross-section T-T' and U-U' that cross each other and run roughly northwest to southeast across the boundary between the Mound and Forebay basins. Cross-section T-T' and U-U' are very similar to each other. The land surface elevation seen in the cross-section decreases abruptly (Appendix D) on the Forebay side of the boundary to the southeast as the cross-section obliquely transverses a terrace. There is a zone of low conductivity that roughly aligns with the basin boundary and the terrace, suggesting different depositional environments for the deposits above the current Santa Clara River floodplain than those below and closer to the active channel or may be suggestive of faulting (see Section 5.6). Geoelectric Layer 1 is not present on the Mound basin side of the boundary. Geoelectric Layer 1 is also absent across the Forebay-Oxnard Plain Boundary in cross-sections A-A' and B-B'.

5.5.2 Forebay-Oxnard Plain Boundary

Figures 4.2-1 and 4.2-2 display the 21 cross-sections as fence diagrams. Cross-Sections A-A', B-B' (Figure 5.3-1), and F-F' (partially blanked due to sparse data) traverse the southwest Forebay/Oxnard Plain basins boundary (Figure 3.3-1). There is an exceptionally thick conductive zone present on the Oxnard Plain side of the boundary that is not present, or is discontinuous, on the Forebay side of the boundary. The conductive zone is interpreted to be an interface between different geologic depositional environments across the Forebay/Oxnard Plain basins boundary. This thick conductive zone does not directly correspond to the actual thickness of an aquitard detectable in electrical logs in the vicinity. Also, the poor-quality semi-perched zone water generally found in the Oxnard Plain in this area is likely increasing the conductivity of the shallow sediments, which may influence the resistivity data obtained below this zone.

Cross-section K-K' extends from the southwest side of Highway 118 and runs roughly parallel to the highway crossing the Forebay/Oxnard Plain basins boundary. The upper grey dashed line in Figure 5.5.2-1 approximates the boundary between the bottom of the Oxnard aquifer and the top of the Mugu aquifer, and the lower grey dashed line approximates the vertical boundary between the bottom of the Hueneme aquifer and the top of the Fox Canyon aquifer, as identified from the electrical logs superimposed on cross-sections K-K' in the figure. The electrical logs correlated (in cross-section) in Figure 5.5.2-1 are located on the northeast side of Highway 118. The furthest any of the electrical logs are laterally off the cross-section K-K' line is 600 feet.

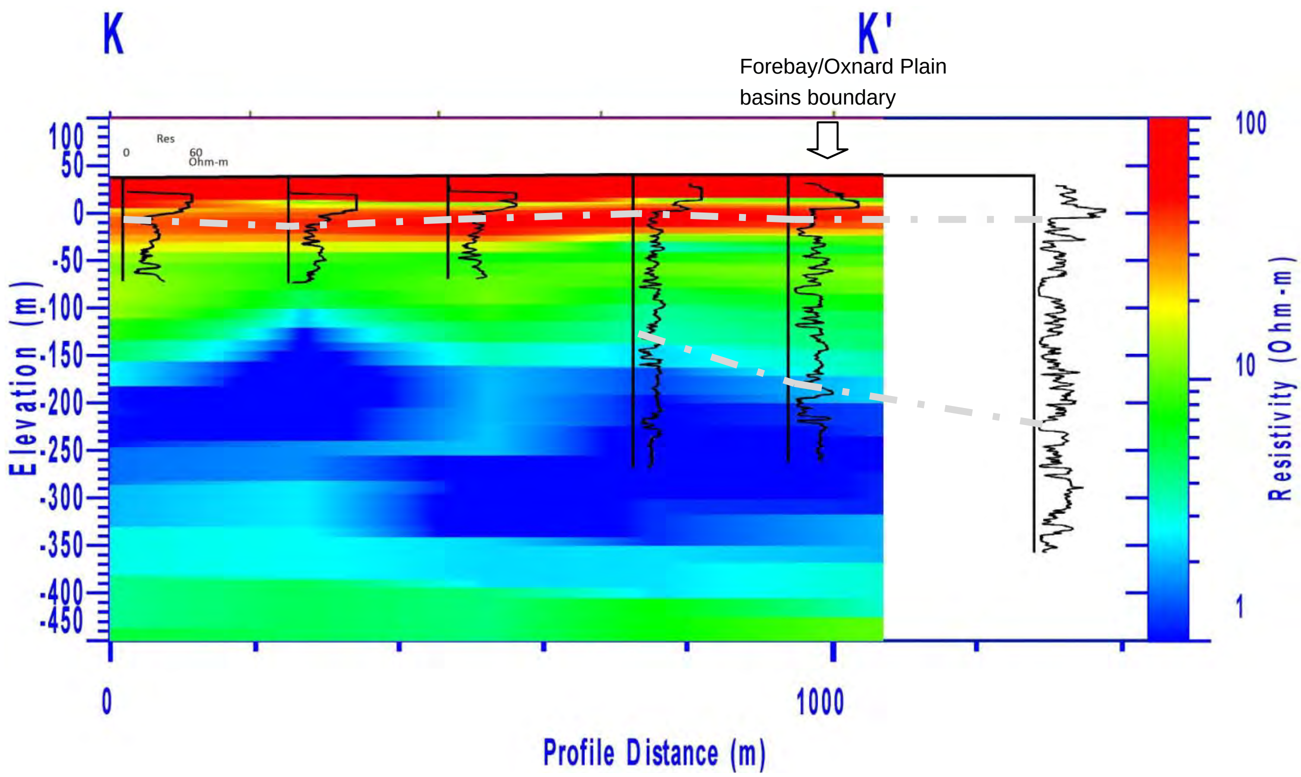

Figure 5.5.2-1: Cross-section K-K' (note horizontal scale) with superimposed nearby borehole resistivity electrical logs.

Cross-section K-K' which crosses the southeast Forebay/Oxnard Plain basin boundary shows geoelectric Layer 3 becoming deeper (or possibly offset) as the cross-section transverses the Forebay basin boundary into the mapped Oxnard Plain basin. This is seen in most of the northwest-to-southeast trending cross-sections.

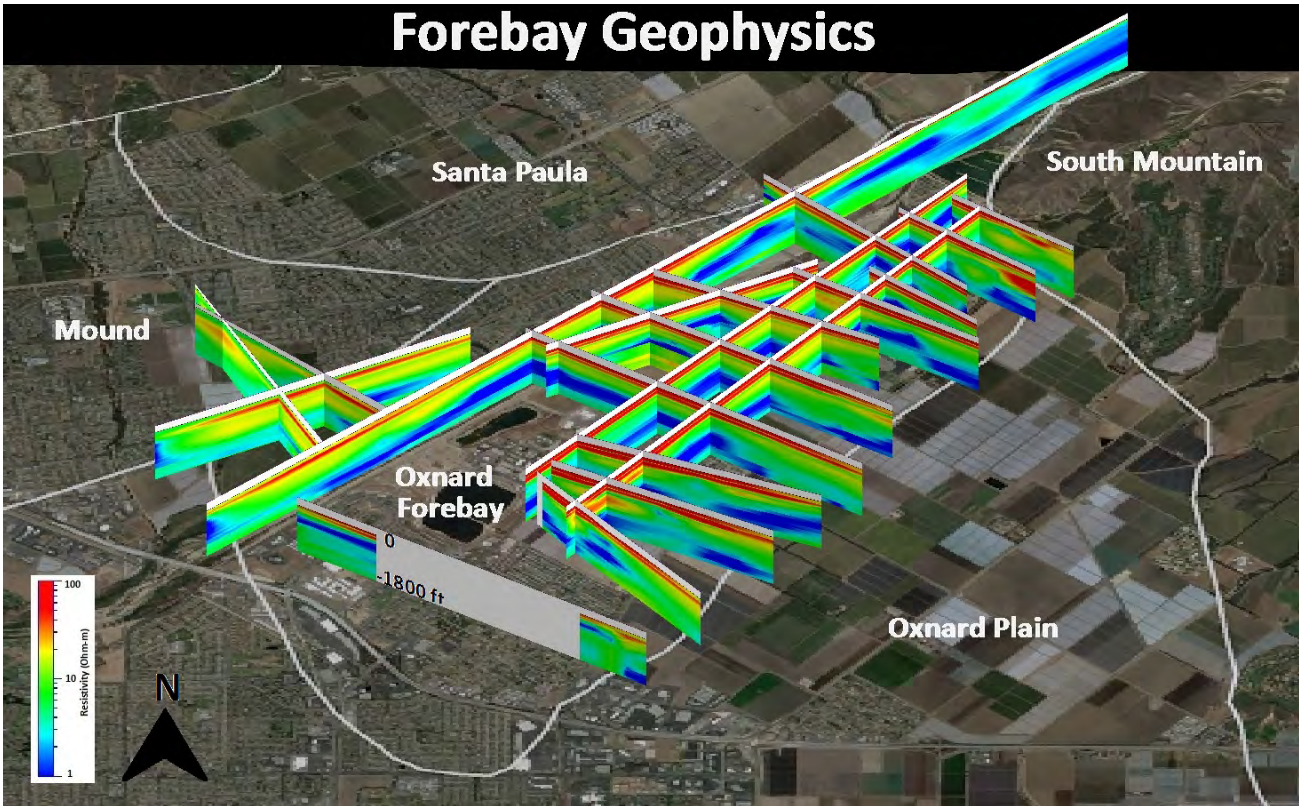

Figure 5.5.2-2: Fence Diagram of cross-Sections (1 -50 Ohm-m color ramp) looking obliquely north.

Figure 5.5.2-2 shows cross-sections with sections F-F' and G-G' stripped away so that the cross-sections that traverse the southeast Forebay/Oxnard Plain basins boundary can be viewed. Geoelectric Layer 3 appears to change (or possibly offset) across this boundary, but the presence of an aquitard separating the upper and lower aquifer systems cannot be determined from these data alone. The TDEM data are suggestive of faulting in this area. Several of the northwest-southeast cross-sections (e.g., H-H', I-I', J-J', L-L', M-M', N-N') imply offset in the low resistivity intervals in geoelectric Layer 3, but the offset is not so apparent in geoelectric Layer 2, and absent in geoelectric Layer 1.

5.6 FAULTING

Figure 5.6-1 is a fault map showing the Forebay and surrounding basins.

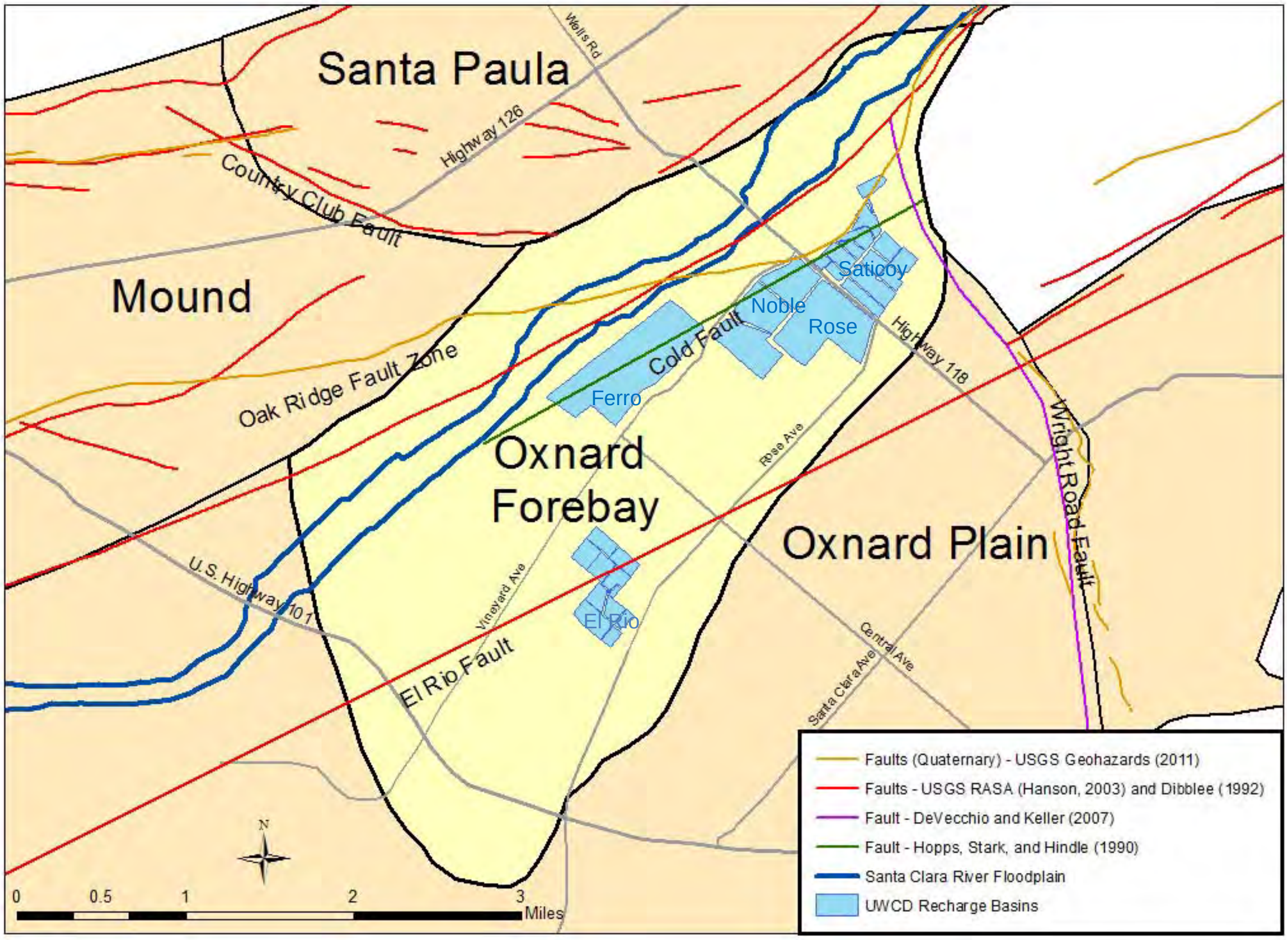

Figure 5.6-1: Oxnard Forebay Fault map.

Northwest-southeast trending cross-sections P-P’ and Q-Q’ that cross the Forebay/Oxnard Plain basin boundary suggest possible faulting near Central Avenue and Rose Avenue. The mapped trace of the El Rio Fault (Figure 5.6-1) is coincident with this possible faulting in this area suggested from the data.

Southwest-northeast trending cross-sections such as F-F’ and G-G’ cross the mapped trace of the Wright Road fault (Figure 5.6-1) in the northeastern portion of the Forebay. Cross-section F-F’ suggests offset across this fault.

The Oak Ridge fault zone runs sub-parallel to the Montalvo anticline which is presently used as the Forebay/Mound basin boundary. Different investigators have mapped the Oak Ride Fault following different traces with differing degrees of offset (United, 2012b). Cross-sections T-T’ and U-U’ transverse the Oak Ridge fault zone and the Montalvo anticline. Facies changes across the Forebay/Mound basin boundary were noted in section 5.5-1, suggestive of changes in depositional environments near the present day Santa Clara River floodplain. While, distinct offsets due to faulting were not apparent from the data, the presence of the vertically oriented lower resistivity zone (at about 1000m along T-T’ and about 1200m along U-U’) is highly suggestive of faulting. The coincident location of these anomalies with mapped locations of the Oak Ridge fault zone supports this interpretation.

6 FINDINGS AND CONCLUSIONS

Based on the results of this study, United Water offers the following conclusions:

- The interpretation of data collected for the TDEM Oxnard Forebay surface geophysical survey generally conforms to prior publications of geologic conditions within the Forebay. Changes in resistivity were observed in cross-section across the Forebay basin boundary. Anomalous zones of high and low resistivity (indicating sands/gravels and silts/clays, respectively) were identified within and near United Water's recharge facilities that will aid in future recharge planning.

- The resistivity data from the Oxnard Forebay can be roughly divided into three geoelectric layers. This grouping does not hold true for all of the soundings, especially those near the Forebay boundary, but are useful for the purpose of general interpretation of the data. Geoelectric Layer 1 is continuous throughout the Forebay and ranges in thickness from approximately 200 to 280 feet (approximately 61 to 85m). Although it protrudes down into the Upper Mugu aquifer, it roughly corresponds to the Oxnard aquifer.

- Geoelectric Layer 2 is interpreted to roughly correspond to the Lower Mugu and Upper Hueneme aquifers. This geoelectric layer is approximately 800 feet (244m) thick in the middle of the Forebay and nearly disappears near South Mountain. Layer 2 contains several noticeable anomalies. The high-resistivity anomalies are interpreted as aquifer material (areas of relatively low porosity and high permeability) and the low-resistivity anomalies are interpreted as silts and clays (areas of high porosity and low permeability).

- Geoelectric Layer 3 is fairly continuous, and likely corresponds with the Lower Hueneme and Fox Canyon aquifers, and the Santa Barbara Formation. The Lower Hueneme and Fox Canyon aquifers both appear to be relatively conductive and cannot be distinguished from each other with the surface geophysics method employed here.

- The large transmitter loop laid on the ground surface required to obtain the desired depth of investigation for this project produces notable lateral influence (averaging) of the modeled geoelectric layers. The method is good for showing the degree of continuity of units, but not absolute depths of aquifer units.

- The modeled resistivity data collected for this project show that sediments within the Oxnard Forebay are notably conductive at depth. This is not surprising since the Lower Hueneme and Fox Canyon aquifers (San Pedro Formation) consist of more fined-grained marine sands, in contrast to the predominately coarse-grained terrestrial deposits (with intermixed marine deposits due to changes in sea level) of the Upper Hueneme, Mugu and Oxnard aquifers.

- Very low resistivities may correspond to the Lower Hueneme and Fox Canyon aquifers, but they may also correspond to discontinuous clay lenses (aquitards) that are present, at more shallow depths, at some locations in the Forebay. Clay lenses appear to be discontinuous and are shown as anomalies (blobs of low resistivity) within the dataset. The deeper Lower Hueneme and Fox Canyon aquifers appear as a somewhat continuous geoelectric layer. Deeper clay lenses, if present, may not be distinguished from the Lower Hueneme and Fox Canyon aquifers (Layer 3) using the TDEM surface geophysical technique in the Forebay.

- Several of the northwest-southeast cross-sections imply offset in the low resistivity intervals in geoelectric Layer 3, but the offset is not so apparent in geoelectric Layer 2, and absent in geoelectric Layer 1.

- Changes in the geoelectric layers are apparent in the cross-sections that transverse both the mapped Forebay/Mound and Forebay Oxnard Plain basin boundaries. These facies changes are interpreted to be changes in depositional/erosional environments and/or suspected faulting.

7 RECOMMENDATIONS

United Water suggests the implementation of a similar geophysical investigation on the agricultural land on either side of the Santa Paula/Mound basins boundary, and further investigation on the Mound side of the Forebay/Mound basins boundary. This would be useful data, especially considering the continued development of agricultural land for commercial and municipal uses that significantly complicates geophysical investigations.

United Water also recommends comparisons of supposed faulting identified in the TDEM data with structural isopleths on selected aquifers (e.g. Top of Fox Canyon Aquifer) to aid in quantifying offset amounts.

8 REFERENCES

California Department of Water Resources, 1954, Seawater intrusion: Oxnard Plain of Ventura County: Bulletin No. 63-1, 59p.

Daniel B. Stephens & Associates, 2008, Final Draft Report: Oxnard Forebay Deep Pit Recharge Study; prepared for United Water Conservation District; report dated May 30, 2008.

DeVecchio, D.E., and Keller, E.A., 2007, Earthquake Hazard of the Camarillo Fold Belt: An Analysis of the Unstudied Fold Belt in Southern California “Hot Zone”. Final Report USGS/NEHRP, Award Number 07HQGR0040.

Dibblee, Thomas W. Jr., edited by Helmut E. Ehrenspeck. 1992a, Geologic map of the Santa Paula quadrangle: Ventura County, California: Santa Barbara, Calif., Dibblee Geological Foundation, Dibblee Foundation Map series, DF-41, scale 1:24,000.

Dibblee, Thomas W. Jr., edited by Helmut E. Ehrenspeck. 1992b, Geologic map of the Saticoy quadrangle: Ventura County, California: Santa Barbara, Calif., Dibblee Geological Foundation, Dibblee Foundation Map series, DF-42, scale 1:24,000.

Fox Canyon Groundwater Management Agency, 2007, 2007 Update to the Fox Canyon Groundwater Management Agency Groundwater Management Plan dated May 2007.

Hanson, R.T., Martin, P. and Koczot, K.M., 2003, Simulation of Ground-Water/Surface-Water Flow in the Santa Clara–Calleguas Ground-Water Basin, Ventura County, California, U.S. Geological Survey, Water-Resources Investigations Report 02-4136, 32, 43, 157p.

Hopps, T.E., H.E. Stark, and R.J. Hindle, 1990, Website Titled: Ventura Basin Study Group Maps & Cross Sections, http://projects.eri.ucsb.edu/hopps/

Mukae, M., and Turner, J., 1975, Ventura County Water Resources Management Study, Geologic Formations, Structures and History in the Santa Clara-Calleguas Area, in Compilation of Technical Records for the Ventura County Cooperative Investigation: California Department of Water Resources, 28p.

Sylvester, A.G., and Brown, G.C., 1988, Santa Barbara and Ventura Basins; Tectonics, Structure, Sedimentation, Oilfields along an East-West Transect: Coast Geological Society Guidebook 64, Ventura, California, 167 p.

Turner, J.M., 1975, Aquifer delineation in the Oxnard-Calleguas area, Ventura County, in Compilation of Technical Information Records for the Ventura County Cooperative Investigation: California Department of Water Resources, 45p.

United Water Conservation District, 2010, Oxnard Plain Time Domain Electromagnetic Study for Saline Intrusion, United Water Conservation District Open-File Report 2010-003.

United Water Conservation District, 2012a, Groundwater and Surface Water Conditions Report - 2011, United Water Conservation District Open-File Report 2012-02.

United Water Conservation District, 2012b, Hydrogeologic Assessment of the Mound Basin, United Water Conservation District Open-File Report 2012-001, June 11, 2012 update.

United States Geological Survey, 2011, Website Titled: Quaternary Fault and Fold Database of the United States, http://earthquake.usgs.gov/hazards/qfaults/

Yeats, R.S., Clark, M.N., Keller, E.A., and Rockwell, T.K. 1981, Active Fault Hazard in Southern California: Ground Rupture Versus Seismic Shaking: Geol. Soc. America Bull, Part 1, v. 92, 189-196p.

APPENDIX A – FURTHER EXPLANATION OF METHODOLOGY AND DATA INTERPRETATION

The first panel in Figure A-1 shows the waveform of the transmitter current and primary magnetic field generated by the transmitter. The second panel shows the induced electromotive force (primary field impulse) which creates the secondary currents (referred to as eddy currents) immediately below the transmitter loop. These eddy currents approximate a mirror image of the transmitter loop. As the initial near surface eddy currents decay, they in turn induce eddy currents at greater depths. The third panel in Figure A-1 shows the waveform of the secondary magnetic field generated by the series of eddy currents induced in the ground. The magnitude and rate of decay of those secondary currents depend upon the conductivity of the medium (i.e. electrical resistivity of the soil) and the geometry of the subsurface. The TDEM receiver measures the decay of the magnetic fields (secondary magnetic fields) created by those secondary currents.

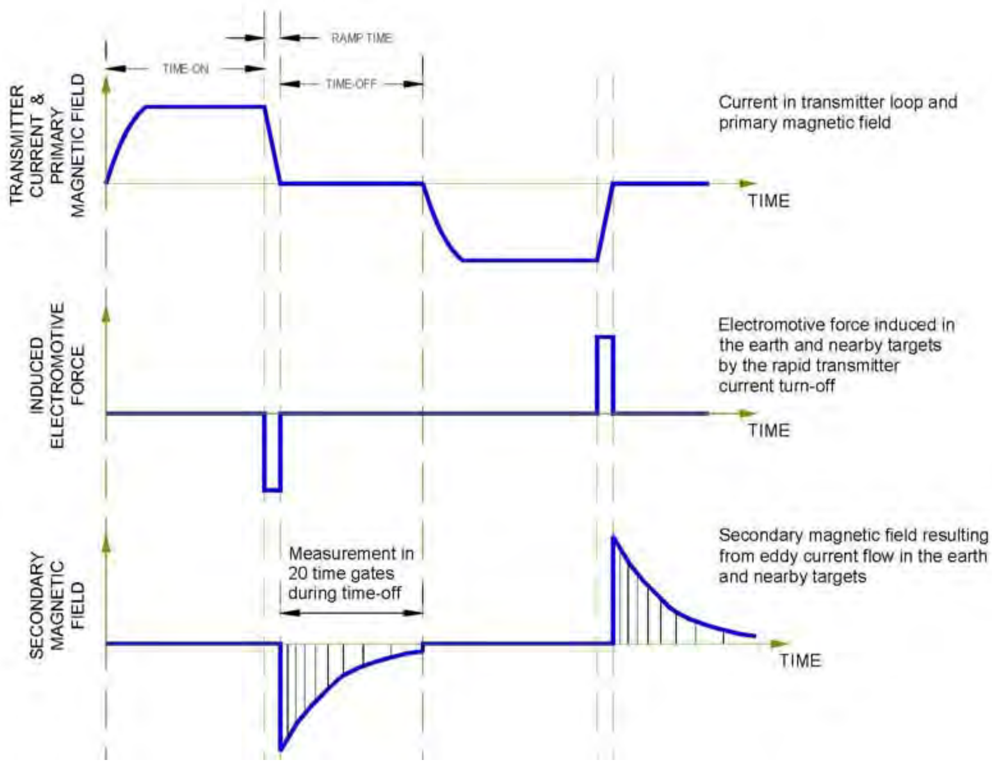

Figure A-1: TDEM Waveforms.

In TDEM techniques the inducing signal is a sharp pulse, or transient signal. The induced currents in the earth (eddy currents) are initially concentrated immediately below the transmitter loop. This is depicted schematically in Figure A-2. Those currents will diffuse down and away from the transmitter with time. This is also depicted in Figure A-2. An analogy with smoke rings is often used to describe the behavior of the currents in the ground. Initially strong currents form in the ground adjacent to the transmitting loop. The “smoke ring” then expands, weakens, and travels down through the earth. The rate of diffusion depends upon the earth resistivity. In resistive media the current will diffuse very rapidly. In conductive media (low resistivity) the currents will diffuse more slowly. A conductive layer at depth may “trap” currents in that layer, while currents elsewhere decay more rapidly.

Measurements of the secondary magnetic field are typically made in the time range from 10 micro-seconds to 10 milli-seconds following the “turn-off” of the primary field. Measurements are made in 20 to 30 discrete “time gates” (or time intervals) following the primary inducing pulse. For deeper exploration in conductive areas, measurement times can extend up to one second. Because measurements are made while the transmitting current is turned off, more sensitive measurements of the secondary field can be made.

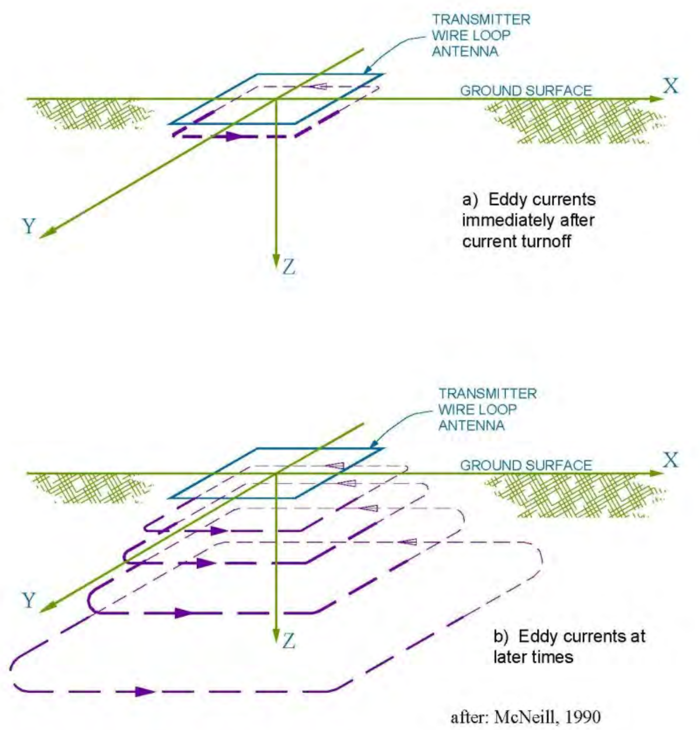

Figure A-2: TDEM Eddy Current Flow - a) early time and b) late time.

The measured decay values of the secondary magnetic field are used to generate values of apparent resistivity. Apparent resistivity is the resistivity of homogeneous and isotropic ground which would give the same voltage current relationship as measured. However, non-homogeneous and anisotropic media consist of different “true resistivities” which result in that measured value. Therefore, the data must be modeled to achieve a solution for resistivity structure and depth.

Interpretation procedures generally use forward and inverse modeling. A hypothetical layered earth model is generated and then the theoretical response for that model is calculated. The model is then refined until the calculated response matches the observed or measured field response. The model refinements can be made using an automated iterative process or “inversion modeling”. There are several conditions that will affect the sounding data (perched aquifer, vadose zone, complex geology, etc.).

Figure A-3 shows the decay of the secondary magnetic field. It decays over three decades during the course of the recording from 0.006 milli-seconds (ms) to 7 ms. The electrical potential induced in the receiver coil is proportional to dBZ/dt and is reported as “normalized voltage”, normalized to the receiver coil moment and transmitter current of 2.6 amperes (A).

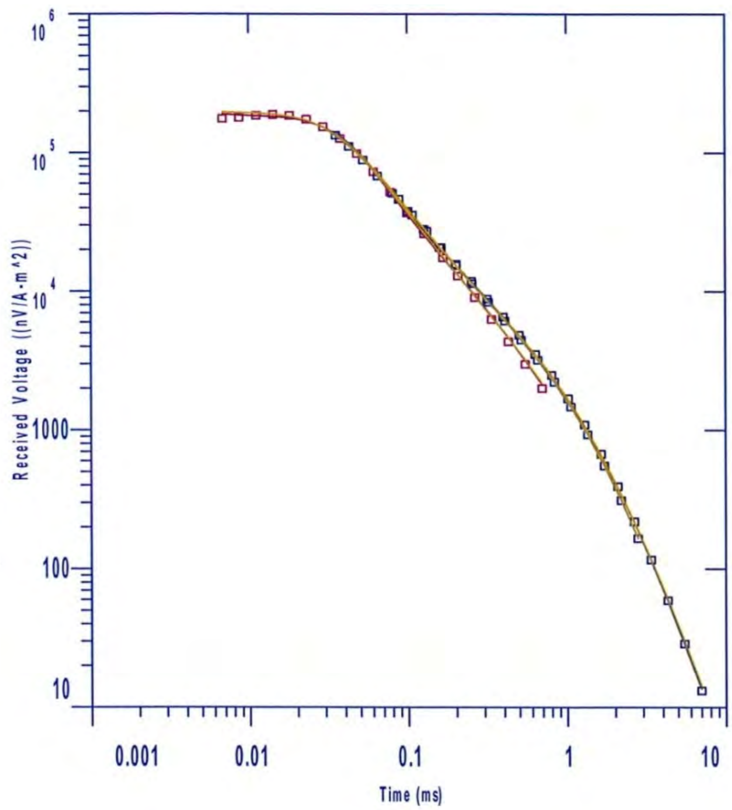

Figure A-3: TDEM Decay of Secondary Magnetic Field.

The right hand panel of Figure A-4 is a forward and inverse model refined using automated inverse modeling. The left hand panel shows a plot of the same data as Figure A-3 converted to “late stage” apparent resistivity. The apparent resistivity curve gives a somewhat more intuitive feel for the geoelectric section. However, as explained in the following paragraph, TDEM apparent resistivity is not a true apparent resistivity as observed in DC resistivity of frequency domain techniques.

In concept, the “apparent resistivity” is the resistivity of a uniform earth which will produce the observed instrument response. However, the observed TDEM field is a non-linear function of time and earth resistivity. In fact, the instrument response is not a single valued function of the resistivity over the time range of the instrument.

For most TDEM soundings a “late stage” apparent resistivity is used, which is a “true” apparent resistivity only for a later stage of the decay curve. It is generally attempted to make measurements in this time range but often the first portion of the curve is not truly in late stage, hence the numerical values may not accurately indicate the earth resistivity for the first few time gates. This discussed in Appendix B.

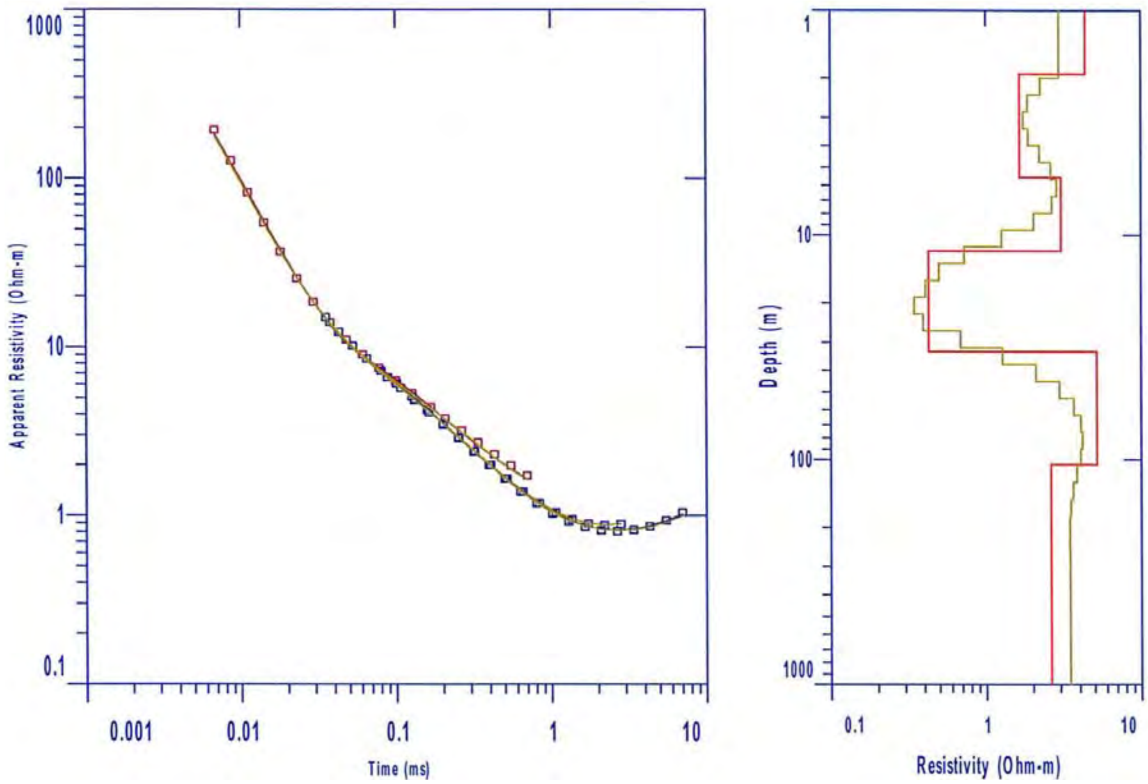

Figure A-4: TDEM Sounding in Late Stage and Model.

The green line in right hand panel of Figure A-5 shows the way in which the data was modeled for this project with the forward model (red line in right hand panel) approach superimposed on top of it. The model shown is the smooth model automatically generated using IX1D 3.51 modeling software. The modeled resistivity is considered to be the “true resistivity” which is used to calculate the given response in attempt to match the observed or field data (small squares on the left hand panel are apparent resistivity or measured data). The different resistivity values represent varying earth materials with inherent true resistivities (sand versus clay versus silt versus rock, etc.). The true resistivity is dependent upon many factors some of which include: grain size, composition, water content, consolidation/lithification, weathering, etc..

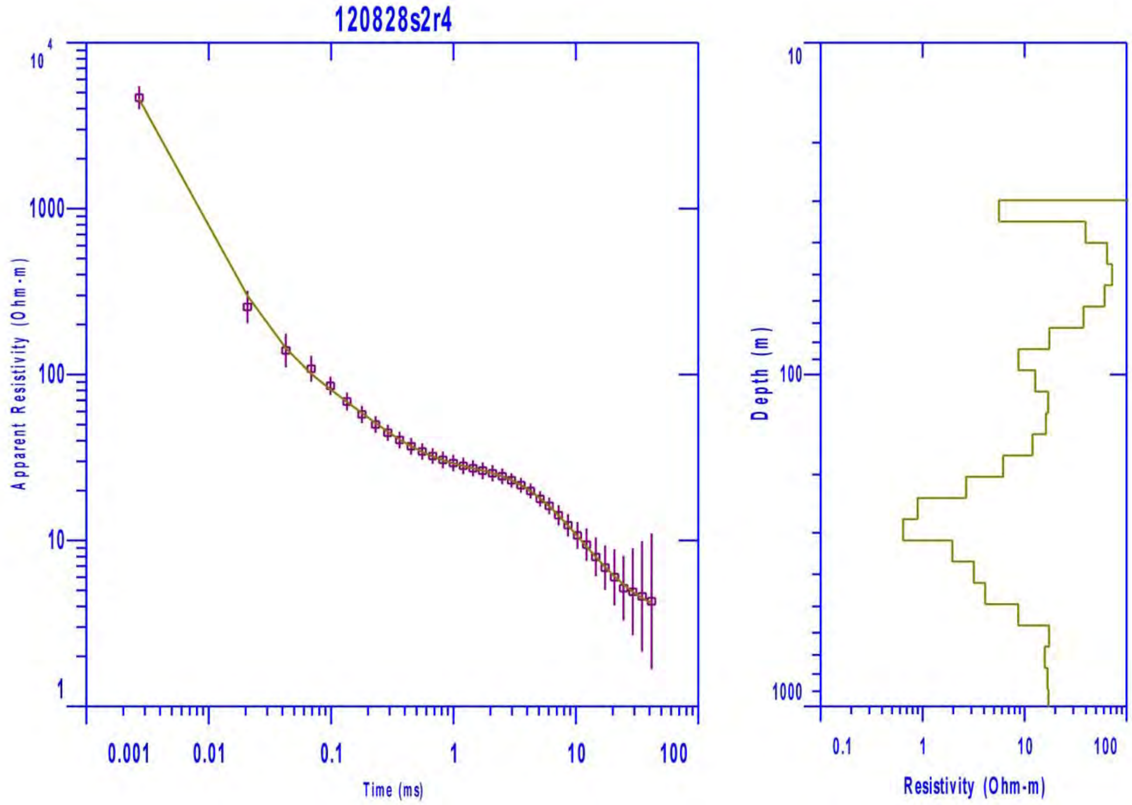

Figure A-5: TDEM Sounding and Model for Sounding 120828s2r4.

APPENDIX B – APPARENT RESISTIVITY IN TDEM SOUNDINGS

Figure B-1 shows, schematically, a linear plot of a typical TDEM transient response from the earth. The vertical axis is instrument response (output voltage) in nV/m^2. It is useful to examine this response when plotted logarithmically against the logarithm of time for a homogeneous earth (i.e. the resistivity does not vary with either lateral distance or depth). Such a plot is shown in Figure B-2. It suggests that the response can be divided into an early stage (where the response is constant with time), an intermediate stage (response continually varying with time), and a late stage (response is now a straight line on the log-log plot). The response is generally a mathematically complex function of conductivity and time; however, during the late stage, the mathematics simplifies considerably, and it can be shown that during this time the response varies quite simply with time and conductivity as

$$e(t) = \frac{k_1 M \sigma^{3/2}}{t^{5/2}}, \qquad (1)$$

$e(t)$ = output voltage from a single-turn receiver coil of area 1 m^2
k_1 = a constant
M = product of Tx current x area (a-m^2)
σ = terrain conductivity (siemens/m = S/m = 1/Ωm)
t = time (s)

For conventional resistivity methods (DC resistivity) the measured voltage varies linearly with terrain resistivity. For TDEM, the measured voltage [e(t)] varies as $\sigma^{3/2}$, therefore, it is intrinsically more sensitive to small variations in the conductivity than conventional resistivity methods. Note that during the late stage, the measured voltage is decaying at the rate $t^{-5/2}$, which is very rapidly with time. Eventually the signal disappears into the system noise, and further measurement is impossible. This is the maximum depth of exploration for the particular system.

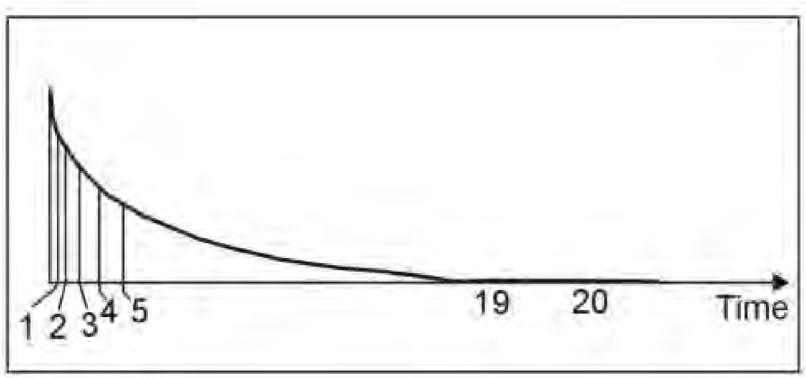

Figure B-1: Receiver time gate locations.

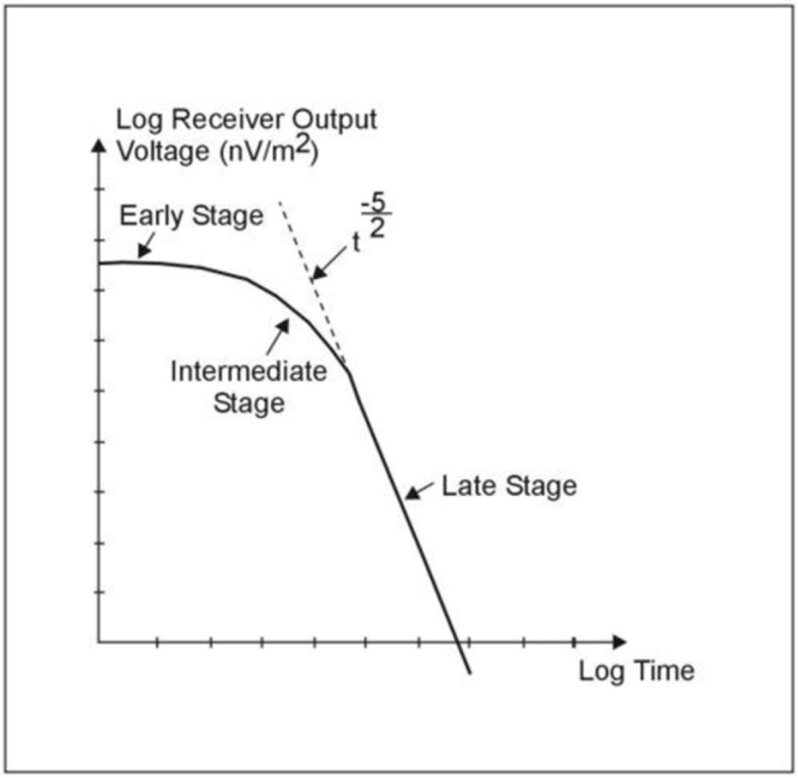

Figure B-2. Log plot-receiver output voltage versus time (one transient).

With conventional DC resistivity methods, for example the Wenner array, the measured voltage over a uniform earth can be shown to be

$$V(a) = \frac{\rho I}{2\pi a} \qquad (2a)$$

a = inter-electrode spacing (m)
ρ = terrain resistivity (Ω-m)
I = current into the outer electrodes
V(*a*) = voltage measured across the inner electrodes for the specific value of *a*

In order to obtain the resistivity of the ground, equation 2a is rearranged to give equation 2b:

$$\rho = 2\pi a \frac{V(a)}{I}, \qquad (2b)$$

If ground resistivity is homogeneous and isotropic (uniform half space), and the inter-electrode spacing (*a*) is increased, the measured voltage decreases directly with *a* so that the right-hand side of equation 2b stays constant, and the equation gives the true resistivity. Suppose now that the ground is horizontally layered (i.e., that the resistivity varies with depth). For example, it might consist of an upper layer of thickness *h* and resistivity ρ1, overlying a more resistive basement of resistivity (ρ2 > ρ1). This is called a two-layered earth. At very short inter-electrode spacing (*a*<<*h*), virtually no current penetrates into the more resistive basement, and resistivity calculation from equation 2b will give the value ρ1. As the inter-electrode spacing (a) is increased, the current

(I) is forced to flow to greater and greater depths. Suppose that, at large values of *a* ($a \gg h$), the effect of the near-surface material of resistivity ρ1 will be negligible, and resistivity calculated from equation 2b will give the value ρ2. At intermediate values of *a*, the resistivity given by equation 2b will lie somewhere between ρ1 and ρ2.

Equation 2b is, in the general case, used to define an apparent resistivity which is a function of a ($\rho_a(a)$). The variation of $\rho_a(a)$ with *a*

$$\rho_a(a) = 2\pi a \frac{V(a)}{I}, \tag{3}$$

is descriptive of the variation of resistivity with depth. The behavior of the apparent resistivity $\rho_a(a)$ for a Wenner array for the two-layered earth above is shown schematically in Figure B-3. With conventional resistivity sounding, to increase the depth of exploration, the inter-electrode spacing must be increased. In the case of TDEM soundings it was observed earlier that as time increases, the depth to the eddy current loops increases. This phenomenon is used to perform the sounding of resistivity with depth in TDEM. Thus, in analogy with equation 3, equation 1 can be inverted to read (since $\rho = 1/\sigma$)

$$\rho_a(t) = \frac{k_2 M^{2/3}}{e(t)^{2/3} t^{5/3}}. \tag{4}$$

Suppose once again that resistivity does not vary with depth (uniform half-space) and is of resistivity ρ1. For this case, a plot of $\rho_a(t)$ against time would be as shown in Figure B-4. Note that at late time the apparent resistivity $\rho_a(t)$ is equal to ρ1, but at early time $\rho_a(t)$ is much larger than ρ1. The reason for this is that the definition of apparent resistivity is based (as seen from Figure B-2) on the time behavior of the receiver coil output voltage. At earlier and intermediate time, Figure B-2 shows that the receiver voltage is too low (the dashed line indicates the voltage given by the late stage approximation) and thus, from equation 4, the apparent resistivity will be too high. For this reason, there will always be, as shown on Figure B-4, a "descending branch" at early time where the apparent resistivity is higher than the half-space resistivity (or, as will be seen later, is higher than the upper layer resistivity in a horizontally layered earth). This is not a problem, but it is an artifact of which we must be aware.

Suppose the earth is two-layered with upper layer resistivity ρ1 (thickness *h)* and basement resistivity ρ2 (>ρ1). At early time when the currents are entirely in the upper layer of resistivity ρ1 the decay curve will look like that of Figure B-2. However, later on the currents will lie in both layers, and at much later time, they will be located entirely in the basement (resistivity ρ2). Since ρ2>ρ1, equation 4 shows that the measured voltage will now be less than it should have been for the homogeneous half-space of resistivity ρ1 (as indicated in Figure B-5). The effect on the apparent resistivity curve is shown in Figure B-6a. Since at late times all the currents are in the basement, the apparent resistivity $\rho_a(t)$ becomes equal to ρ2, completely in analogy with Figure B-3 for conventional resistivity measurements. In the event that ρ2<ρ1, the inverse behavior is also as expected. At late times the measured voltage response, shown in Figure B-5, is greater than that from a homogeneous half-space of resistivity ρ1, and the apparent resistivity curve correspondingly becomes that of Figure B-6b, becoming equal to the new value of ρ2 at late time. Note that for the case of a (relatively) conductive basement, there is a region of intermediate time (shown as *t**), where the voltage response temporarily falls before continuing on to adopt the value appropriate to ρ2. This behavior, which is a characteristic of TDEM, is again not a problem, as long as it is recognized. The resultant influence of the anomalous behavior on the apparent resistivity is also shown on Figure B-6b at *t**.

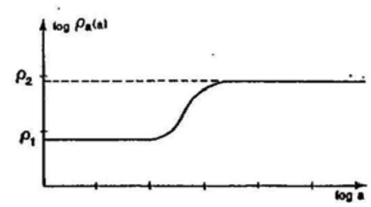

Figure B-3: Wenner array: apparent resistivity, two layer curve.

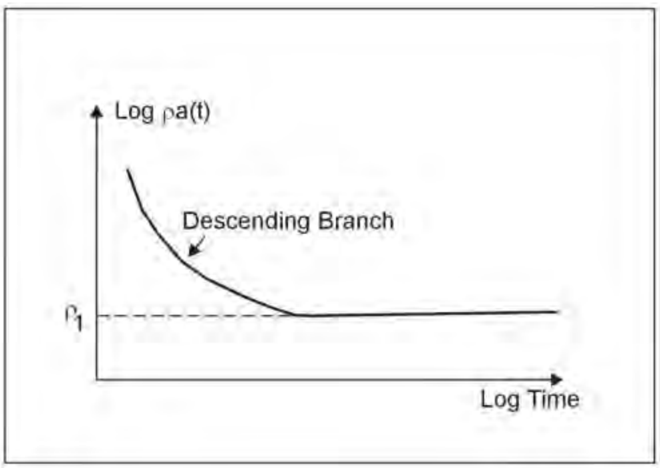

Figure B-4. Time Domain Electromagnetic (TDEM): apparent resistivity, homogeneous half space.

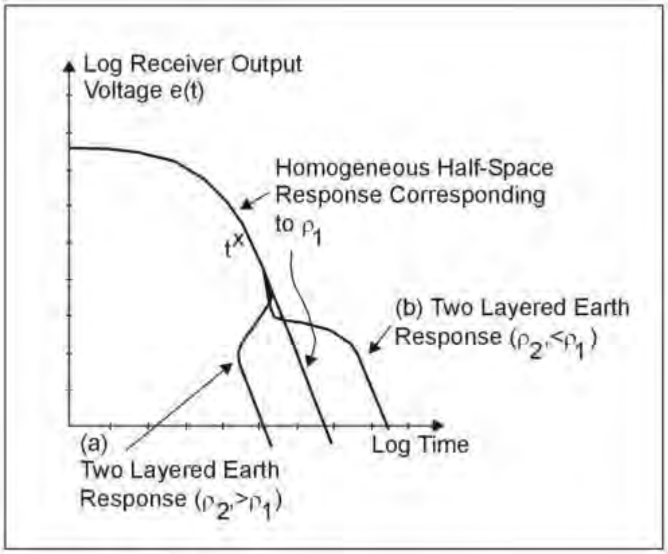

Figure B-5. Time Domain Electromagnetic (TDEM): receiver output voltage, two layer earth.

To summarize, except for the early-time descending branch and the intermediate-time anomalous region described above, the sounding behavior of TDEM is analogous to that of conventional DC resistivity if the passage of time is allowed to achieve the increasing depth of exploration rather than increasing inter-electrode spacing.

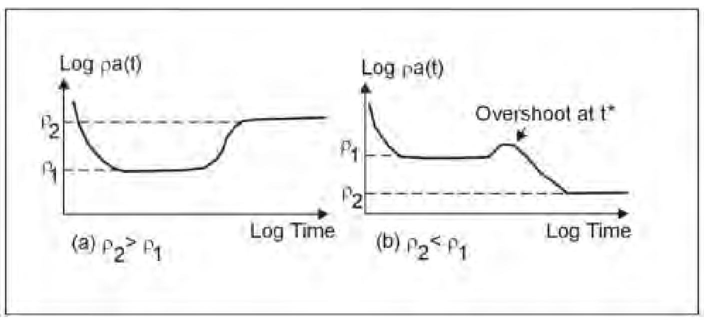

Figure B-6. Time Domain Electromagnetic (TDEM): apparent resistivity, two layered earth.

Curves of apparent resistivity such as Figure B-6 tend to disguise the fact, that at very late times, there is simply no signal, as is evident from Figure B-5. In fact, in the TDEM central loop sounding method, it is unusual to see, in practical data, the curve of apparent resistivity actually asymptote to the basement resistivity due to loss of measurable signal. Fortunately, both theoretically and in practice, the information about the behavior of the apparent resistivity curve at early time and in the transition region is generally sufficient to allow the interpretation to determine relatively accurately the resistivity of the basement without use of the full resistivity-sounding curve.

APPENDIX C – OXNARD FOREBAY 2011 GROUNDWATER ELEVATIONS CONTOURS AND AVAILABLE GROUNDWATER STORAGE

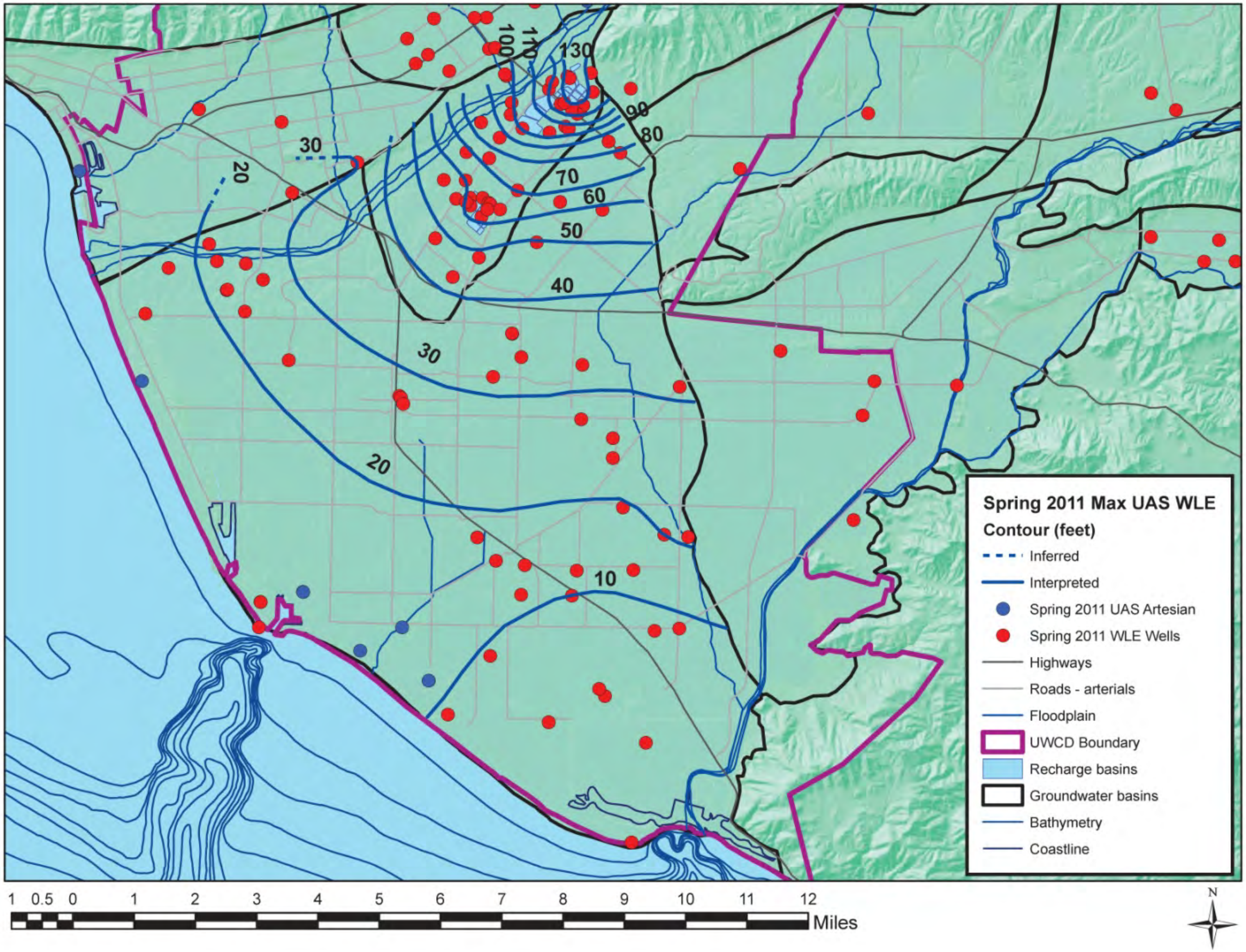

Figure C-1. Oxnard Forebay-Oxnard Plain Upper Aquifer System (UAS) groundwater elevations for spring 2011.

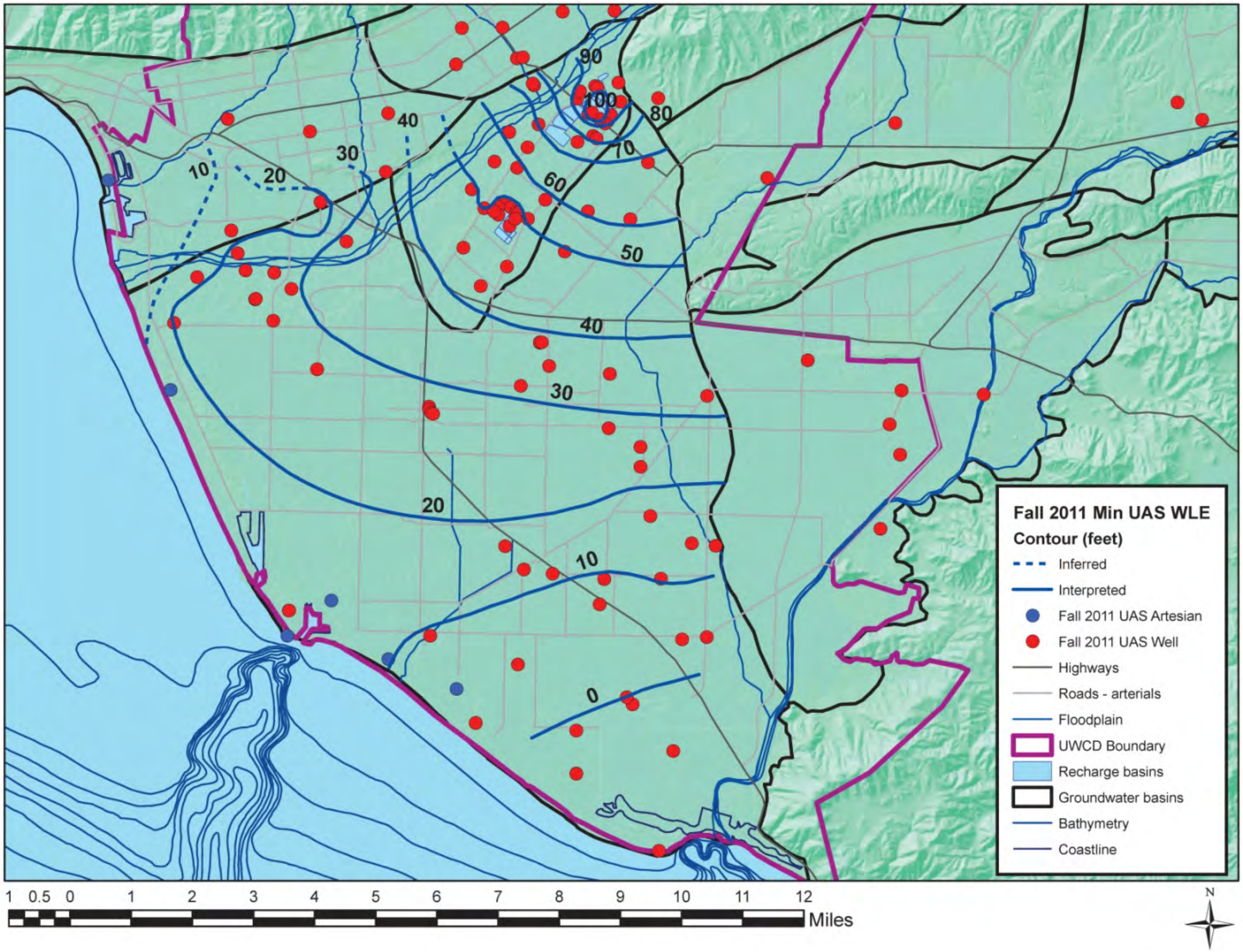

Figure C-2. Oxnard Forebay-Oxnard Plain Upper Aquifer System (UAS) groundwater elevations for fall 2011.

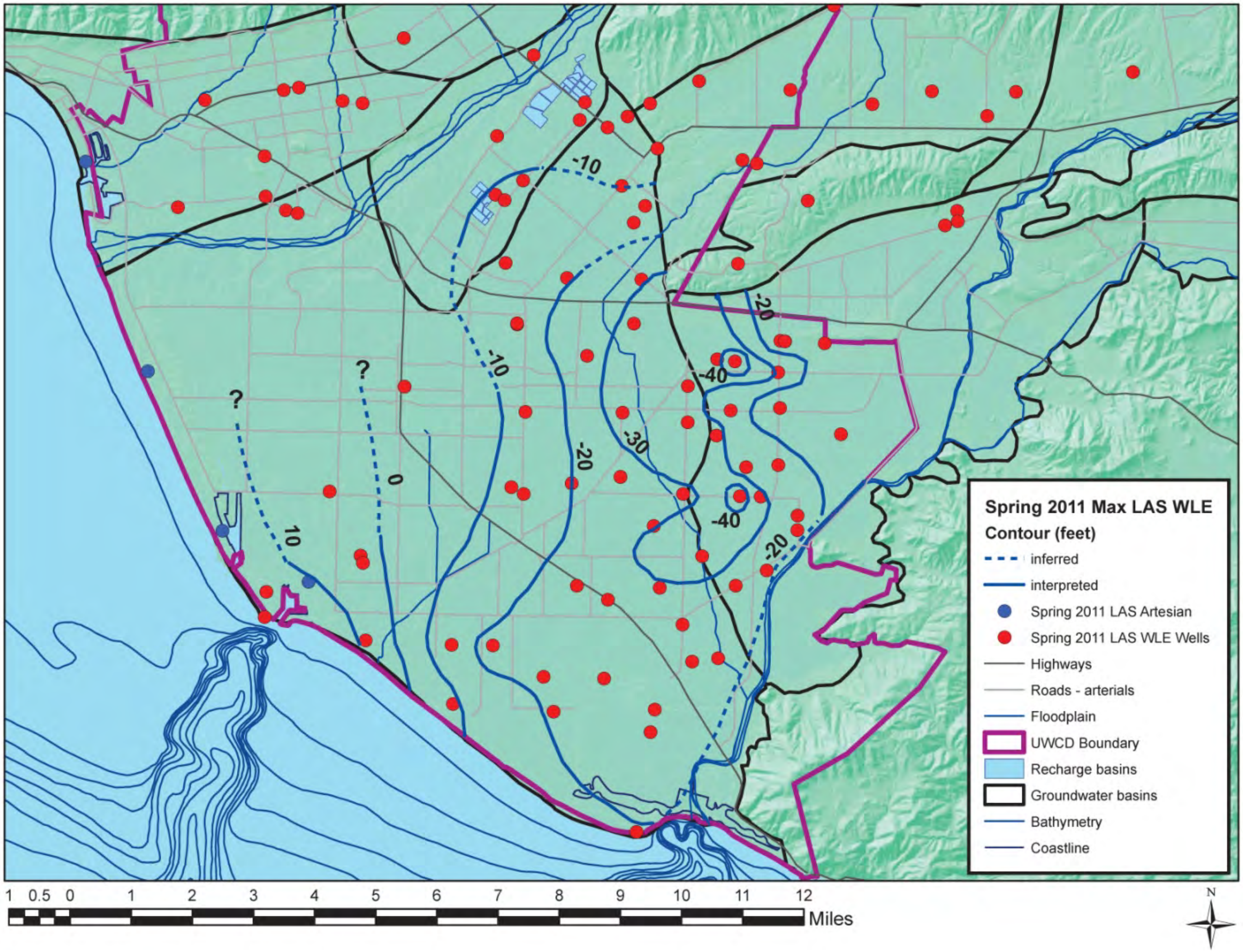

Figure C-3. Oxnard Forebay-Oxnard Plain Lower Aquifer System (LAS) groundwater elevations for spring 2011.

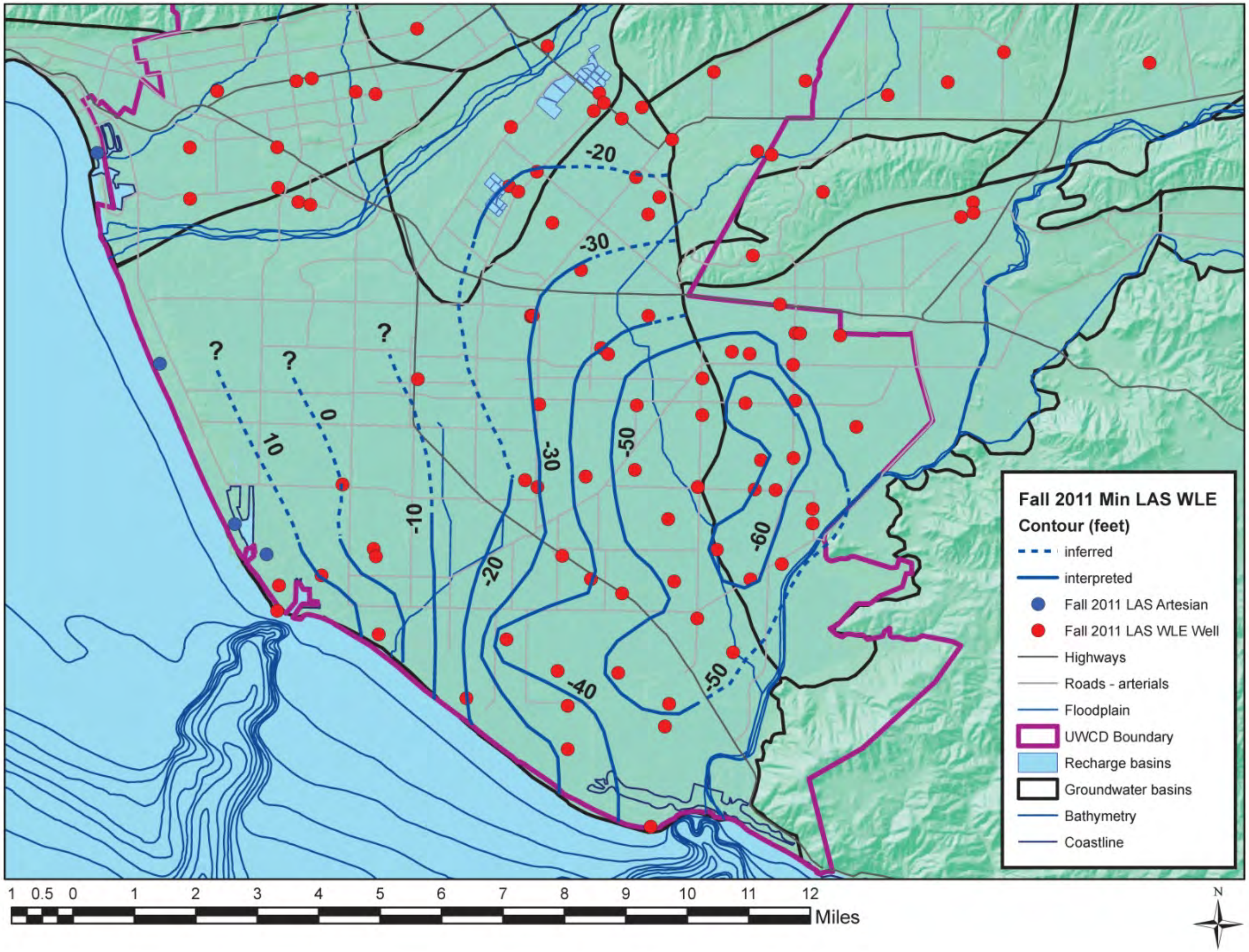

Figure C-4. Oxnard Forebay-Oxnard Plain Lower Aquifer System (LAS) groundwater elevations for fall 2011.

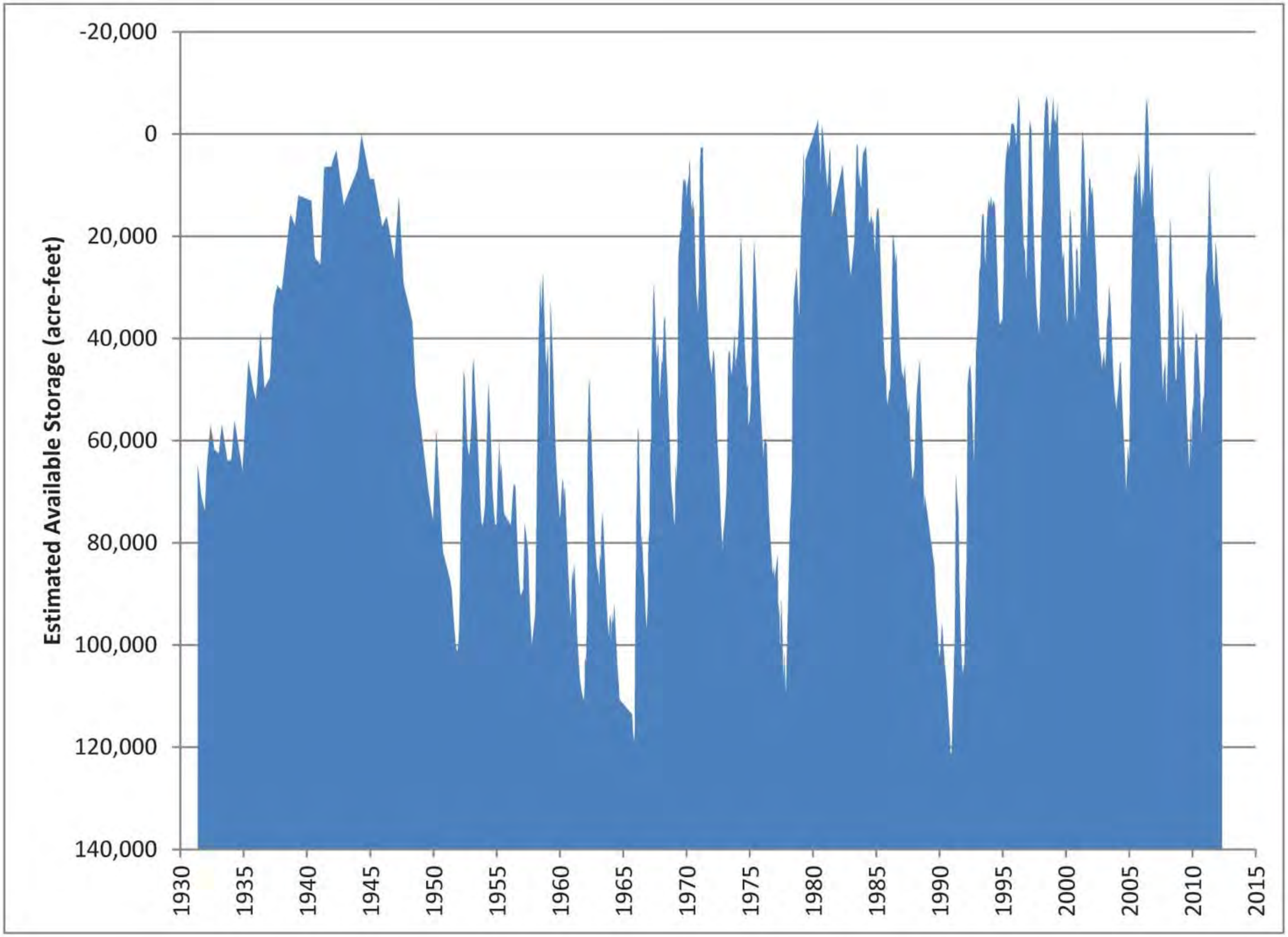

Figure C-5. Oxnard Forebay basin historical estimates of available groundwater storage.

APPENDIX D – CROSS-SECTIONS

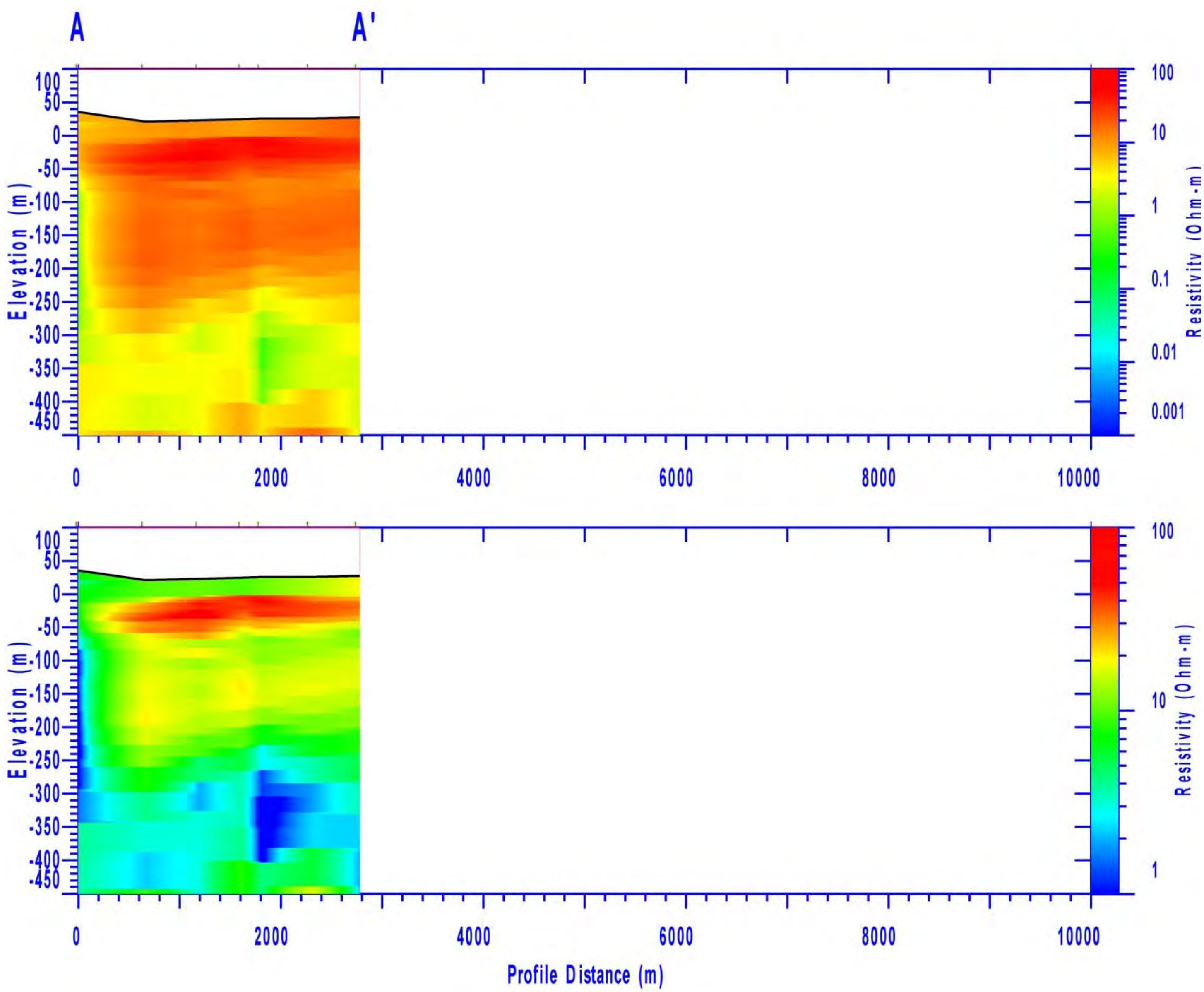

Figure D-1. Cross-section A-A'.

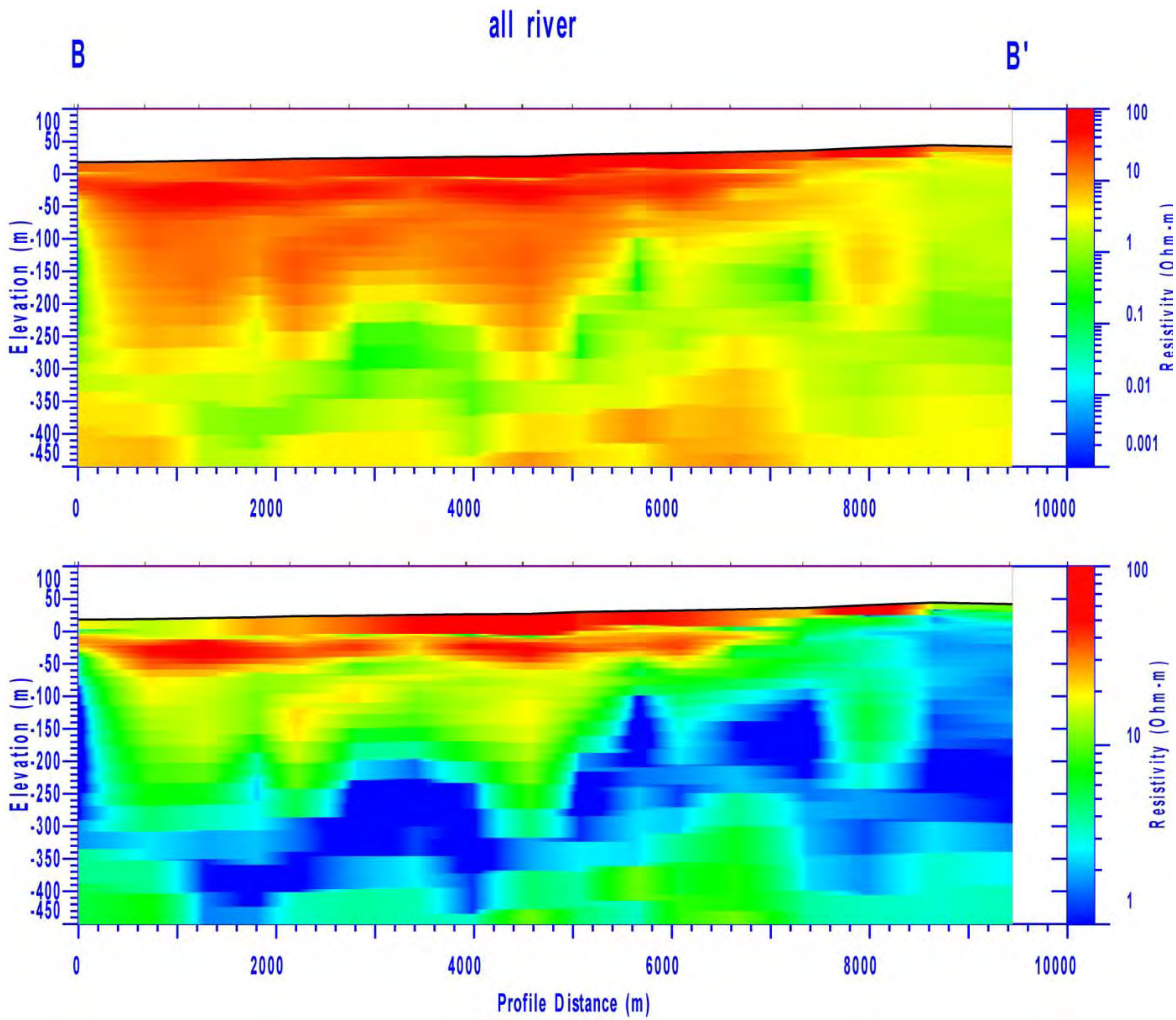

Figure D-2. Cross-section B-B'.

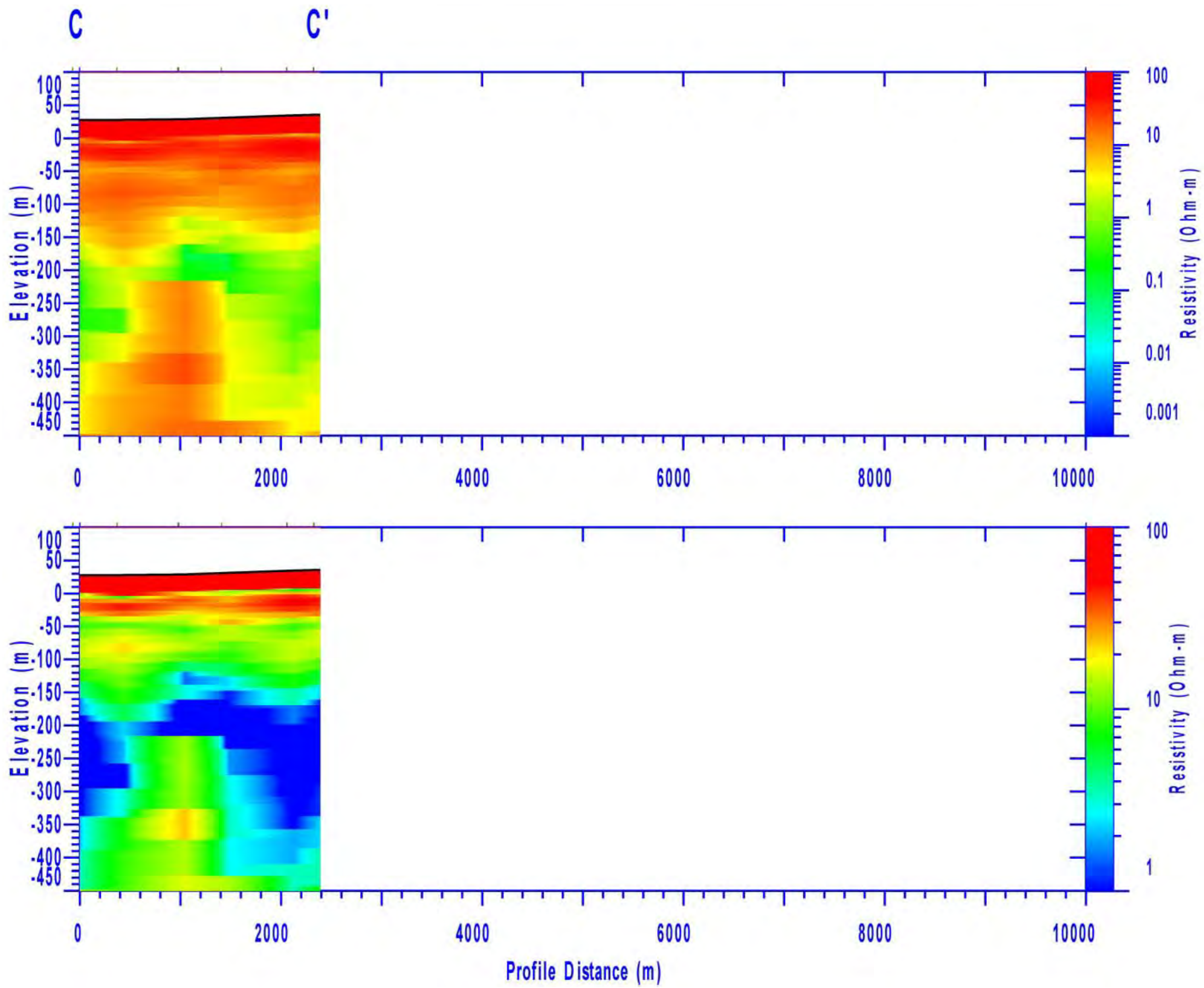

Figure D-3. Cross-section C-C'.

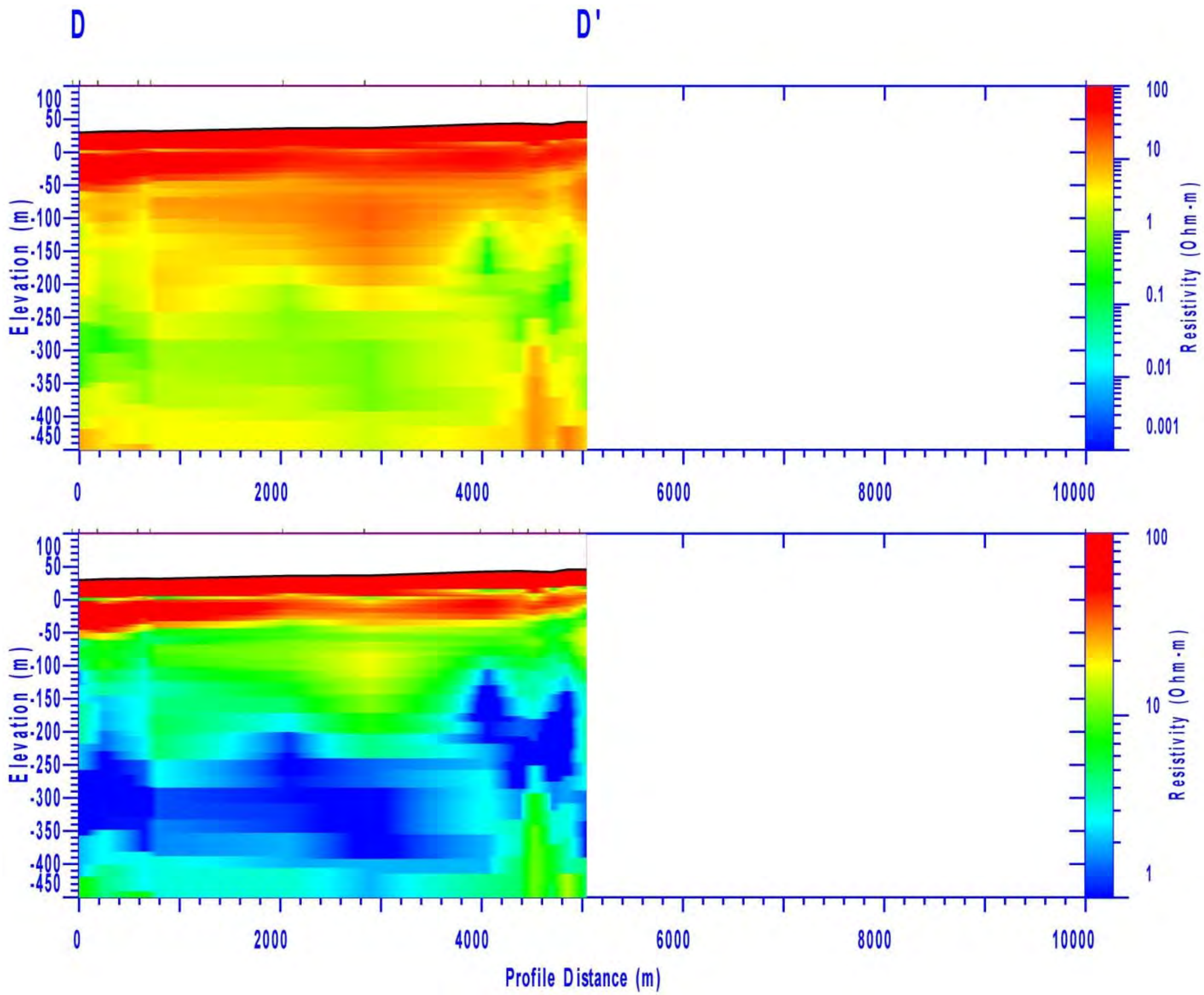

Figure D-4. Cross-section D-D'.

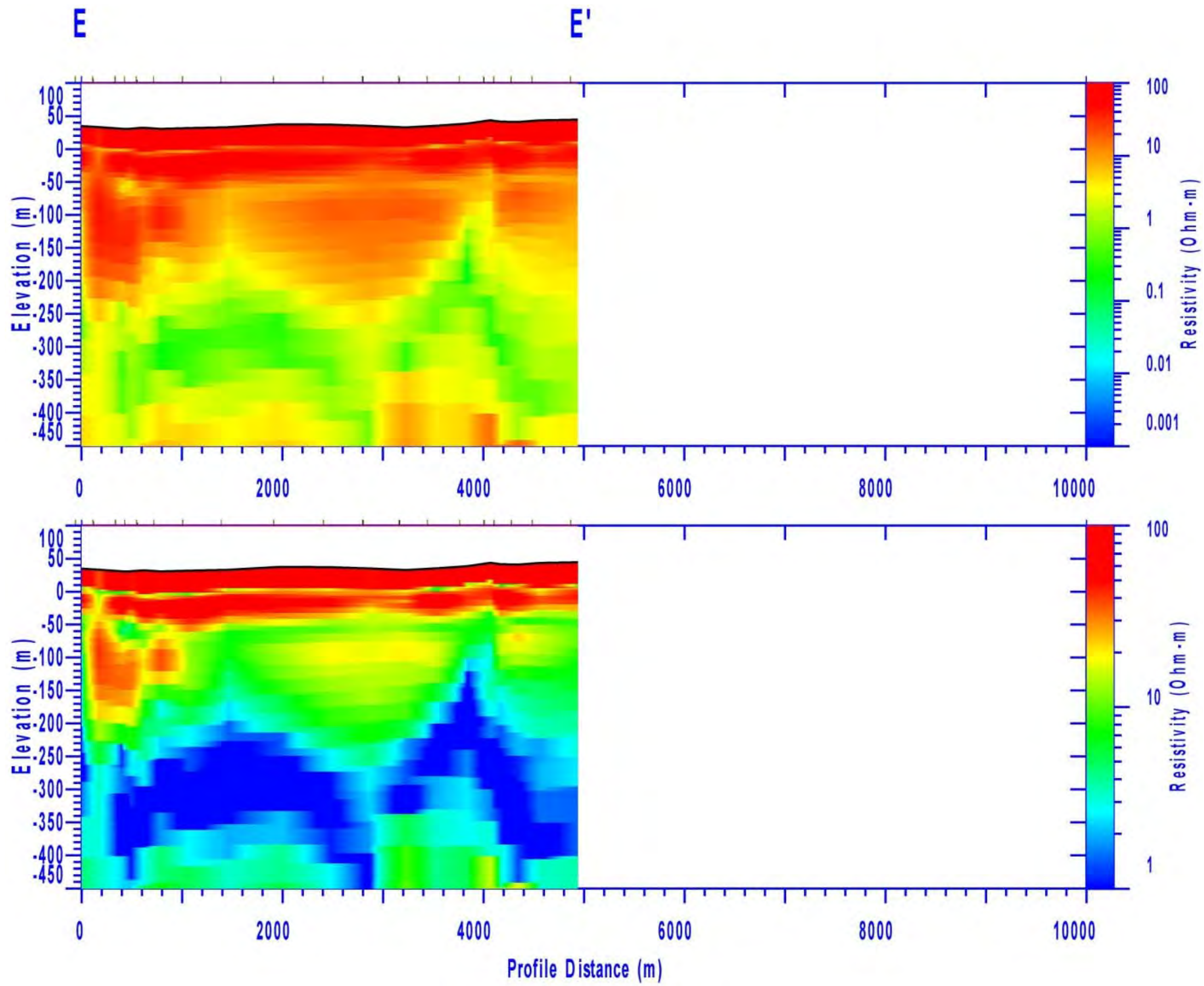

Figure D-5. Cross-section E-E'.

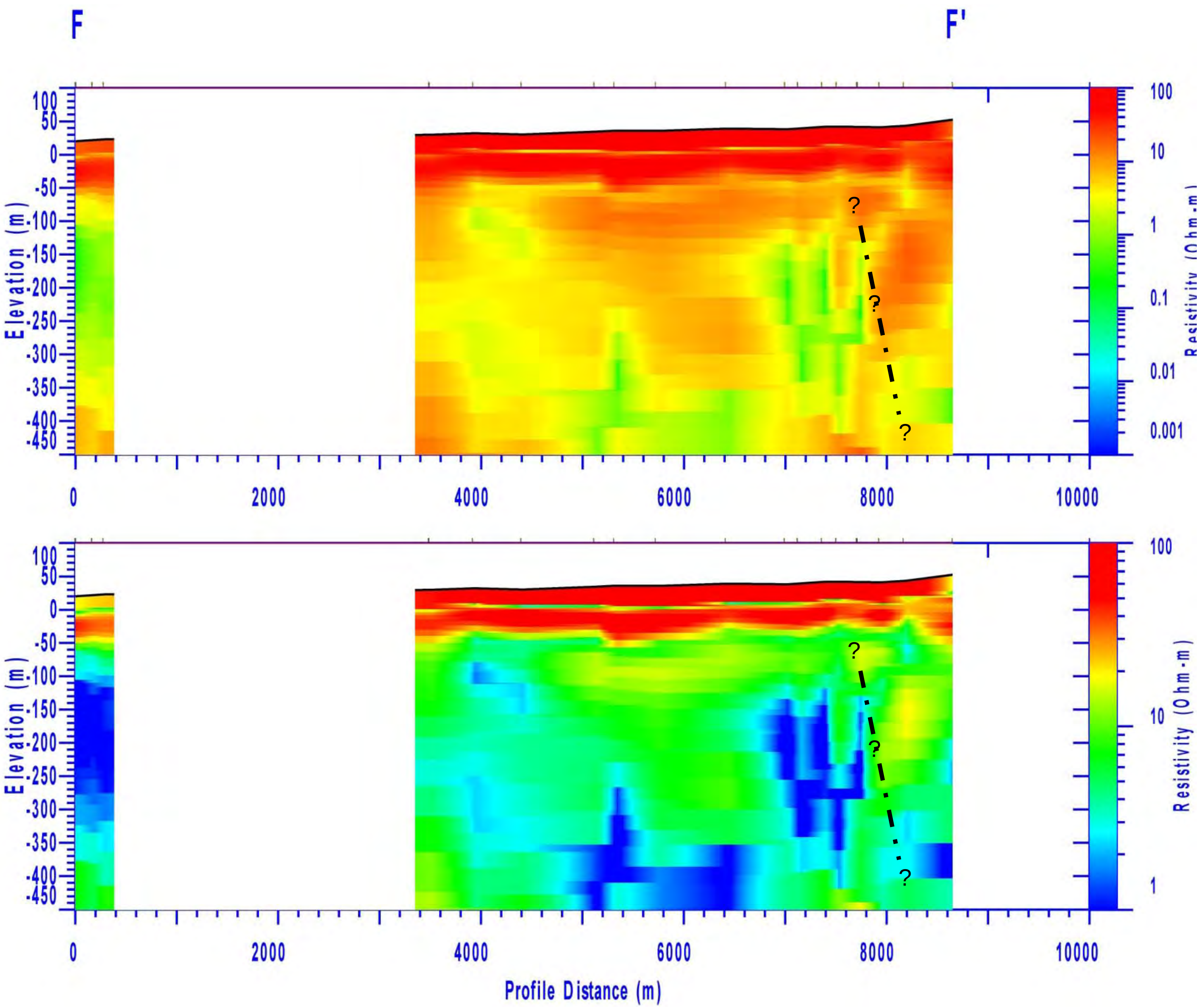

Figure D-6. Cross-section F-F'.

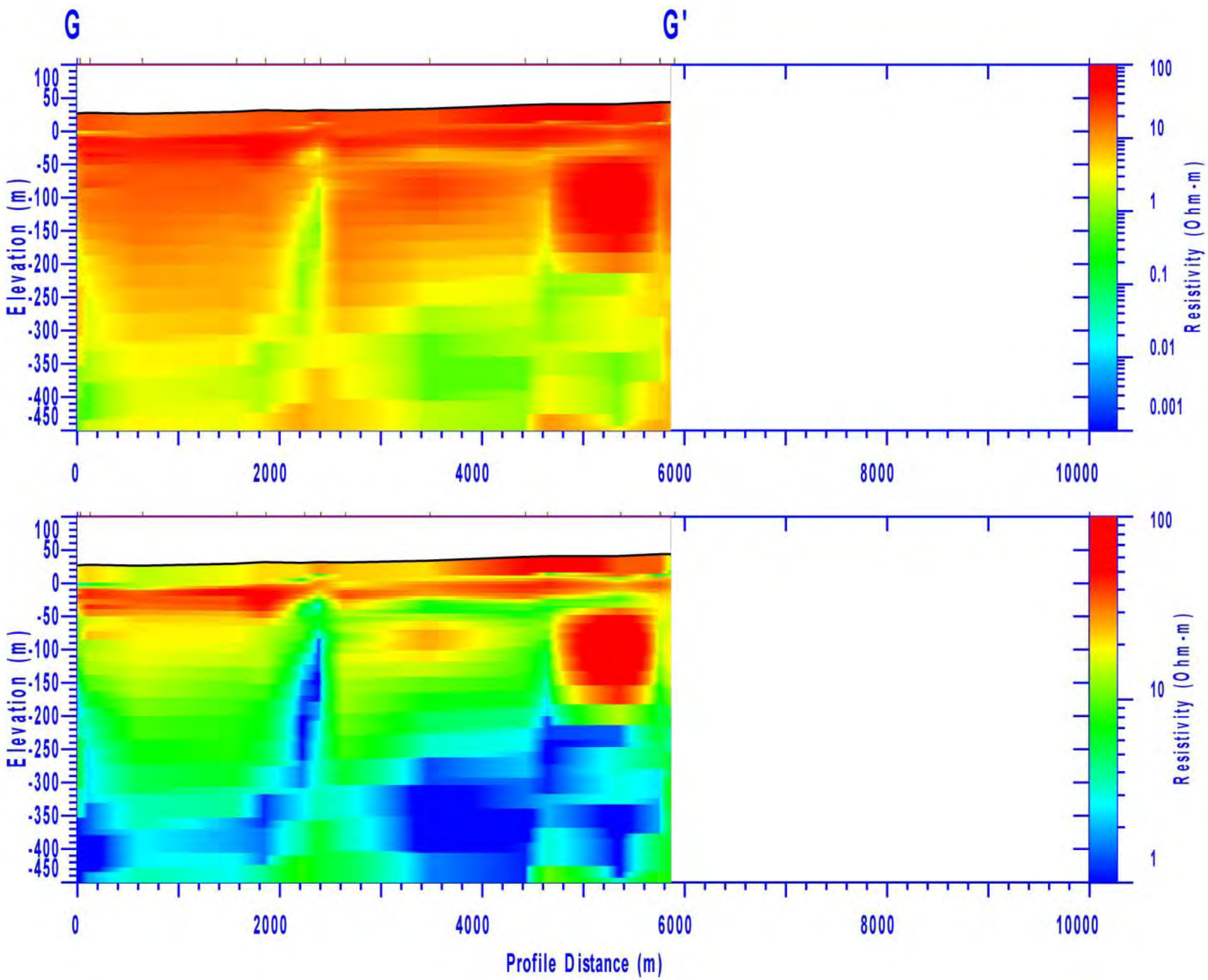

Figure D-7. Cross-section G-G'.

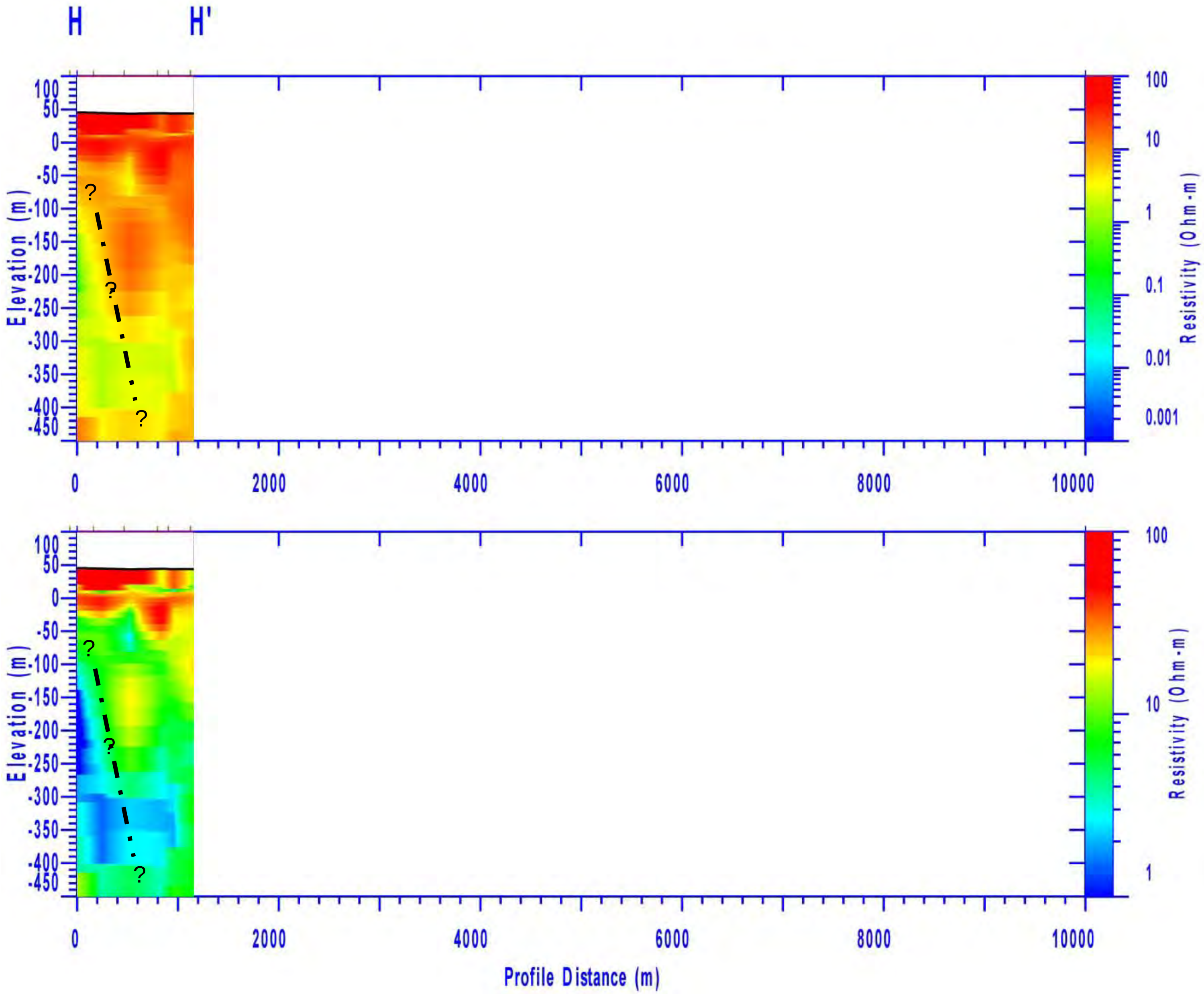

Figure D-8. Cross-section H-H'.

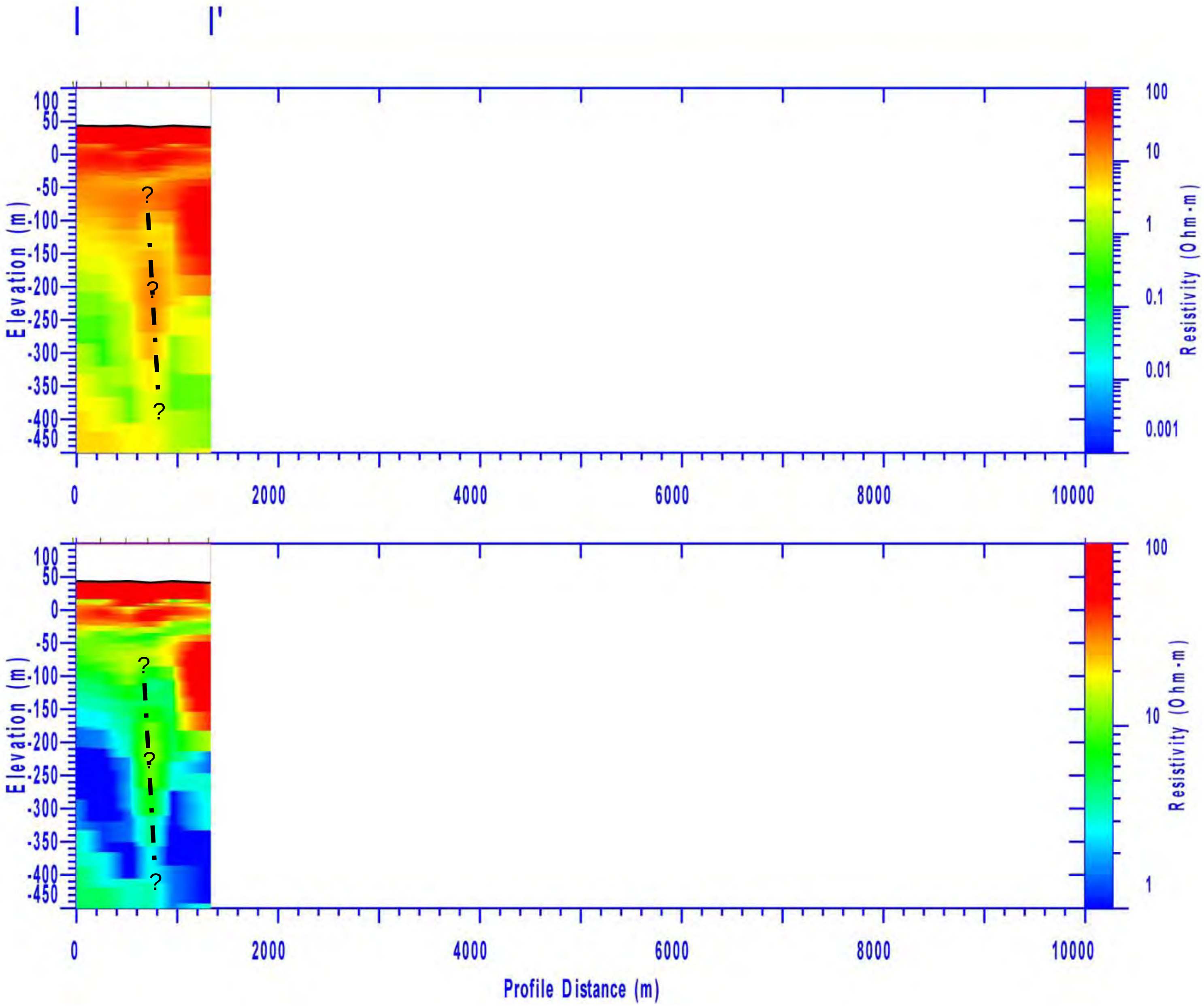

Figure D-9. Cross-section I-I'.

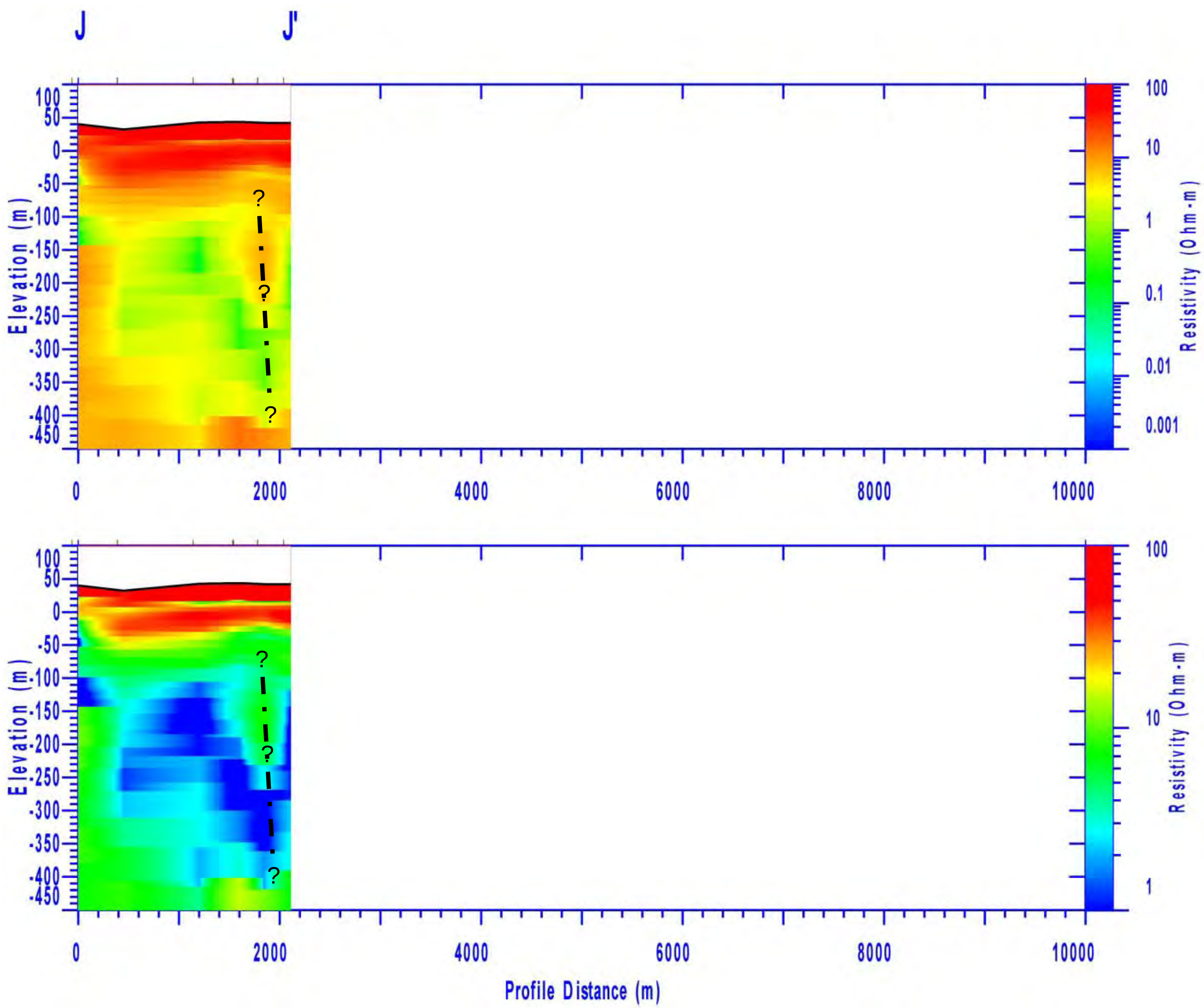

Figure D-10. Cross-section J-J'.

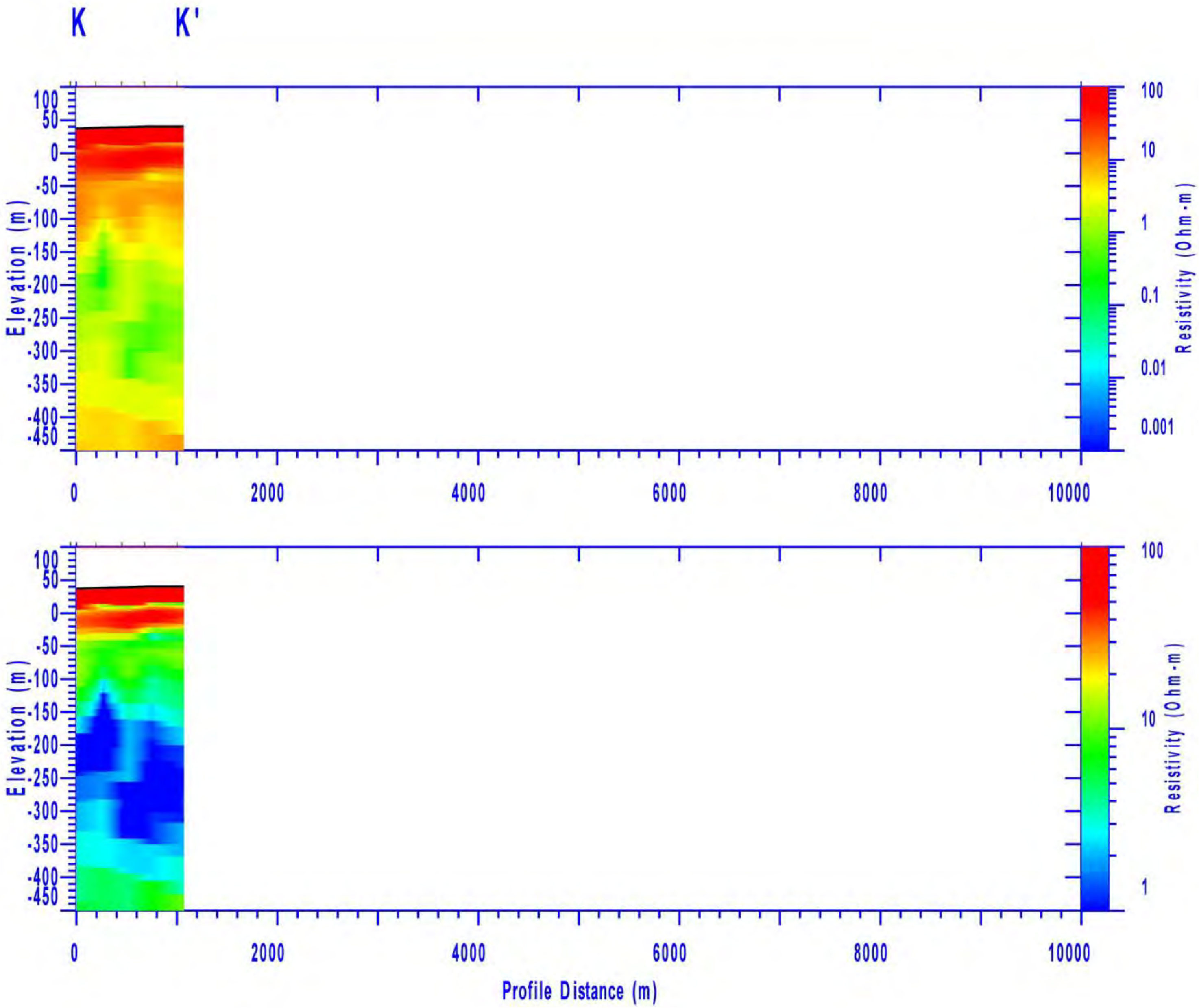

Figure D-11. Cross-section K-K'.

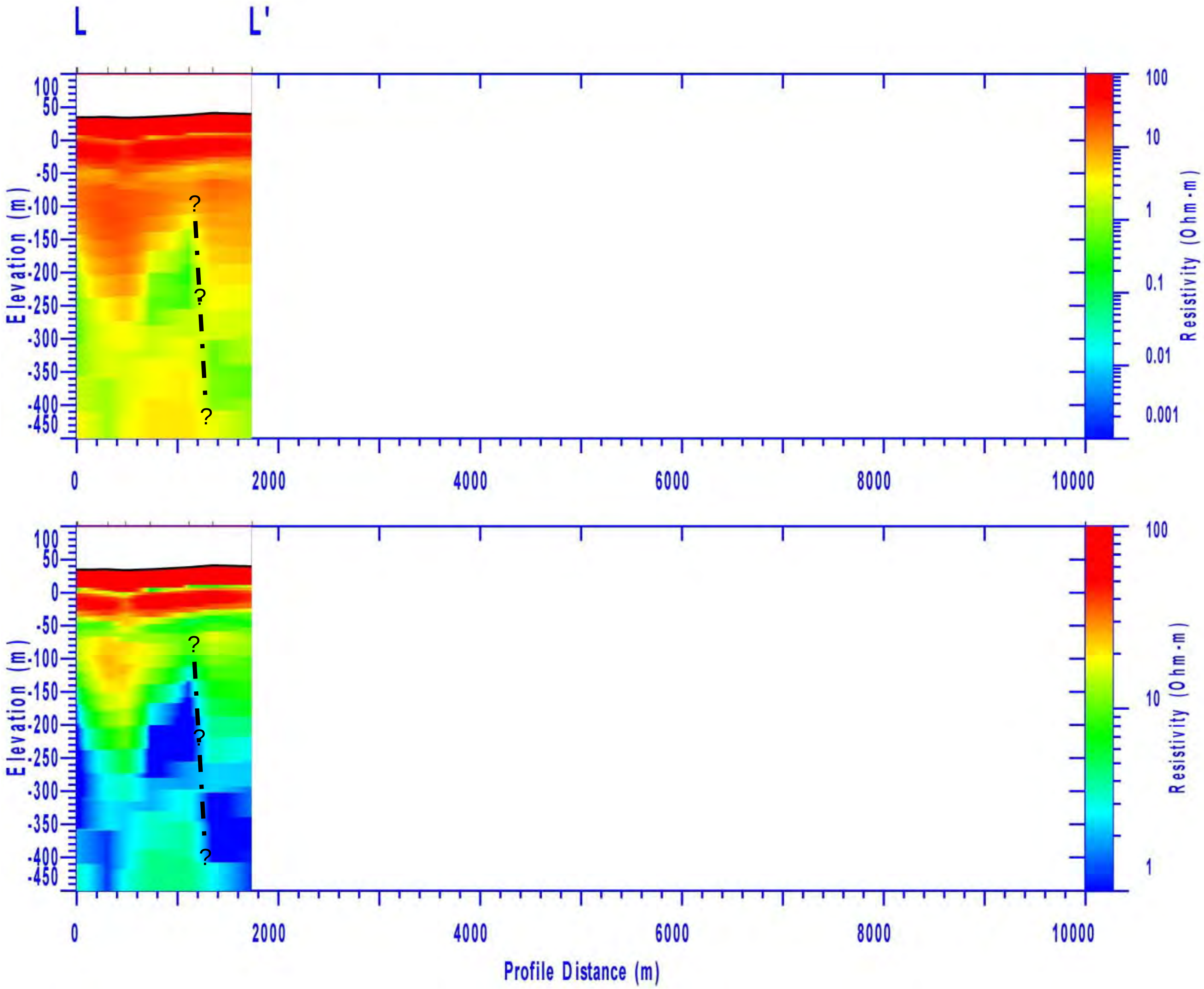

Figure D-12. Cross-section L-L'.

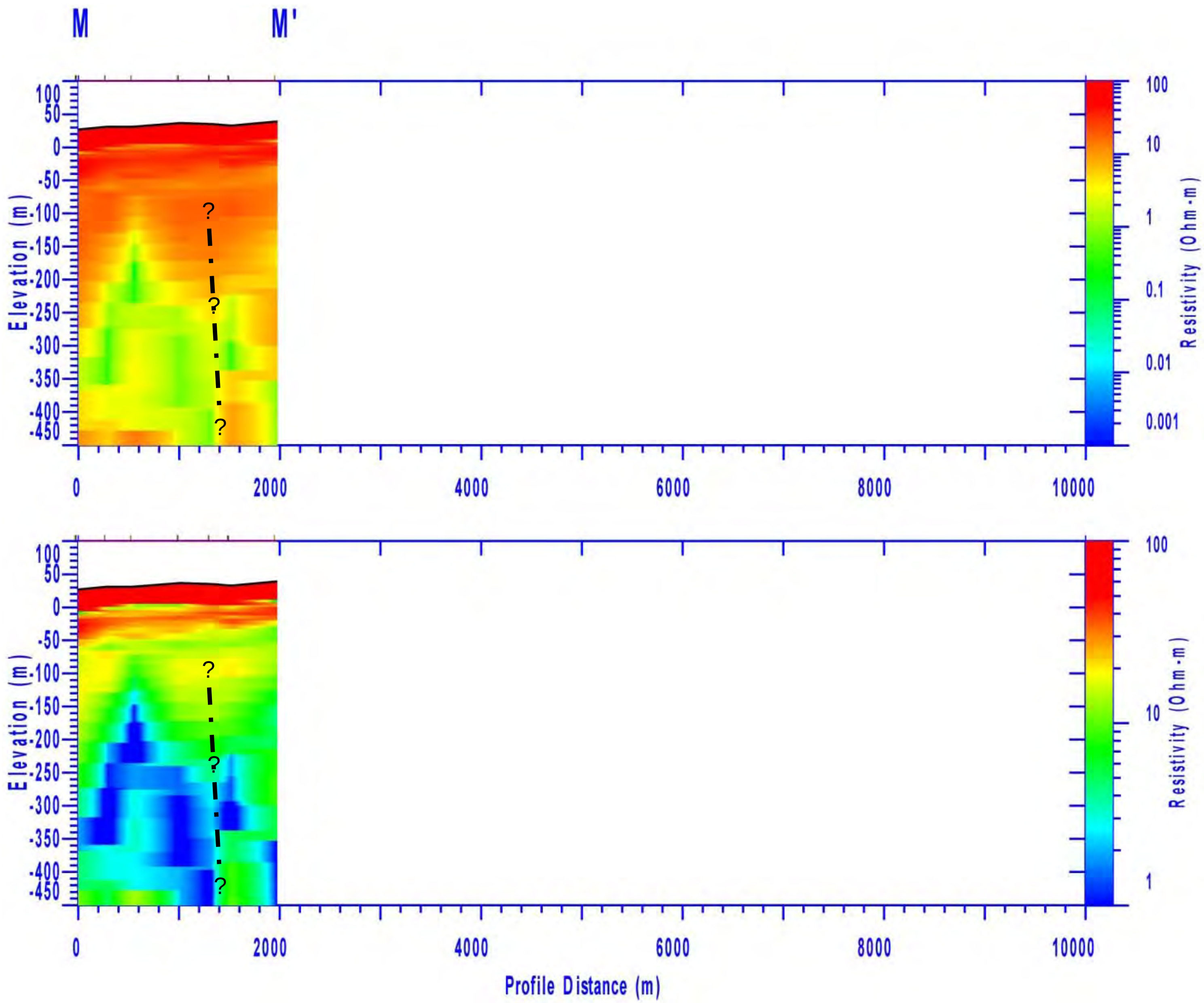

Figure D-13. Cross-section M-M'.

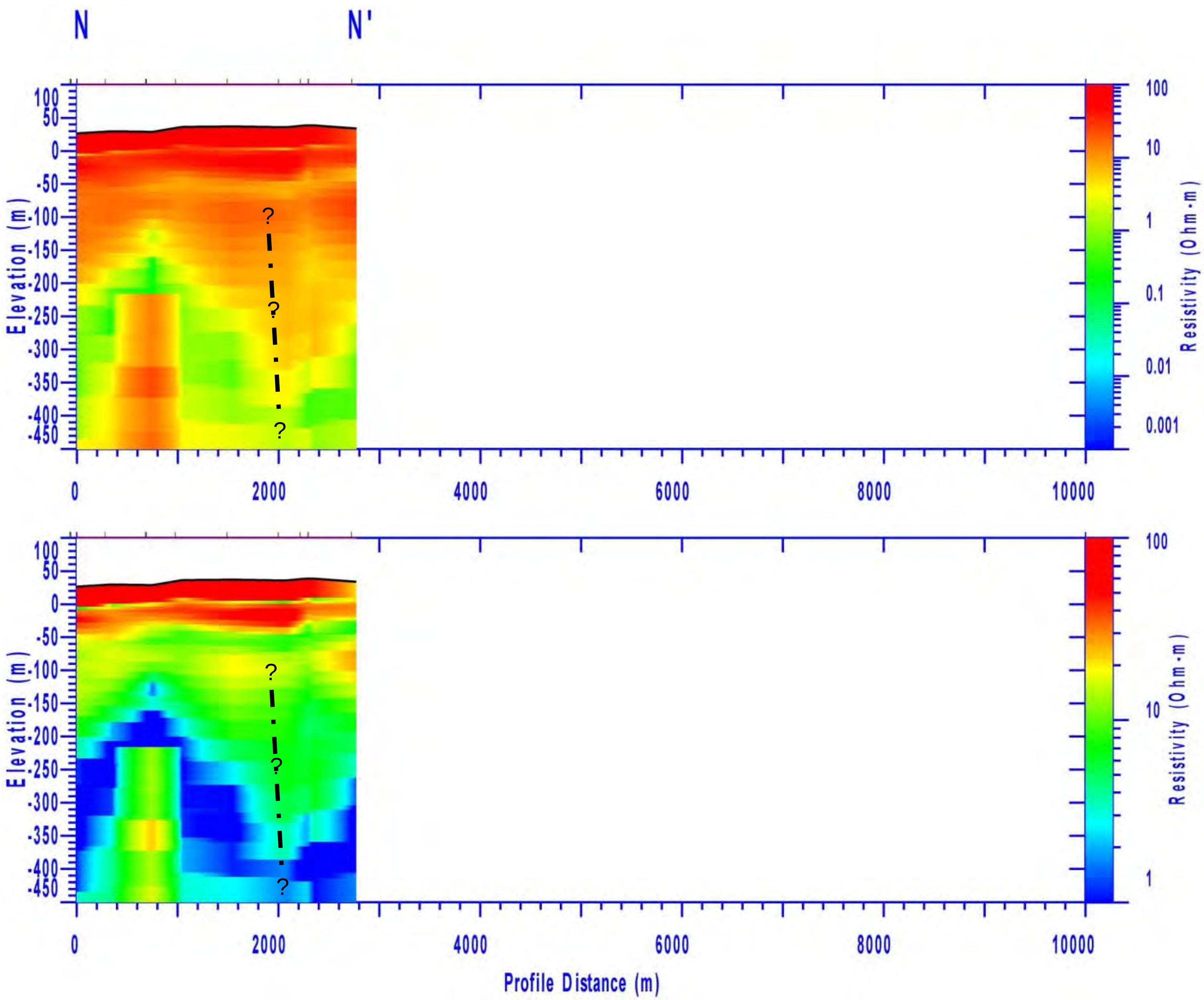

Figure D-14. Cross-section N-N'.

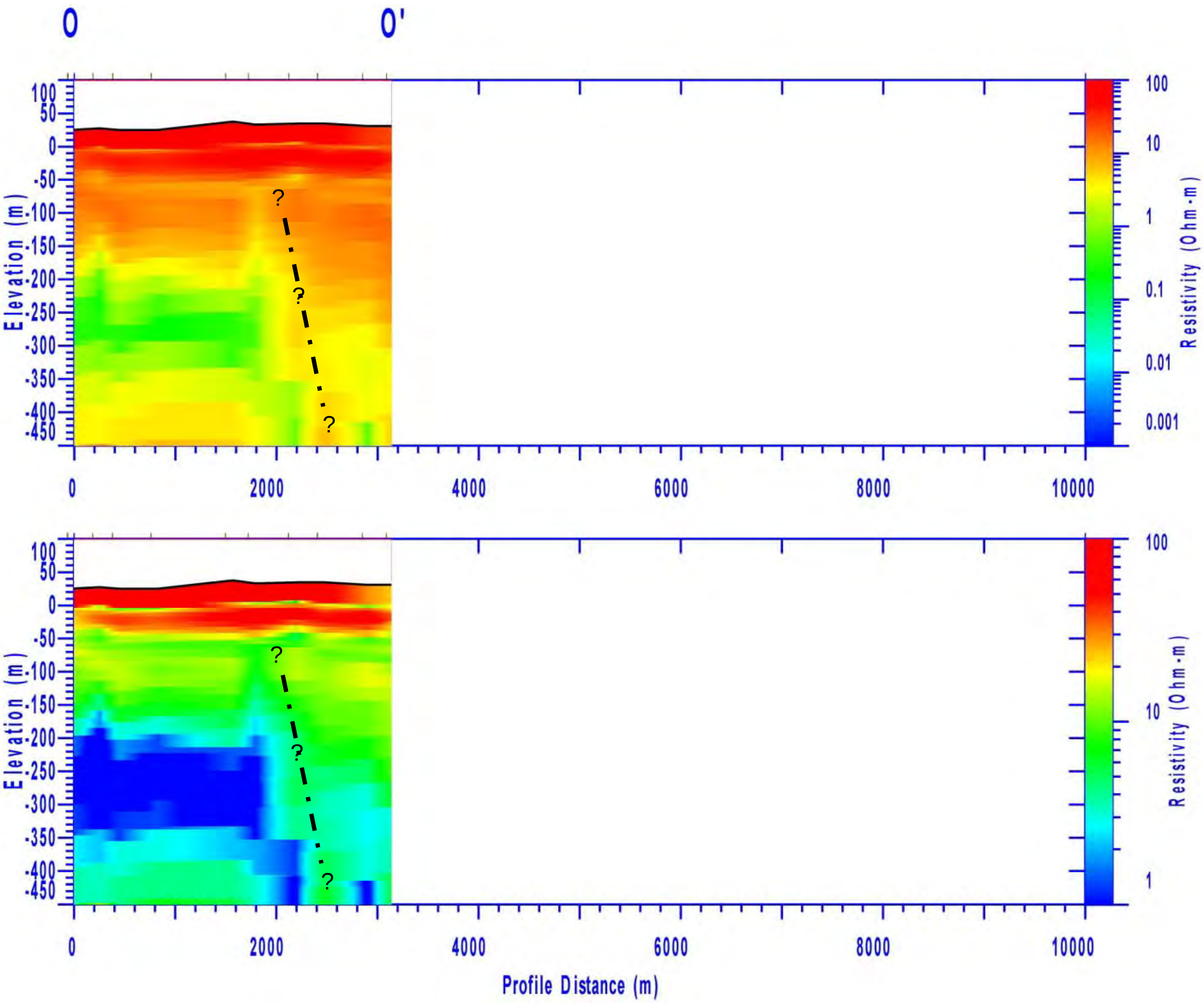

Figure D-15. Cross-section O-O'.

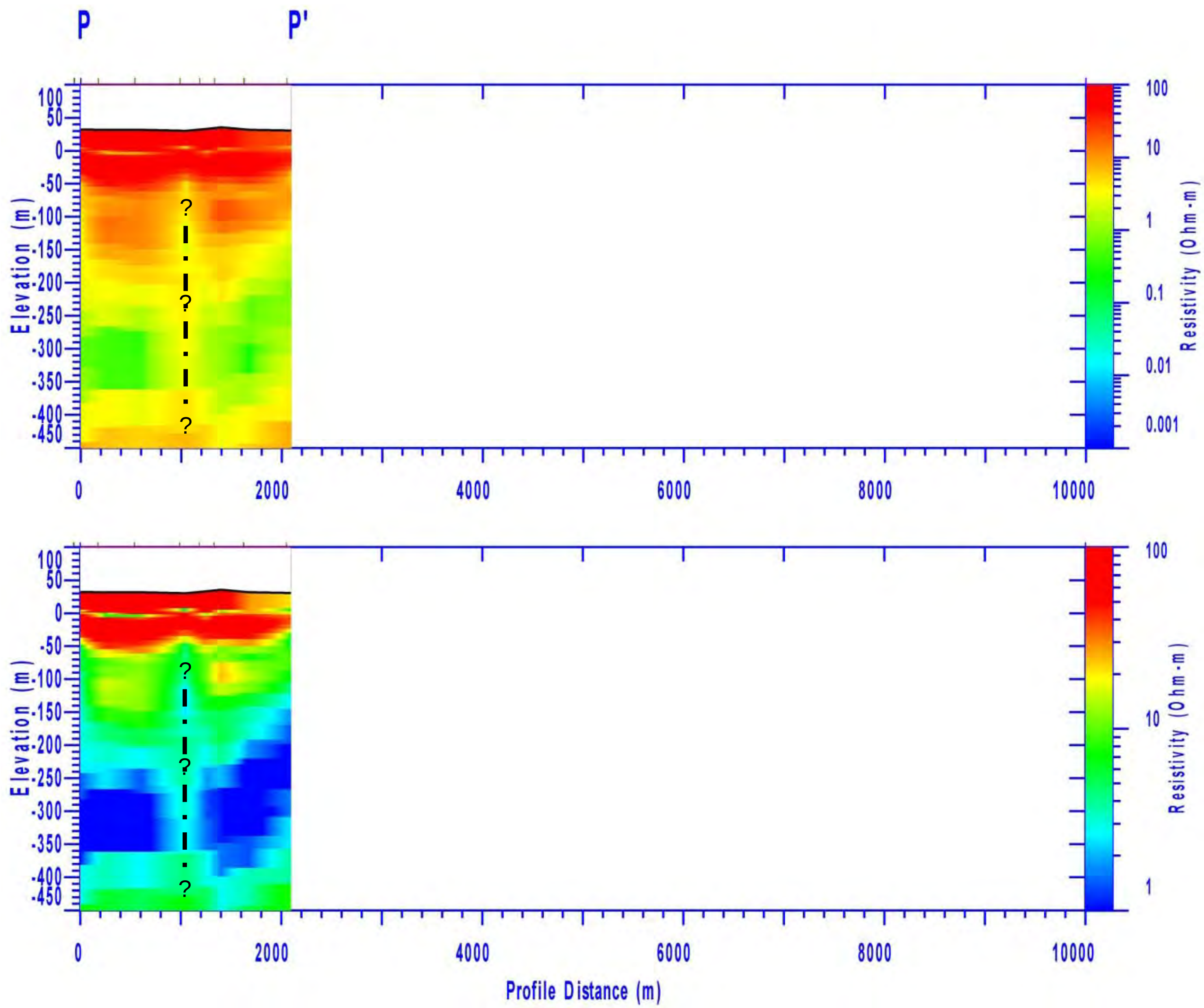

Figure D-16. Cross-section P-P'.

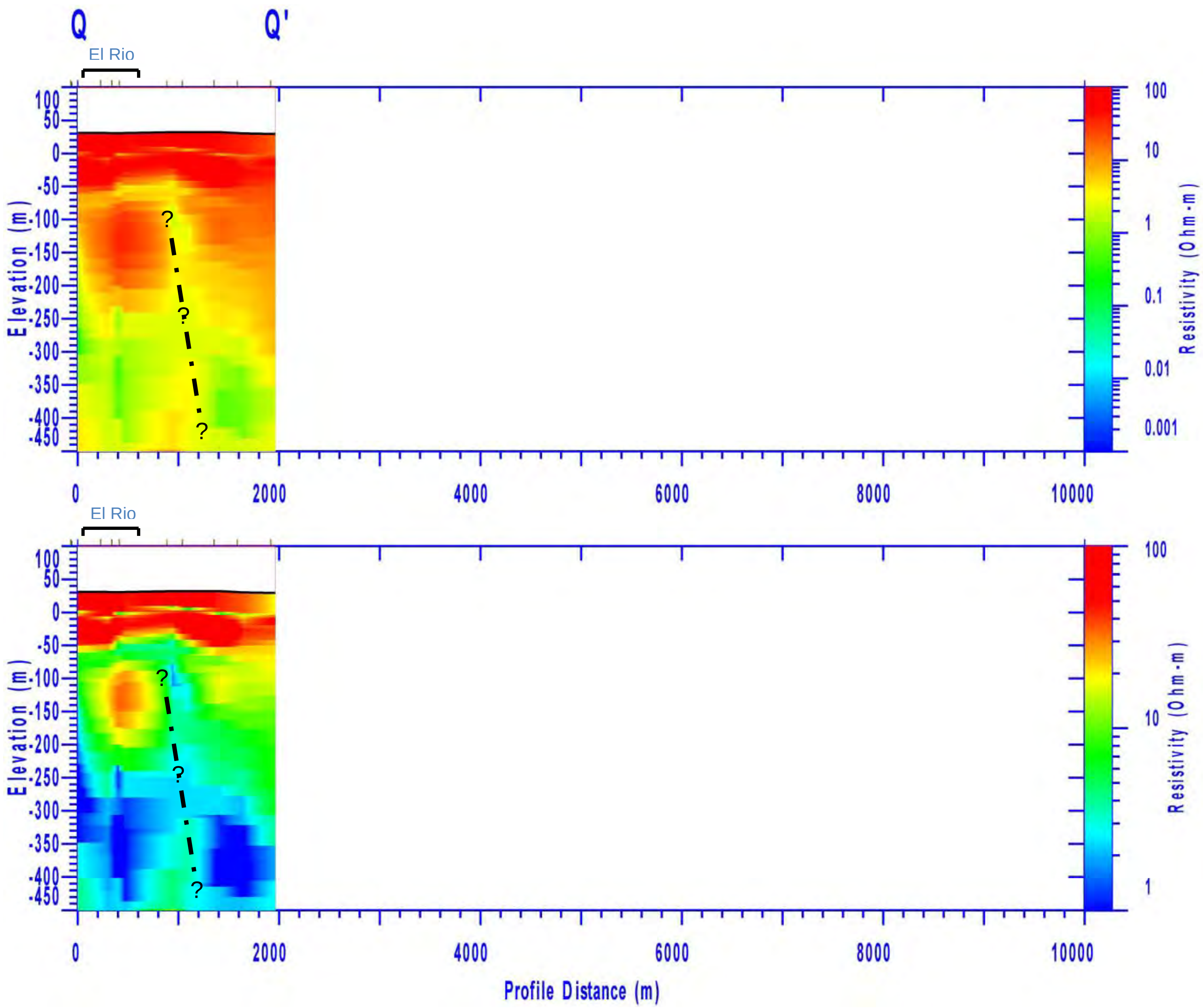

Figure D-17. Cross-section Q-Q'.

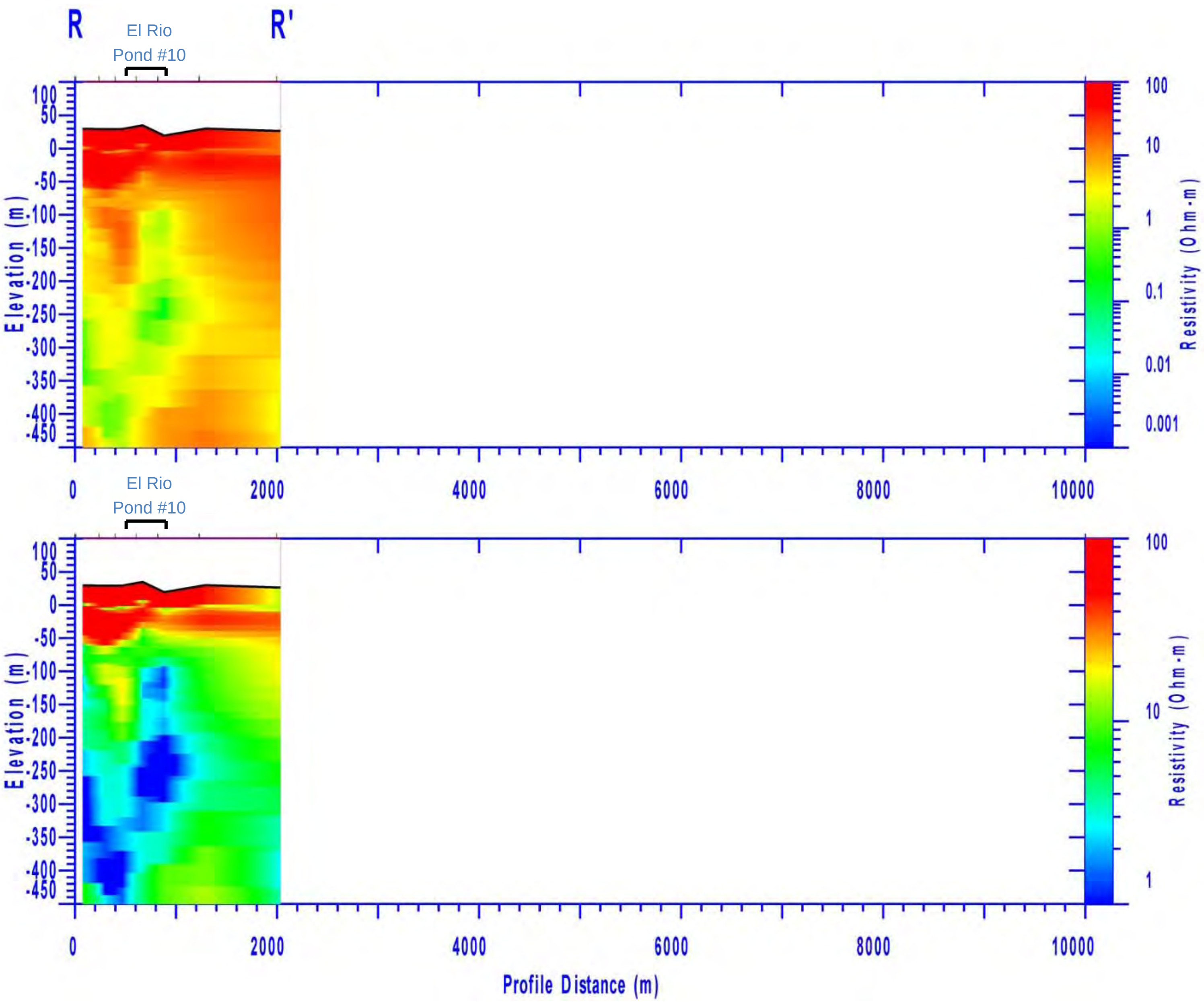

Figure D-18. Cross-section R-R'.

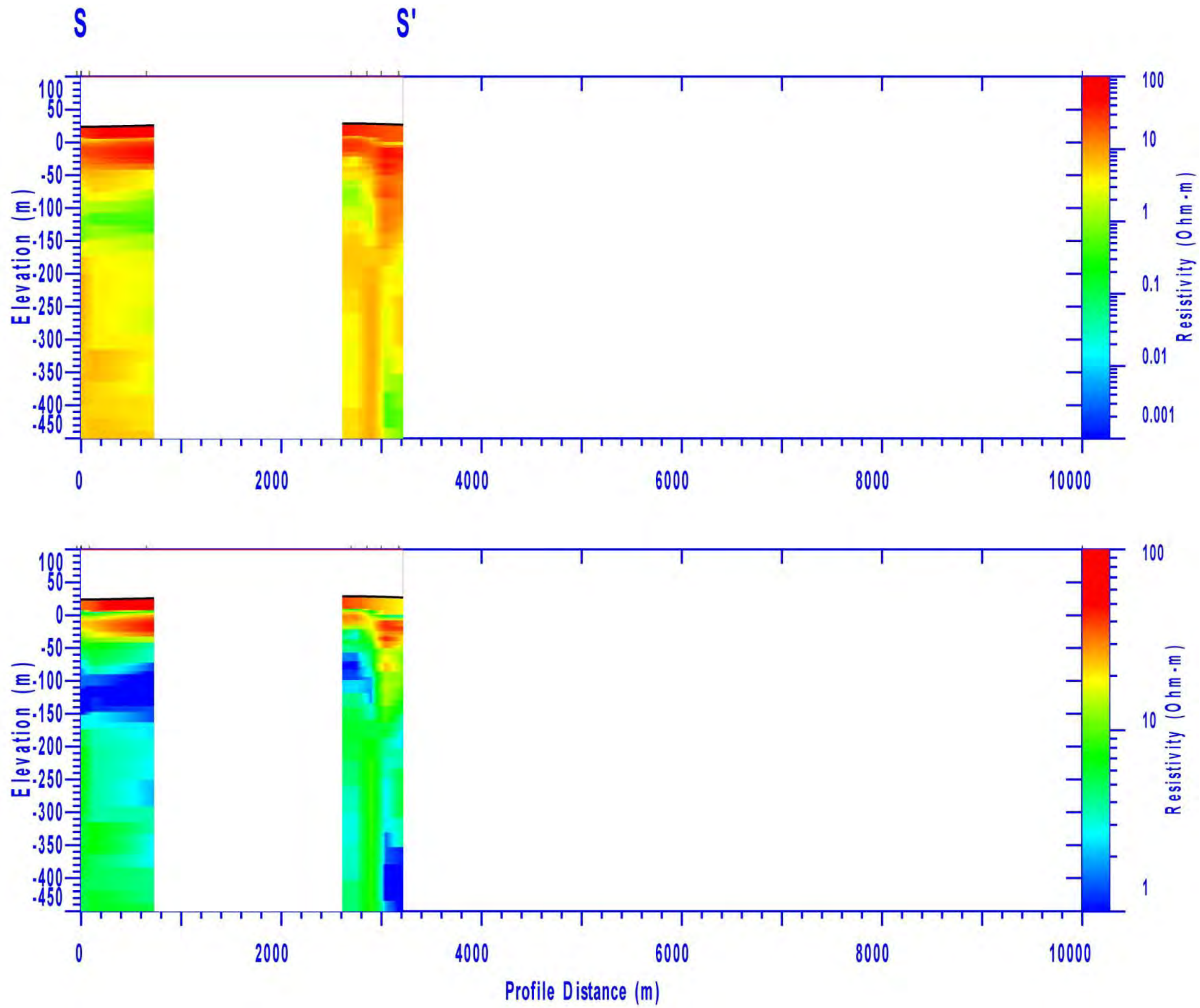

Figure D-19. Cross-section S-S'.

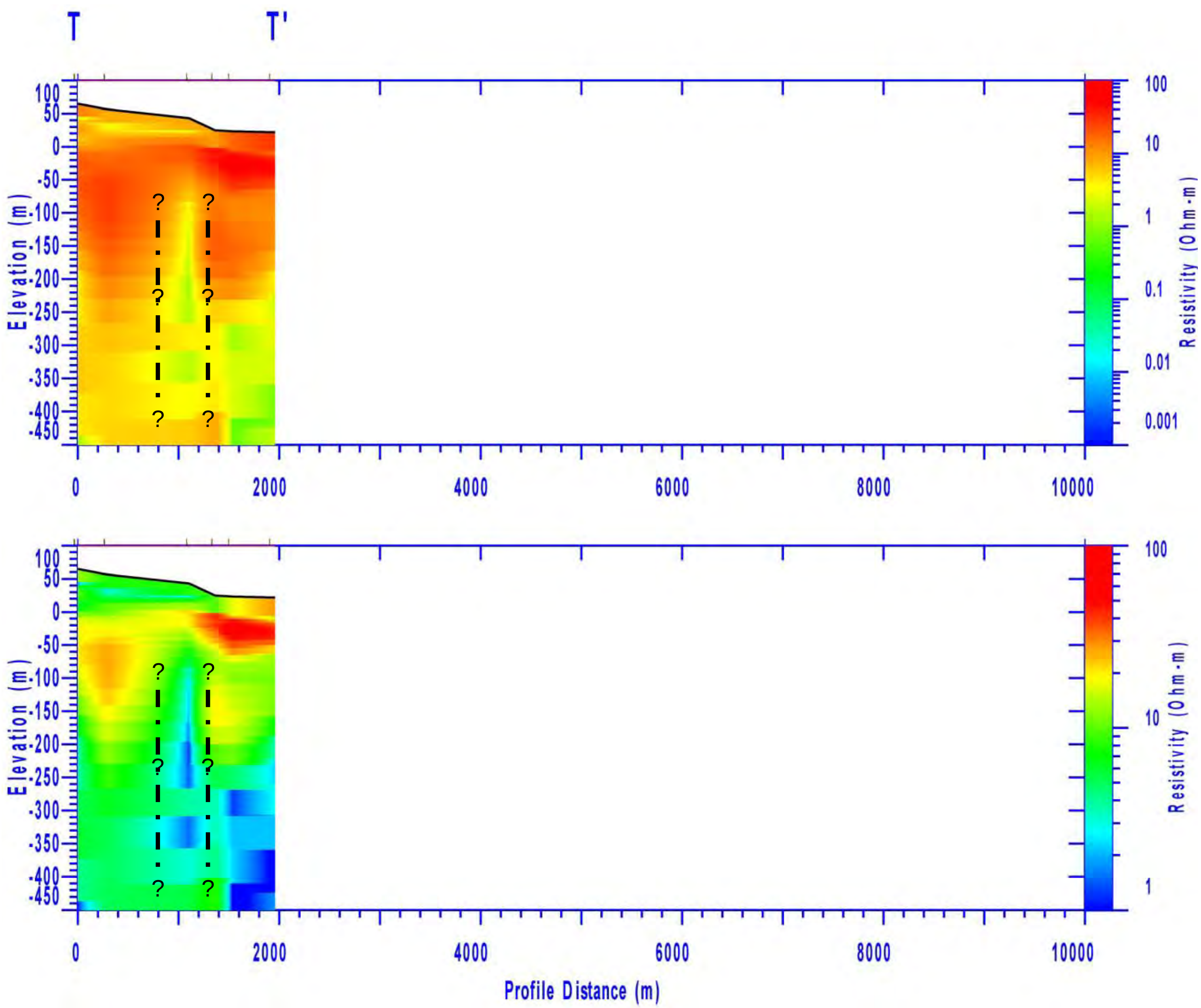

Figure D-20. Cross-section T-T'.

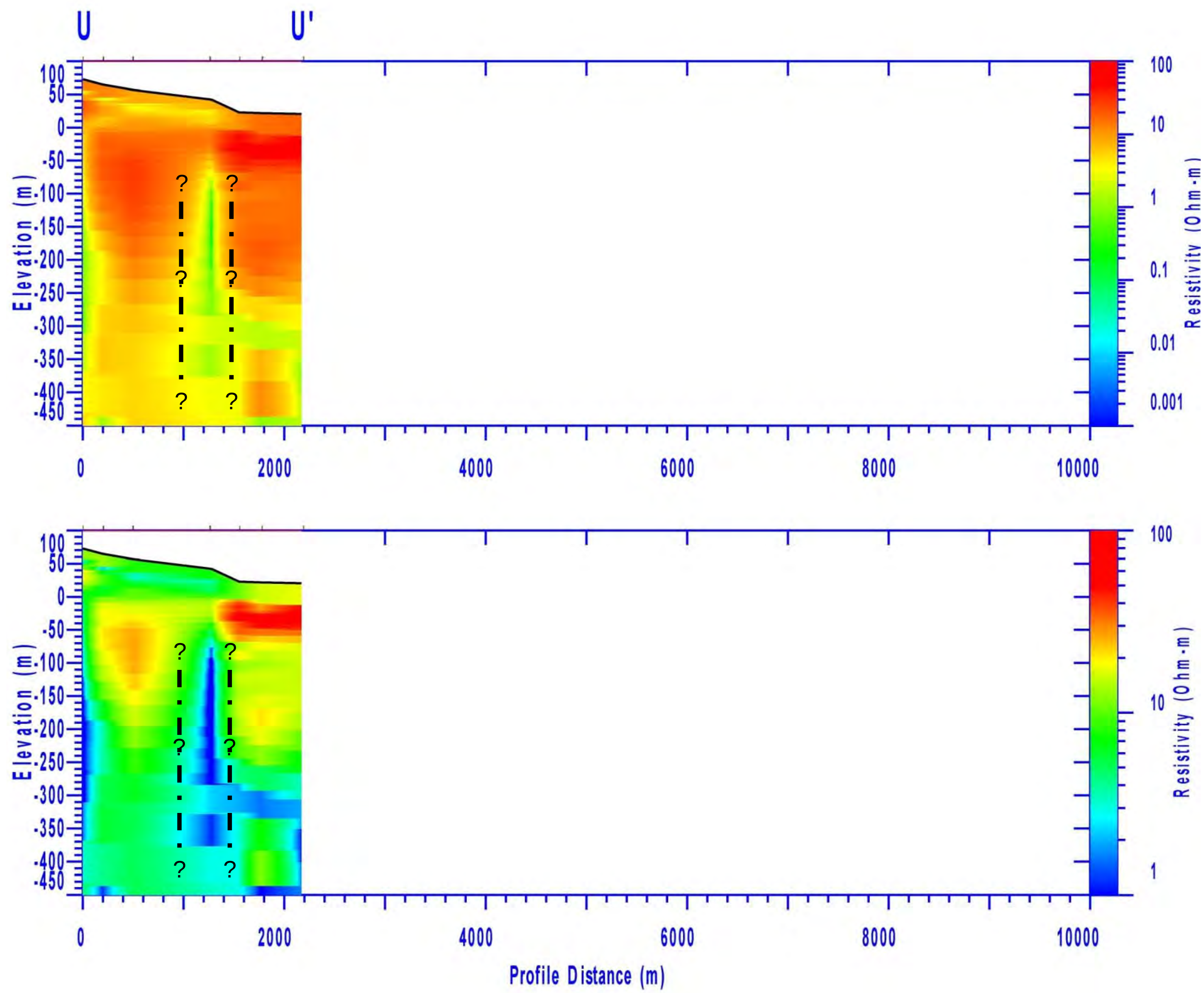

Figure D-21. Cross-section U-U'.